



Investigating the Combination of MNK1/2 and BET Inhibitors in Melanoma

Omar Moussa

Faculty of Medicine, Division of Experimental Medicine
McGill University, Montreal

April 2022

A thesis submitted to McGill University in partial fulfillment of the requirements of the degree of
MSc in experimental medicine

© Omar Moussa – 2022

TABLE OF CONTENTS

1.	ENGLISH ABSTRACT	5
2.	FRENCH ABSTRACT	6
3.	ACKNOWLEDGEMENTS	7
4.	AUTHOR CONTRIBUTIONS	8
5.	RESEARCH OBJECTIVES	9
6.	LITERATURE REVIEW	10
6.1.	MELANOMA: THE DEADLIEST FORM OF SKIN CANCER.....	10
6.2.	CLASSIFICATION OF MELANOMA SUBTYPES.....	10
6.3.	PATHOPHYSIOLOGY OF DRIVER MUTATIONS IN CUTANEOUS MELANOMA	10
6.4.	ADDITIONAL MUTATIONS ARE REQUIRED FOR THE OCCURRENCE OF ADVANCED STAGE DISEASE	11
6.5.	THE CURRENT THERAPEUTIC LANDSCAPE OF METASTATIC MELANOMA	12
6.6.	ACTIVATION OF PARALLEL SIGNALLING PATHWAYS AS A COMMON RESISTANCE MECHANISM TO MAPK INHIBITION IN MELANOMA	14
6.7.	RATIONALE OF INHIBITING THE MNK1/2-EIF4E AXIS IN MELANOMA.....	15
6.8.	MNK1 AND MNK2 KINASES: ISOFORMS AND FUNCTION	18
6.9.	NUCLEAR AND CYTOPLASMIC SUBCELLULAR LOCALIZATION OF MNK1/2 KINASES SUGGESTS ADDITIONAL BIOLOGICAL FUNCTIONS.....	19
6.10.	CURRENTLY AVAILABLE INHIBITORS OF MNK1/2 KINASES	20
6.11.	TRANSLATIONAL AND EPIGENETIC REPROGRAMMING IN MELANOMA UNDERLIE PHENOTYPE SWITCHING	21
6.12.	LYSINE ACETYLATION AND BROMODOMAIN PROTEINS IN CANCER.....	22
6.13.	STRUCTURE AND FUNCTION OF BET-FAMILY PROTEINS.....	22
6.14.	THE ROLE OF BET-FAMILY PROTEINS IN MELANOMA AND OTHER CANCERS	25
6.15.	INHIBITING BET-FAMILY OF PROTEINS IN CANCER.....	26
6.16.	CROSSTALK BETWEEN THE MNK1/2-EIF4E AXIS AND BET-FAMILY PROTEINS.....	26
7.	METHODS	28
7.1.	CELL LINES AND REAGENTS	28
7.2.	CRISPR-KO SCREEN	28
7.3.	VIRAL TRANSDUCTION OF A375	28

7.4.	IMMUNOBLOTTING	28
7.5.	DOSE RESPONSE CURVES.....	29
7.6.	CELL VIABILITY ASSAYS	29
7.7.	COLONY FORMATION ASSAY	29
7.8.	CELL CYCLE ANALYSIS	30
7.9.	ANNEXIN V-PI.....	30
7.10.	CFSE PROLIFERATION ASSAY	30
7.11.	BOYDEN CHAMBER INVASION ASSAY.....	31
7.12.	SENESCENCE ASSAY.....	31
7.13.	<i>IN VIVO</i> MOUSE STUDY	31
7.14.	IMMUNOHISTOCHEMISTRY STAINING MNK1	32
7.15.	IMMUNOHISTOCHEMISTRY STAINING P-EIF4E.....	32
7.16.	IMMUNOHISTOCHEMISTRY STAINING KI67.....	33
7.17.	STATISTICAL ANALYSES.....	33
8.	RESEARCH FINDINGS.....	34
8.1.	A SEL201-CRISPR-KO SCREEN SUGGESTS SYNTHETIC LETHALITY BETWEEN BRD2 AND MNK1/2 KINASES	34
8.2.	COMBINING BET AND MNK1/2 INHIBITORS COMPROMISES MELANOMA CLONOGENIC OUTGROWTH BETTER THAN EITHER DRUG ALONE.....	36
8.3.	BRD4 KNOCKDOWN IN A375 RECAPITULATES PHARMACOLOGICAL EFFECTS OF BET1 IN COMBINATION TREATMENT	45
8.4.	EFT508 RECAPITULATES PHARMACOLOGICAL EFFECTS OF SEL201 IN BLM BUT NOT IN A375 WHEN COMBINED WITH OTX-015	46
8.5.	TREATMENT OF A375 CELLS WITH OTX-015 AND SEL201 DOES NOT INDUCE CELL CYCLE ARREST	46
8.6.	COMBO-TREATED A375 CELLS DO NOT EXHIBIT DECREASED CELLULAR PROLIFERATION BY CFSE DESPITE SHOWING LOWER CELLULAR ABUNDANCE	47
8.7.	THE COMBINATION OF SEL201 AND OTX-015 DOES NOT ENHANCE APOPTOSIS IN A375	49
8.8.	DUAL THERAPY USING SEL201 AND OTX-015 DOES NOT INDUCE CELLULAR SENESCENCE IN A375.....	50

8.9.	COMBINING SEL201 AND OTX-015 DOES NOT FURTHER DECREASE THE INVASIVE POTENTIAL <i>IN VITRO</i> OF A375 AND BLM MELANOMA CELL LINES.....	51
8.10.	COMBINING SEL201 AND OTX-015 IN A SYNGENEIC MOUSE MODEL SHOWS IMPROVED SURVIVAL THAN VEHICLE OR SINGLE AGENT TREATMENTS	52
8.11.	PHARMACOLOGICAL EFFECTS OF SEL201 IN THE COMBINATION TREATMENT ARE LIKELY NOT ATTRIBUTABLE TO P-EIF4E INHIBITION	54
8.12.	TREATMENT OF MELANOMA CELLS WITH OTX-015 DOES NOT CONSISTENTLY ENHANCE P-EIF4E EXPRESSION.....	55
9.	DISCUSSION	57
10.	CONCLUSION	62
11.	SUPPLEMENTAL FIGURES	63
12.	REFERENCES	66

1. ENGLISH ABSTRACT

Melanoma is the deadliest type of skin cancer comprised of various molecular subtypes, most of which do not exhibit durable responses to clinically approved targeted therapies. Moreover, while the predominant subtype of cutaneous melanomas, that is BRAF^{V600E}-mutant, initially respond to combined BRAF and MEK inhibition, resistance almost always occurs. Similarly, other subtypes of melanoma exhibiting NF1, NRAS mutations or triple wild-type for BRAF, NF1 and NRAS remain hard-to-treat with currently approved targeted therapies. Thus, novel therapeutic avenues are required to widen the spectrum of available targeted therapies in melanoma. Using CRISPR-KO screening, we show a synthetic lethal interaction between SEL201, a MNK1/2 kinase inhibitor, and BRD2, a member of the BET-family of proteins. Dual inhibition of MNK1/2 kinases and BET-family proteins in BRAF- and NRAS-mutant melanoma cell lines showed decreased cell viability and clonogenic outgrowth relative to single agents alone. Moreover, the combined inhibition of MNK1/2 and BET-family proteins slightly enhanced the survival of syngeneic mice subcutaneously injected with Yummer 1.7 melanoma cells. While the mechanism of this combination treatment remains to be investigated, we propose that combining MNK1/2 and BET inhibitors may provide an potential avenue for the treatment of hard-to-treat subtypes and therapy-resistant melanomas.

2. FRENCH ABSTRACT

Le mélanome est le type de cancer de la peau le plus mortel, composé de divers sous-types moléculaires, dont la plupart ne présentent pas de réponses durables aux thérapies ciblées qui sont cliniquement approuvées. De plus, alors que le sous-type prédominant de mélanomes cutanés, c'est-à-dire le BRAFV600E-mutant, répond initialement à l'inhibition de BRAF et de MEK, une résistance se développe presque toujours. De plus, d'autres sous-types de mélanome présentant des mutations NF1, NRAS ou autre que BRAF, NF1 et NRAS restent difficiles à traiter avec présentement aucune thérapie ciblée approuvée. Ainsi, de nouvelles avenues thérapeutiques sont nécessaires pour élargir le spectre des thérapies ciblées disponibles pour le mélanome. En utilisant un dépistage CRISPR-KO, nous montrons une interaction létale synthétique entre SEL201, un inhibiteur des kinases MNK1/2, et BRD2, un membre de la famille des protéines BET. La double inhibition des kinases MNK1/2 et des protéines de la famille BET dans les lignées cellulaires de mélanome mutantes BRAF et NRAS a montré une diminution de la viabilité cellulaire et de l'excroissance clonogénique par rapport aux agents seuls. De plus, l'inhibition combinée des protéines de la famille MNK1/2 et BET a légèrement amélioré la survie des souris syngéniques injectées par voie sous-cutanée avec des cellules de mélanome Yummer 1.7. Bien que le mécanisme de ce traitement combiné reste incertain, nous proposons que la combinaison des inhibiteurs de MNK1/2 et BET peut fournir une avenue intéressante pour le traitement des mélanomes résistants aux thérapies et des sous-types difficiles à traiter.

3. ACKNOWLEDGEMENTS

I sincerely acknowledge the tremendous support provided by the Miller-Del Rincon laboratory, especially my supervisor Dr. Sonia Del Rincon, which has provided significant input for the present thesis, and my mentor Dr. Antoine Meant. I also would like to thank my co-supervisor Dr. Wilson Miller Jr., my academic advisor Dr. Volker Blank and committee members Dr. Michael Witcher and Dr. Rene Zahedi for their valuable advice and guidance. Special thanks to the FRQS and the Andy-Lena Chabot CRS Studentship for providing financial support throughout my masters.

4. AUTHOR CONTRIBUTIONS

Figures 1, 2 and 3 of the introduction were all done by myself. The CRISPR-KO screen was performed by the lab of Dr. Michael Tyers as a collaborative effort and analyzed by Dr. Antoine Meant (figure 4). Dose response curves and cell viability assays for *BRAF*-mutant cell lines were performed by Dr. Antoine Meant, while those for *NRAS*-mutant cell lines were done by myself. I performed most of the clonogenic assays with the help of Dr. Meant. All flow cytometry experiments (cell cycle analysis, CFSE and Annexin V-PI), western blots (excluding for BET-KD), senescence, invasion assays, dose response curves for MDMel cell lines, and IHC staining (Yummer 1.7 tumors and MNK1 Breast cancer TMA) were exclusively done by myself. *In vivo* experiments (e.g. tumor monitoring and measurement) were performed by Dr. Antoine Meant with occasional help by myself. Staining of p-eIF4E Breast cancer TMA (Supplemental figure 2B) was done by Samuel Preston, a PhD student in the Miller-Del Rincon lab, but analyzed by myself.

5. RESEARCH OBJECTIVES

Given that single agent MNK inhibitors only display cytostatic effects on tumor cells, these inhibitors were suggested to be used in combination therapy for enhanced efficacy¹. Additionally, currently available therapies for melanoma exhibit limited clinical efficacy². Thus, we aimed to identify genetic vulnerabilities that sensitize tumor cells to MNK kinase inhibition, and provide a pre-clinical rationale for dual therapy. To achieve this global objective, we specifically aimed to:

1. Perform a CRISPR-KO screen in the presence of a MNK kinase inhibitor to identify synthetic lethal genes with MNK1/2 inhibitors.
2. Identify a druggable synthetic lethal target gene from the CRISPR-KO screen and validate the efficacy of its pharmacologic inhibition with MNK inhibitors *in vitro* using melanoma cell lines.
3. Elucidate a mechanism by which the combination treatment inhibits melanoma cell viability.
4. Finally, characterize the efficacy of the drug combination *in vivo* using a melanoma mouse model.

6. LITERATURE REVIEW

6.1. Melanoma: The Deadliest Form of Skin Cancer

Melanoma is a type of skin cancer that arises in pigment-producing cells of the body known as melanocytes. Given its high metastatic potential, melanoma is the deadliest type of skin cancer accounting for about 75% of skin cancer-related deaths³. Currently, the 5-year relative survival in patients diagnosed with metastatic lesions is at 29.8% compared to 99.4% in patients with localized tumors, thereby highlighting the importance of early diagnosis (seer.cancer.gov/statfacts/html/melan.html). Despite a continuous increase in the incidence of melanoma, recent advances in the therapeutic landscape of metastatic melanoma have enabled a steady decrease in mortality⁴.

6.2. Classification of Melanoma Subtypes

Historically, the classification of melanoma was restricted to histopathological features of the primary tumor which comprised cutaneous, acral, mucosal and uveal melanomas⁵. Cutaneous melanoma (CM) arises in non-glabrous skin and is characterized by C>T nucleotide transitions as a result of ultraviolet (UV)-radiation⁶. On the other hand, less commonly observed melanomas include acral melanoma (AM), which arises in non-glabrous skin (palms, soles and nail beds), mucosal melanoma (MM), which develops in mucous membranes lining internal tissues, and uveal melanoma (UM), which emerges in the uveal tract of the eye. Despite providing valuable information in terms of disease pathology, the histopathologic classification provided limited clinical insight⁷. Therefore, a recent classification by The Cancer Genome Atlas in 2015 distinguished four main genomic subtypes of cutaneous melanoma based on the occurrence of driver mutations alone, that is *BRAF*, *NRAS*, *NF1* and triple wild-type (wild-type *BRAF*, *NRAS* and *NF1*)⁸. Cutaneous melanoma is dominated by *BRAF* mutations (45-50%) followed by *NRAS* (30%) and *NF1* (10-15%)⁵. Other frequently observed mutations in cutaneous melanoma include amplification of *KIT* (10%), and loss of the tumor suppressors *TP53* (15-18%) and *CDKN2A* (45%)⁵. Uveal, acral and mucosal melanomas are mostly associated with mutations found in the triple wild-type subgroup (e.g. *KIT* mutations).

6.3. Pathophysiology of Driver Mutations in Cutaneous Melanoma

Driver mutations in melanoma often result in the activation of major signalling pathways including the mitogen-activated protein kinase (MAPK) and phosphoinositide 3-kinase (PI3K)/AKT

pathways⁹. In fact, aberrations in the MAPK pathway are observed in about 90% of melanomas, thereby causing cell cycle progression and inhibition of apoptosis⁹. Most notably, the deregulation of the MAPK pathway can occur following oncogenic activation of BRAF, which results in sustained downstream signalling of MEK/ERK. Such mutations in BRAF mainly occur as single nucleotide substitutions at position 600, of which 80-90% are characterized by a valine-to-glutamic acid substitution (BRAF^{V600E})^{9,10}. Deregulation of the MAPK signalling pathway can also occur as a result of activating mutations in the NRAS GTPase. In 80% of NRAS-mutant melanoma cases, a glutamine residue at position 61 is substituted to arginine, lysine or leucine (NRAS^{Q61R/K/L}) which enhance the GTP-bound form¹¹. In contrast, loss of function mutations in NF1, a Ras GTPase activating protein (GAP), causes depletion of GTP-bound Ras which occurs in 63% of NF1-mutant melanomas¹². In addition to activating the MAPK signalling pathway through phosphorylation of RAF, GTP-bound RAS proteins also activate PI3K. Similarly, dual activation of the MAPK and PI3K/AKT pathways also occurs upon activation of the KIT receptor-tyrosine kinase (RTK). This latter is also a driver mutation in melanoma, whereby it is altered in 22% of triple wild-type tumors and is frequently observed in acral and mucosal melanomas¹³. Specifically, constitutive activation of c-KIT is caused by translocations within exons 11 and 13 of *KIT*, generating c-KIT^{L576P} and c-KIT^{K624E} mutants respectively¹⁴.

6.4. Additional Mutations are Required for the Occurrence of Advanced Stage Disease

While driver mutations initiate melanomagenesis, rarely do these primary oncogenic alterations cause progression to metastatic disease on their own¹⁵. Rather, additional mutations are required for the tumor to acquire invasive properties. Through whole genome sequencing (WGS) of patient samples at different stages of disease, Shain et al. identified a common pattern of sequential and non-mutually exclusive mutations in melanoma that progressively lead to metastatic disease¹⁶. Shortly after the emergence of driver mutations, subsequent gain of function mutations commonly occur in the *TERT* (telomerase reverse transcriptase) promoter followed by biallelic inactivation of *CDKN2A* and loss of function mutations in subunits of the SWI/SNF complex (specifically *ARID2* and *ARID1A*)¹⁶. Mutations in the *TERT* promoter create *de novo* binding sites for ETS transcription factors, thus enhancing *TERT* transcription and subsequent cellular proliferation¹⁷. Moreover, *CDKN2A* encodes for the tumor suppressors p16^{INK4A} and p14^{ARF}. On one hand, p16^{INK4A} negatively regulates the activity of cyclin-dependent kinases 4/6 (CDK4/6), thereby preventing cells from progressing to S phase¹⁸. On the other hand, p14^{ARF} sequesters MDM2 in the nucleolus, thus preventing proteasomal

degradation of p53¹⁹. The SWI/SNF chromatin remodeling complex regulates global gene transcription and is mutated in ~20% of human malignancies²⁰. Mutations in the SWI-SNF complex causes genomic instability and are associated with chromosomal aberrations¹⁶. Shain et al. also observed loss of function of both *PTEN* and *TP53* uniquely in thicker melanocytic lesions, which further indicates the occurrence of these mutations in later disease stages¹⁶. Functionally, PTEN is a dual phosphatase capable of dephosphorylating phospho-peptides and phospho-lipids²¹. Namely, PTEN dephosphorylates phosphatidylinositol-3, 4, 5-triphosphate (PIP3), thereby inhibiting PI3K signalling. P53 is known as the “guardian of the genome” and induces cell cycle arrest and apoptosis upon DNA damage²². Interestingly, one of the most commonly employed mouse models of metastatic melanoma exploit the dual mutations in BRAF and PTEN²³.

Although less investigated, studies have highlighted the pro-tumorigenic role of p38 MAPK in melanoma, where it is sometimes found to be deregulated²⁴⁻²⁶. In response to cellular stresses and cytokines, the MEKK/MKK3-6/p38 pathway is activated, which in turn regulates several cellular processes including transcription, protein synthesis and cytoskeletal organization among others²⁷. Paradoxically, p38 activation in early stages of cancer manifests tumor suppressive effects²⁸, whereas in later stages p38 favours cell survival and invasion²⁹.

6.5. The Current Therapeutic Landscape of Metastatic Melanoma

Over the past decade, several regimens of targeted therapies and immunotherapies have revolutionized the treatment of advanced melanoma². Initially in 2011, Chapman et al. showed the efficacy of a BRAF^{V600E}-specific inhibitor, vemurafenib (PLX4032), in patients with metastatic melanoma³⁰. Specifically, this study was a phase-III randomized clinical trial conducted in 675 patients with metastatic melanoma harboring a BRAF^{V600E} mutation. Results indicated a 48% response rate to vemurafenib, compared to 5% for dacarbazine, a chemotherapeutic agent that was the standard therapy for metastatic melanoma since 1972. Despite several adverse events, vemurafenib displayed an increased overall survival (84%) when compared to dacarbazine (64%) after 6-months. Shortly after, another BRAF inhibitor, dabrafenib, was approved by the FDA for the treatment of malignant melanoma³¹. Whereas the use of BRAF inhibitors as single agents had shown promise in the treatment of advanced melanoma, progression-free survival (PFS) only lasted for 5 months with resistance rapidly developing^{30,31}. Interestingly, mechanisms of resistance to BRAF-targeted therapies include the recovery of MAPK signalling pathway in 70% of BRAF-mutant patients and the activation of the PI3K-PTEN-AKT pathway in 22% of cases³². Moreover, continued vemurafenib treatment of

vemurafenib-resistant melanomas in a preclinical study was shown to further support tumor growth owing to drug dependency³³. Specifically, BRAF-inhibitor resistance patterns included recovery of p-ERK signalling³⁴, *RAS* mutations³², *BRAF* amplification³², *MAP3K8* overexpression³⁵ and *MEK* mutations³⁶ among others. Therefore, given the frequent reactivation of MAPK signalling upon BRAF-inhibitor resistance, dual inhibition of BRAF and MEK was proposed to sustain cytotoxicity of tumor cells and further delay the onset of resistance³⁴. Numerous BRAF- and MEK-inhibition combination therapies were subsequently approved for the treatment of metastatic melanoma, including dabrafenib and trametinib³⁷, vemurafenib and cobimetinib³⁸ and more recently encorafenib and binimetinib³⁹. Although BRAF- and MEK-inhibition therapy exhibited response rates exceeding 60% and a median PFS above 10 months, the occurrence of resistance remained. These resistance mechanisms are similar to those occurring following single-agent BRAF inhibition (reviewed in ⁴⁰) with an increased proportion of resistant tumors acquiring reactivation of MAPK signalling in dual BRAF- and MEK-inhibitor therapy as compared to monotherapy with BRAF-inhibitors⁴¹. Moreover, adverse events occurred in almost all patients treated with such combination therapy⁴². Nevertheless, the superior efficacy of combined BRAF- and MEK-inhibition establishes this treatment regimen as the standard of care targeted therapy for advanced melanoma².

Melanoma displays the highest somatic mutational burden of any cancer subtype⁴³. This increased production of antigens by cancer cells generates an immunogenic tumor microenvironment that favours immune cell infiltration. Thus, melanomas quickly develop mechanisms to suppress the activity of the immune system, namely through manipulation of immune checkpoints. In normal conditions, the binding of programmed cell death protein 1 receptor (PD-1) – present on T-cells – to its ligands (PD-L1/2) – expressed by epithelial, hematopoietic, and immune cells – ensures self-tolerance and suppresses autoimmunity⁴⁴. However, in the context of melanoma, this process is hijacked whereby tumor cells overexpress PD-L1/2, thus inhibiting T-cell mediated cytotoxicity⁴⁵. Another immune checkpoint is the expression of cytotoxic T-lymphocyte-associated protein 4 (CTLA-4) mainly by CD4+ helper T cells⁴⁵. CTLA-4 outcompetes the co-stimulatory receptor CD28 for binding to CD80 and CD86 expressed on antigen-presenting cells (APCs), thus effectively compromising anti-tumor immunity⁴⁴. In recent years, immune checkpoint inhibition through PD-1 and CTLA-4 blockade were proposed to potentiate anti-tumor T-cell response in melanoma³. During the past decade, four immune checkpoint inhibitors have been approved for the treatment of metastatic melanoma including ipilimumab, a monoclonal antibody against CTLA-4, anti-PD1 antibodies nivolumab and pembrolizumab and the anti-PD-L1 antibody atezolizumab³. Current

standard of care immunotherapy in metastatic melanoma remains the combination of nivolumab and ipilimumab, showing an overall survival of 52% compared to 44% and 26% for single agents nivolumab and ipilimumab respectively⁴⁶. Despite exhibiting favorable prognosis, combining checkpoint inhibitors considerably enhances immune-related adverse events (irAEs) relative to checkpoint monotherapy⁴⁷. Specifically, irAEs can affect any organ and include colitis, pneumonitis, and hepatitis among others⁴⁸, all which can result in the patient being taken off immunotherapy and sometimes even result in mortality in extreme cases of unresolved toxicity.

In practice, melanoma patients with severe tumor burden are initially treated with targeted therapy given the more rapid response observed when compared to immunotherapy². However, a recent phase-III clinical trial has shown enhanced progression free survival when using a combination of atezolizumab, vemurafenib and cobimetinib (15.6 months) relative to combined vemurafenib and cobimetinib (10.6 months) in unresectable BRAF^{V600}-mutant advanced melanoma, thus highlighting the potential of combining immunotherapy and targeted therapy⁴⁹.

6.6. Activation of Parallel Signalling Pathways as a Common Resistance Mechanism to MAPK Inhibition in Melanoma

Despite showing improved progression-free survival over the past decade, current standard of care targeted therapies in melanoma are rapidly rendered inefficient due to diverse mechanisms of drug resistance (reviewed in ⁵⁰). In most cases, resistance to BRAF inhibition may occur through reactivation of the MAPK pathway or through MAPK-independent mechanisms⁵⁰. In particular, resistance to BRAF inhibition includes the activation of parallel signalling pathway, most conspicuously by triggering the PI3K/AKT pathway. One way that this is achieved is through loss of the *PTEN* tumor suppressor, which causes AKT signalling upon BRAF-inhibitor treatment and the subsequent suppression of apoptosis⁵¹. Whereas loss of *PTEN* remains an intrinsic resistance mechanism to BRAF inhibition, the PI3K/AKT pathway can also be activated through acquired resistance to BRAF inhibition. For instance, Jiang et al. have shown that melanoma cells with acquired resistance to BRAF-inhibition employ AKT to induce ERK signalling independent of MEK⁵². Consistently, melanoma cells with AKT-dependent ERK phosphorylation circumvent both BRAF and MEK inhibition⁵². While activation of the PI3K/AKT pathway highlights the importance of concurrently inhibiting parallel signalling pathways along with MAPK inhibition, clinical development of a PI3K β -selective inhibitor (SAR260301) was halted due to rapid drug clearance in patients with advanced solid tumors⁵³. Moreover, whereas an AKT inhibitor (GSK2141795B) has been shown to

potentiate the effect of BRAF and MEK inhibitors *in vitro*, its efficiency has yet to be shown in the clinic⁵⁴. Interestingly, inhibition of mTOR downstream of the PI3K/AKT pathway overcomes acquired BRAF- and MEK-inhibitor resistance in melanoma⁵⁵. The combination of vemurafenib and mTOR inhibitor Everolimus in melanoma patients was well tolerated and showed partial responses in a phase I clinical trial⁵⁶. This underlines the potential of targeting downstream effectors of major signalling pathways to overcome or further delay the occurrence of resistance.

6.7. Rationale of Inhibiting the MNK1/2-eIF4E Axis in Melanoma

Another way to circumvent the activation of parallel signalling mechanisms is to target downstream effectors that intersect between major signalling pathways. Most notably, the MNK1/2-eIF4E axis lies at the nexus of the MAPK and the PI3K/AKT pathways, two of the most deregulated pathways in melanoma (figure 1)⁵⁷. Specifically, ERK1/2 and p38 MAPKs phosphorylate and activate (MAPK)-interacting kinases 1 and 2 (MNK1/2), which in turn phosphorylate eukaryotic initiation factor 4E (eIF4E)⁵⁸. Interestingly, phosphorylation of eIF4E has been associated with enhanced translation of a specific subset of mRNAs with oncogenic properties¹. eIF4E recognizes and binds to the 7-methylguanosine cap (m⁷G) at the 5' end of mRNAs, whereby it is joined by other components of the eIF4F complex⁵⁹. These include eIF4A, an RNA helicase that unwinds mRNA secondary structures, and the scaffold protein eIF4G⁶⁰. Moreover, the availability of eIF4E is tightly controlled by the PI3K/AKT/mTOR pathway. Hypophosphorylated 4E-binding proteins (4E-BPs) compete with eIF4G for binding eIF4E, whereas mTOR signalling causes hyperphosphorylation of 4E-BPs, thus releasing eIF4E, which then joins the eIF4F complex and enables cap-dependent mRNA translation⁶¹.

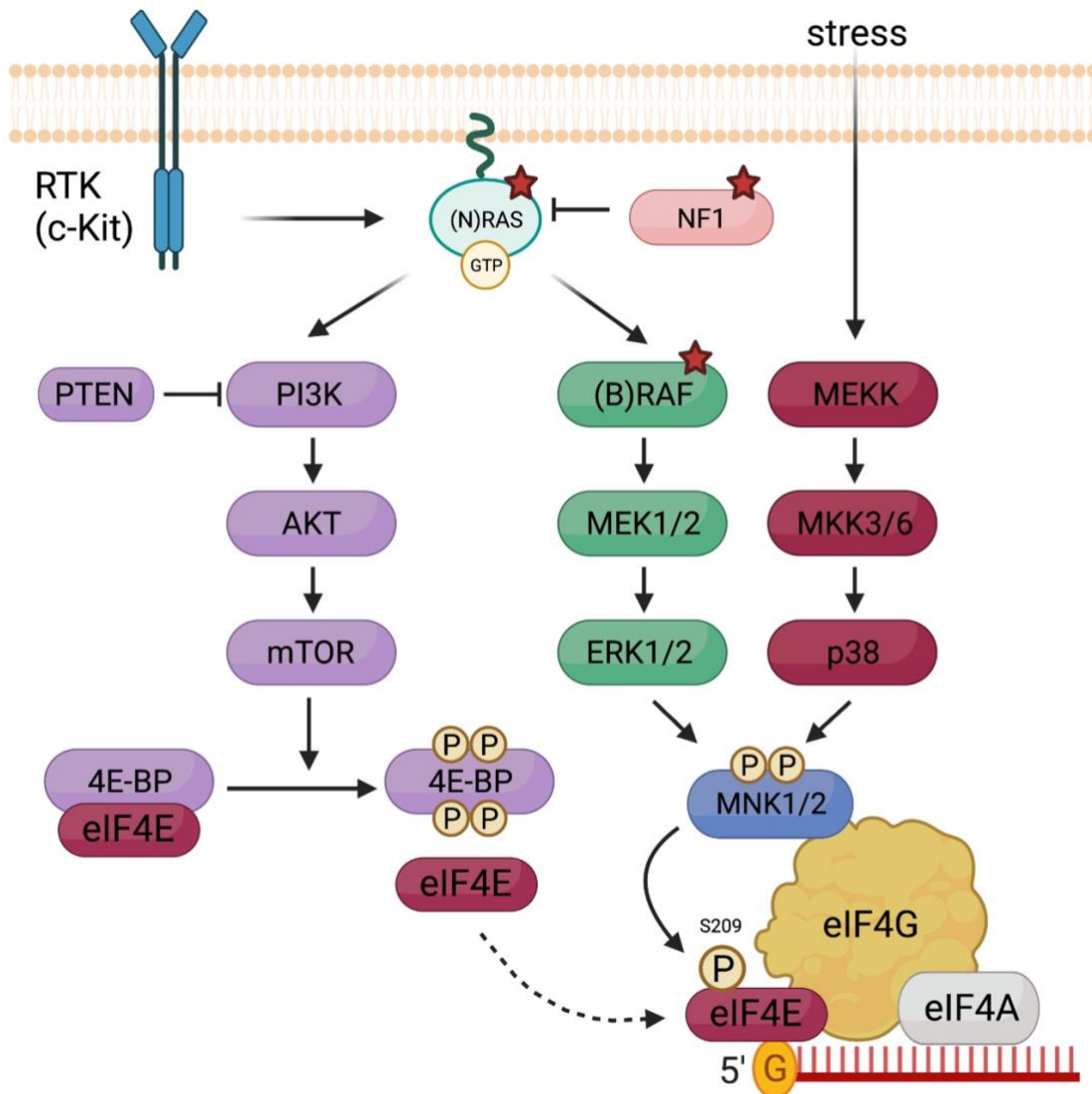


Figure 1 (adapted from⁵⁷). The MNK1/2-eIF4E axis lies at the nexus of major signalling pathways in melanoma. Major driver mutations in cutaneous melanoma are depicted with a red star. See text for details. Figure designed using biorender.com.

Involvement of the MNK1/2-eIF4E axis in cancer has been highlighted in numerous studies (extensively reviewed in ⁶²). Initially, Lazaris-Karatzas et al. (1990) have shown that overexpression of eIF4E in NIH 3T3 or Rat 2 cells causes tumor formation when injected in nude mice, which was the first study to address the role of eIF4E as a proto-oncogene⁶³. Later studies further emphasized the poor prognostic significance of elevated eIF4E levels in diverse cancer subtypes including prostate⁶⁴, breast⁶⁵⁻⁶⁷, lung adenocarcinoma⁶⁸, gallbladder⁶⁹, colon⁷⁰, colorectal adenocarcinoma⁷¹ and

hepatocellular carcinoma⁷². Furthermore, increased eIF4E is associated with advanced disease stage in esophageal cancer⁷³ and squamous cell carcinoma⁷⁴. While eIF4E alone seems to correlate with poor outcomes in cancer, its oncogenic activity is thought to be tightly linked with its phosphorylation by MNK kinases⁷⁵. Consistently, the phosphorylation of eIF4E (p-eIF4E) is an independent prognostic factor in astrocytoma⁷⁶, non-small-cell lung cancer (NSCLC)⁷⁷, and was associated with decreased overall survival in nasopharyngeal carcinoma along with p-MNK1⁷⁸. High MNK1 levels are also correlated with poor prognosis in epithelial ovarian cancer⁷⁹, hepatocellular carcinoma⁸⁰, kidney, liver and prostate cancer⁶², while increased MNK2 levels are associated with poor prognosis in NSCLC⁸¹, low grade glioma and prostate cancer⁶². In sum, these previous studies strongly suggest the inhibition of the MNK1/2-eIF4E axis for the treatment of cancer.

Other studies have also particularly accentuated the relevance of the MNK1/2-eIF4E axis in melanoma, particularly for its involvement in metastasis⁵⁷. For instance, Khosravi et al. showed that high eIF4E expression was correlated with advanced stage melanomas, and poor overall survival across melanoma stages⁷¹. These observations were attributed to the enhanced invasiveness conferred by upregulated eIF4E activity. Similarly, Curtin et al. have shown that malignant melanomas express higher levels of eIF4E or p-eIF4E when compared to benign nevi⁸². Furthermore, elevated levels of eIF4E and p-eIF4E were associated with increased metastatic potential and poor survival⁸². Our group also showed increased MNK1, p-MNK1 and p-eIF4E levels in *KIT*-mutant melanoma relative to *KIT*-wild-type melanomas, whilst inhibition of MNK1/2 activity compromised lung metastasis in a xenograft mouse model¹³. More recently, a study by Huang et al. additionally highlighted the role of MNK kinases in promoting melanoma phenotype switching, a process by which melanocytes dedifferentiate and lose melanocytic antigens, and showed the efficacy of MNK1/2 inhibitors in enhancing response to anti-PD-1 immunotherapy⁸³. Taken together, the MNK1/2-eIF4E axis plays a pivotal role in melanoma and presents an exploitable therapeutic target.

Additionally, disruption of MNK1/2 kinase activity is also expected to exhibit limited side-effects and toxicities *in vivo*⁵⁷. This prediction is further supported by numerous studies in which mice engineered to harbor a genetic knockout in MNK1 and 2 or inactive eIF4E phosphorylation do not manifest embryonic lethality or developmental defects. In fact, Ueda et al. showed that mice with single or double knockout of MNK1 and MNK2 kinases undergo normal development⁵⁸. Similarly, Furic et al. showed that mice harboring a non-phosphorylatable version of eIF4E (eIF4E^{S209A/S209A}) also develop normally⁸⁴. In contrast, double knockout of eIF4E remained embryonic lethal, whereas

mouse engineered with a haploinsufficient eIF4E develop almost identically to their wild-type counterparts⁸⁵.

6.8. MNK1 and MNK2 Kinases: Isoforms and Function

The serine/threonine kinases MNK1 and MNK2 are encoded by two distinct genes, that are *MKNK1* and *MKNK2* respectively (figure 2)⁸⁶⁻⁸⁸. MNK1/2 kinases are activated by ERK1/2 in response to mitogens and p38 kinases following stress signalling⁸⁸. Isoform variants for both proteins have been exclusively reported in humans, whereby alternative splicing of *MKNK1/2* generates a and b isoforms^{86,89}. MNK1a and MNK2a include all exons of their respective genes (referred to as MNK1 and MNK2 in the literature). These full-length isoforms possess a MAPK-binding motif, wherein a single amino acid difference between both motifs (MNK1a – LARRR; MNK2a – LAQRR) confers preferential binding of p38 to MNK1a and ERK1/2 to MNK2a^{88,90}. Subsequent activation of MNK kinases occurs upon phosphorylation of two threonine residues within the T-loop (Thr^{209/214} in MNK1 and Thr^{244/249} in MNK2)⁶². In contrast, MNK1b and MNK2b differ from their a-isoform counterparts particularly at the C-terminus region. Specifically, exon 9 in MNK1b is replaced by 12 novel amino acids, whereas MNK2b is generated by skipping of exon 13a and inclusion of exon 13b, in which cases both alternatively spliced proteins lack a MAPK-binding domain^{89,91}. Nonetheless, MNK1b and MNK2b both manifest the ability to phosphorylate eIF4E independently of MAPK-activation^{89,91,92}. Consistently, basal activity of MNK1b is higher than MNK1a, the latter of which requires MAPK-activation for its ability to phosphorylate eIF4E^{89,93}. An earlier study by Scheper et al. further reported a high basal activity of MNK2a relative to MNK1, while MNK2b displayed very low basal activity⁹¹.

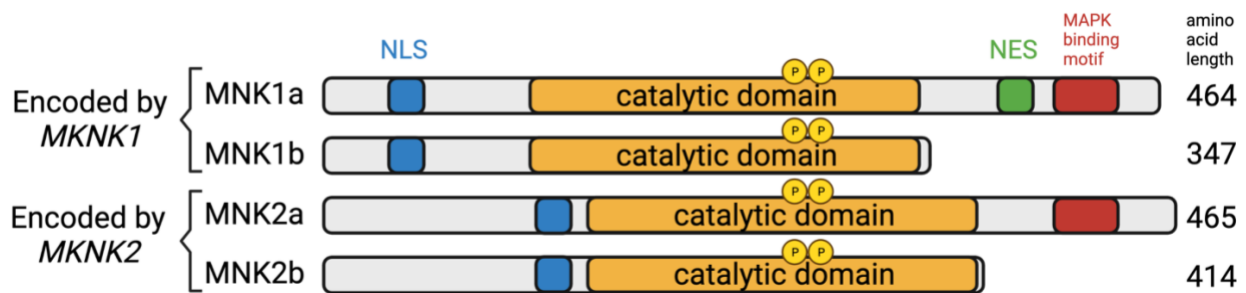


Figure 2 (adapted from ¹ and ⁵⁷). Depiction of human MNK1/2 isoforms. NLS: nuclear localization signal; NES: nuclear export signal. See text for details. Figure designed using biorender.com.

Interestingly, different tumorigenic roles have been established for either MNK isoforms. For instance, Pinto-Diez et al. found a higher expression of both MNK1 splice variants in breast tumors relative to normal tissue, despite only MNK1b correlating with disease outcome⁹². Similarly,

amplification of *SRSF1*, the gene encoding the splicing factor SF2/ASF, favours splicing of *MKNK2*, thus generating increased levels of MNK2b and decreased levels of MNK2a⁹⁴. This in turn enhances phosphorylation of eIF4E in a MAPK-independent manner⁹⁴. Consistently, SF2/ASF was described as an oncoprotein that has increased levels in many cancer subtypes, including colon, thyroid, small intestine, kidney, and lung⁹⁴. Adesso et al. further showed that *SRSF1*-mediated MNK2b expression enhanced gemcitabine resistance in pancreatic ductal adenocarcinoma (PDAC)⁹⁵. Moreover, Maimon et al. show that splicing of the *MKNK2* gene into MNK2a confers tumor-suppressive functions, while its splicing into MNK2b possesses pro-tumorigenic roles⁹⁶. Mechanistically, MNK2a binds to, and phosphorylates p38, which causes its translocation to the nucleus, where p38 triggers stress-induced cell death and inhibits RAS-driven cellular transformation. In contrast, enhanced levels of MNK2b did not associate with p38 activation, while still increasing phosphorylation of eIF4E, thus accounting for its pro-tumorigenic effect. Taken together, these studies highlight the importance of independently studying MNK1 and MNK2 isoforms given their differing effects on tumorigenesis.

6.9. Nuclear and Cytoplasmic Subcellular Localization of MNK1/2 Kinases Suggests Additional Biological Functions

The observed functional differences between a and b isoforms of MNK kinases may be explained in part by their distinct subcellular localization. While all MNK1/2 splice variants contain a nuclear localization signal (NLS) conferring specificity for importin- α , only MNK1a possesses a nuclear export signal (NES) which enables CRM1 (exportin 1)-mediated nuclear export⁹¹. In addition, features in the C-terminus of MNK2a hinder access to the NLS. Consequently, b isoforms are predominantly nuclear, whereas a isoforms are mainly cytoplasmic. Such observations are consistent with the ability of MNK2a to phosphorylate and translocate p38 in the nucleus, a function that MNK2b cannot perform given its compartmentalization in the nucleus. This further raises the question as to whether the subcellular localization of b isoforms can explain their pro-oncogenic functions. No studies have directly investigated the role of MNK kinases in the nucleus, while studies that did address such topic did not necessarily attribute observed functions to specific MNK isoforms. One study by Topisirovic et al. showed that phosphorylation of eIF4E in the nucleus promotes eIF4E-dependent transport of mRNAs including cyclin D1, a function that is likely attributed to MNK1/2 kinases^{1,75}. However, this study did not segregate the role of MNK1/2 a and b isoforms in the regulating the phosphorylation of eIF4E in the nucleus. In sum, further research is necessary to elucidate additional functions of MNK1/2 kinases.

6.10. Currently Available Inhibitors of MNK1/2 Kinases

Given the mounting evidence surrounding the role of MNK kinases in tumor progression, there was increasing interest in identifying and designing MNK inhibitors⁹⁷. This initiative was further motivated by the non-toxic nature of MNK1/2 knockout *in vivo*, suggesting that the use of MNK inhibitors in the clinical setting is a “safer” option for the treatment of various diseases⁵⁸. While early MNK inhibitors such as cercosporamide and CGP57380 showed substantial anti-tumor activity in different cancer subtypes, their effects can be hardly attributable to MNK1/2 inhibition given their numerous off-target effects⁹⁷. Cercosporamide, an anti-fungal compound extracted from the fungus *Cercosporidium benningsii*, showed an IC₅₀ of 0.04 μ M for MNK kinases, but at the same time exhibited a more potent inhibitory effect on other kinases⁹⁸. Similarly, CGP57380, a synthetic compound, is a weak inhibitor of MNK kinases (IC₅₀ of 0.87 μ M for MNK1 and 1.6 μ M for MNK2)⁹⁷. Moreover, CGP57380 inhibits tumorigenic outgrowth at concentrations showing weak repression of p-eIF4E⁹⁸. Therefore, previous studies using early MNK inhibitors need to be interpreted with caution.

More recently, ATP-competitive MNK inhibitors were designed with increased selectivity, namely eFT508 and SEL201. SEL201 has been shown to inhibit both MNK1 and MNK2 at IC₅₀ concentrations of 10.8nM and 5.4nM respectively¹³. On the other hand, eFT508 displays further selectivity for MNK kinases with IC₅₀ concentrations of 2.4nM for MNK1 and 1nM for MNK2⁹⁹. Despite the increased selectivity of recently available MNK inhibitors when compared to their old counterparts, these latter continue to manifest similar or greater inhibitory potential for other kinases. Interestingly, the design of inhibitors with marked specificity for MNK kinases remains possible given an unusual feature in those kinases. In fact, a DFD motif (Asp-Phe-Asp) in MNK1/2 replaces the canonical DFG motif (Asp-Phe-Gly) present in the catalytic domain of other kinases¹⁰⁰. Thus, an auto-inhibited conformation of MNK kinases is expected whereby the phenylalanine residue hinders access to the ATP-binding pocket. As such, proposed novel MNK inhibitors may prevent kinase activity by stabilizing the auto-inhibited state. In contrast to previous MNK inhibitors which acted solely to prevent the binding of ATP, the design of novel inhibitors was proposed to additionally interact with the DFG motif of MNK kinases for increased selectivity¹⁰¹.

While several MNK inhibitors have entered clinical trials in the past, some were withdrawn such as BAY1143269 (NCT02439346) and ETC-206 (NCT03414450) for unclear reasons⁹⁷. Currently, eFT508 remains in clinical trials alone or in combination with paclitaxel, anti-PD1 or anti-PD-L1 therapy (NCT03690141, NCT02937675, NCT03616834, NCT04622007, NCT04261218).

6.11. Translational and Epigenetic Reprogramming in Melanoma Underlie Phenotype Switching

Advanced melanoma displays conspicuous dysregulation in several cellular processes, including metabolism¹⁰², mRNA translation¹⁰³ and epigenetics¹⁰⁴. Collectively, these altered regulatory networks support melanoma phenotype switching, a process by which melanoma cells transition between melanocytic and mesenchymal-like states¹⁰³. Despite the high heterogeneity present within melanoma cell populations, two prevalent transcriptional programmes were identified by gene expression analyses and distinguished the ‘proliferative’ (differentiated, epithelial-like) from the ‘invasive’ (dedifferentiated, mesenchymal-like) phenotype¹⁰⁵. While the ‘proliferative’ state displays high expression of the microphthalmia-associated transcription factor (MITF) and low levels of the receptor tyrosine kinase AXL (MITF^{high} | AXL^{low}), the ‘invasive’ phenotype shows the opposite (MITF^{low} | AXL^{high})¹⁰⁶. Beyond the expression of hallmark genes MITF and AXL, each cell state is also characterized by the expression of additional markers¹⁰⁵. For instance, the ‘proliferative’ phenotype shows marked expression of genes regulating the transcription of MITF (i.e. *SOX10*, *PAX3*, *CREB1*) and downstream targets of MITF (i.e. *MLANA*, *PMEL*, *ZEB2*)¹⁰³. In contrast, the ‘invasive’ phenotype exhibits more complex gene expression patterns (for an extensive list of genes, refer to ¹⁰³). Transition between such transcriptional programs has been shown to occur in response to changes in the epigenome¹⁰⁷. Manning et al. showed that upregulation of genes regulated by EZH2, a histone methyltransferase within the Polycomb repressive complex 2 (PRC2), characterizes motile cells and remains necessary for melanoma invasion¹⁰⁸. Similarly, Ferreti et al. show increased expression of BMI1, a component of the Polycomb repressive complex 1 (PRC1), in metastatic melanoma and induces a gene signature reminiscent of the ‘invasive’ phenotype¹⁰⁹. While epigenetic and transcriptional reprogramming effectively modulate the transition from a melanocytic- to a mesenchymal-like state, such processes are likely not the sole drivers of melanoma cellular plasticity¹¹⁰. Rather, recent studies additionally suggest a pivotal role for mRNA translation^{83,111}. For instance, nutrient deprivation activates the integrative stress response (ISR) through phosphorylation of eukaryotic translation initiation factor 2 α (p-eIF2 α), which in turn decreases global translation and upregulates the translation of ISR-related genes¹¹². These latter include ATF4, a transcription factor that causes a MITF^{low} | AXL^{high} phenotype only in the occurrence of translational reprogramming¹¹¹. Furthermore, enhanced signalling through the MNK1/2-eIF4E axis results in increased translation of oncogenes conferring invasive and metastatic properties to tumor cells, including *MMP3*, *MMP9* and *SNAI1*^{113,114}. Huang et al. also showed that pharmacologic inhibition of the MNK1/2-eIF4E axis

upregulates MITF expression and decreases translation of *NGFR*, a receptor associated with a potentially drug-resistant version of the ‘invasive’ phenotype termed the neural crest stem cell (NCSC)-like state⁸³. Most importantly, inhibition of p-eIF4E abrogated melanoma phenotype switching by blocking melanoma cell invasiveness⁸³. Taken together, both epigenetics and mRNA translation play important roles in melanoma phenotype switching. Consistently, dual targeting of epigenetic and translational mechanisms may provide an important avenue for the design of novel therapies to inhibit the invasive nature of this disease.

6.12. Lysine Acetylation and Bromodomain Proteins in Cancer

Deregulation of cellular epigenetics may occur through numerous processes including post-translational modification of DNA and histones, chromatin remodeling complexes, histone modifiers and readers, microRNAs among others¹¹⁵. In particular, lysine acetylation is known to be deregulated in numerous solid tumours including melanoma^{116,117}. The addition of an acetyl group to the terminal amine of a lysine residue (more specifically, the epsilon nitrogen atom – ϵ -N-acetylation) is catalyzed by lysine acetyltransferases (KATs), whereas its removal is achieved through the activity of lysine deacetylases (KDACs)¹¹⁸. Such post-translational modification can occur on both DNA-binding proteins and histones¹¹⁹. Histone acetylation neutralizes the net positive charge of lysine, which in turn relaxes histone-DNA interactions and ultimately represents a hallmark of open chromatin¹²⁰. Bromodomain-containing proteins are the only ‘readers’ of ϵ -N-acetylated lysine on histones¹²¹. In humans, 46 different proteins contain a total of 61 bromodomains that have roles in chromatin modification and transcription activation¹²¹. While several roles have been attributed to bromodomain-containing proteins, their main function resides in the control of gene expression, leading either to active or repressed transcription¹¹⁹. Most importantly, bromodomain-containing proteins display aberrant expression and mutations in a wide-array of malignancies, thus representing valuable therapeutic targets¹²².

6.13. Structure and Function of BET-Family Proteins

Among this class of epigenetic readers features the bromo- and extra-terminal domain (BET) family proteins that include BRD2, BRD3, BRD4 and BRDT (Bromodomain testis-specific protein)¹²³. Whereas BRDT is solely expressed in germ cells, BRD2/3/4 are ubiquitously expressed¹²⁴. It is important to note, however, that ectopic expression of BRDT has been shown in subtypes of lung cancer, while not being detectable in melanoma¹²⁵. Structurally, BET family proteins share two

bromodomains (BD1 and BD2) at the N-terminus and an extra-terminal domain (ET) at the C-terminus, whereas only BRD4 and BRDT possess a carboxy-terminal domain (CTD – figure 3)¹¹⁹. Additional features of BET proteins also include two casein kinase II (CK2) phosphorylation motifs (NPS and CPS) and a basic residue-enriched interaction domain (BID)¹²⁶. In general, members of the BET family of proteins share similar genomic localization patterns, which partly explains their observed overlapping functions¹²⁷. However, BET-family proteins also display unique functions¹¹⁹.

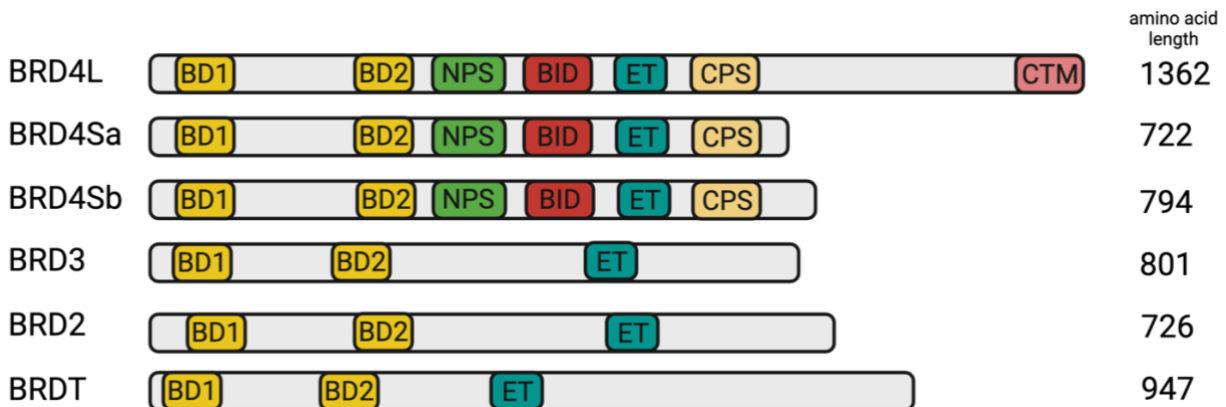


Figure 3 (adapted from ¹²⁸). Functional domain of BET-family proteins. BD1/2: bromodomains 1 and 2; NPS: N-terminal phosphorylation site; BID: basic residue-enriched interaction domain; ET: extra-terminal motif; CPS: C-terminal phosphorylation site; CTM: C-terminal motif. See text for details. Figure designed using biorender.com.

6.13.1. BRD4

BRD4 remains the best studied BET-family protein and has been shown to perform diverse functions ranging from transcriptional regulation to DNA damage repair¹²⁹. BRD4 directly links histone acetylation with gene transcription¹³⁰. The main mechanism by which BRD4 regulates transcription initiation and elongation remains through its association with the mediator complex and PTEFb¹²⁹. Specifically, chromatin acetylation enables the recruitment of BRD4, which in turn recruits the mediator complex to active enhancer regions and enable the formation of the pre-initiation complex (PIC) for transcription initiation¹³¹. Moreover, through its CTD-mediated interaction with positive transcription elongation factor b (PTEFb), BRD4 facilitates transcriptional elongation and mRNA processing¹³². In particular, BRD4 recruits PTEFb to promoter regions, wherein the kinase subunit of PTEFb – cyclin T-CDK9 – phosphorylates DSIF, NELF and the CTD of RNA PolII at serine 2, thus releasing paused RNA polII and enabling mRNA transcription¹³³. Such mechanisms inevitably rely on the ability of BRD4 to bind chromatin. Interestingly, Wu et al. show that CK2-

mediated phosphorylation of BRD4 is required for its acetyl-binding properties¹²⁶. The authors demonstrate that phosphorylation of BRD4 unmasks its bromodomain (BD2) and allows its interaction with acetylated chromatin and p53, thus coregulating p21 transcription. Several other roles have also been attributed to BRD4 including its ability to maintain chromatin acetylation status¹³⁴.

Alternative mRNA splicing of BRD4 yields a longer isoform that include the CTD – termed BRD4L – and two shorter isoforms devoid of a CTD – known as BRD4Sa and BRD4Sb¹³⁵. While little is known about the functional difference between these isoforms, it has been suggested that the longer isoform (BRD4L) exhibits tumor suppressive roles in breast cancer, while the shorter isoform (BRD4S) is oncogenic¹³⁵. Further studies are required to establish whether the different isoforms of BRD4 possess significant implications in melanoma.

6.13.2. BRD2

While BRD4 remains associated with chromatin throughout the cell cycle¹¹⁹, BRD2 (previously referred to as RING3) only localizes to the nucleus in actively cycling cells¹³⁶. Such observations may in part explain the role of BRD2 in cell cycle regulation. BRD2 recruits TATA-binding protein (TBP) to E2F1 transcriptional complexes, which in turn enhances the transcription of genes containing an E2F-binding site¹³⁷. For instance, the specific association of BRD2 with acetylated lysine 12 on histone H4 via its two bromodomains enhances the promoter activity of cyclin D1, cyclin E and cyclin A in a Ras-dependent fashion^{138,139}. Another study by Sinha et al. shows that overexpression of BRD2 upregulates *CCNA2* (cyclin A2) transcription, which induces cell cycle progression¹⁴⁰. Taken together, these studies suggest a crucial role for BRD2 in cell cycle regulation.

BRD2 has also been shown to associate with chromatin insulator CCCTC-binding factor (CTCF)¹⁴¹. Hsu et al. showed that CTCF recruits and associates with BRD2 genome-wide¹⁴¹. Most importantly, loss of BRD2 was also shown to increase the contact frequency between BRD2-insulated regions, thus suggesting a role for BRD2 in modulating chromatin architecture.

Cheung et al. (2017) showed that BRD2 regulates *α*s-regulatory enhancer assembly thus activating transcription¹⁴². BRD2-BD2 binds to Stat3 only when this latter is acetylated at lysine-87, thus facilitating association of Stat3 with Th17 transcription factors including Irf4/Batf, while also increasing the recruitment of RNA polIII¹⁴². Cheung et al. suggested that BRD2 mainly functions as a chromatin organizer, thereby facilitating the assembly of enhancer regulatory elements, while BRD4 regulates transcription elongation by modulating RNA PolIII phosphorylation¹⁴².

6.13.3. BRD3

Despite considerable functional overlap between BET proteins, several unique functions have been uncovered for BRD4 and BRD2. However, few studies have characterized exclusive roles of BRD3. One such study by Lamonica et al. reported that BRD3 associates with GATA1, a pivotal hematopoietic transcription factor, in an acetylation-dependent manner to promote the transcription of erythroid genes¹⁴³.

6.14. The Role of BET-Family Proteins in Melanoma and Other Cancers

In the context of cancer, BET-family proteins were shown to display pro-tumorigenic functions and were suggested as potential therapeutic targets¹⁴⁴. Most strikingly, BRD4 and BRD3 have been shown to drive NUT midline carcinoma (NMC) through genetic fusion with the NUT protein¹⁴⁵. In particular, gene rearrangement on chromosomes 15 and 19 generates the BRD4-NUT fusion oncogene which causes extensive epigenetic reprogramming and poor cellular differentiation¹⁴⁶. The proposed mechanism of BRD4-NUT driven NMC remains through hyperacetylation and activation of oncogenic target genes by recruitment of p300, a histone acetyl transferase (HAT)¹⁴⁷. While BRD-NUT fusion represents a direct mechanism for BET protein-induced carcinogenesis, overexpression of BET proteins alone has been observed in breast cancer, melanoma, NSCLC, glioblastoma, HCC and MPNST^{119,148,149}. Specifically, in the context of melanoma, Segura et al. showed higher BRD2 and BRD4 mRNA expression in tumors relative to nevi¹⁵⁰. Furthermore, the authors specifically underline the role of BRD4 in sustaining melanoma progression, wherein knockdown of BRD4 alone was sufficient to recapitulate pharmacological effect of BET inhibition¹⁵⁰. Finally, BET inhibition caused melanoma cell cycle arrest through downregulation of SKP2 and c-myc and the associated upregulation of p21 and p27¹⁵⁰. Similarly, Gallagher et al. showed that BET inhibition in melanoma compromised NFkB activation and induced programmed cell death¹⁵¹. Moreover, BRD2 was the main BET protein controlling of NFkB activity in melanoma¹⁵¹. Signalling through NFkB decreases the expression of a master regulator of pigmentation MITF (microphthalmia-associated transcription factor) and promotes drug resistance to BRAF and MEK inhibitors, characteristics that are reminiscent of the invasive phenotype¹⁵². As current standard of care BRAF and MEK inhibition imminently develop resistance, Tiago et al. recently highlighted the potential of intermittent BET inhibition to delay the onset of BRAFi and MEKi-driven resistance¹⁵³. The authors showed that BET inhibitor treatment prevented RTK upregulation which usually occurs following dual BRAFi and

MEKi treatment¹⁵³. Taken together, previous studies clearly attribute pro-tumorigenic roles for BET-family proteins in melanoma and other cancer subtypes.

6.15. Inhibiting BET-family of Proteins in Cancer

The design of novel BET inhibitors began over a decade ago amid mounting evidence supporting pro-tumorigenic functions of BET-family proteins¹⁵⁴. Small molecule inhibitors such as JQ1, one of the earliest BET inhibitors, competitively bind to the acetyl-lysine binding pockets of bromodomains, thus effectively displacing BET-family proteins from chromatin¹⁵⁵. While JQ1 displayed anti-tumor effects in NMC-derived cell lines and in mouse xenograft models¹⁵⁵, its low pharmacokinetic activity and oral availability impinged its clinical success¹⁵⁴. In contrast, a JQ1 analogue, termed OTX-015, manifested improved oral bioavailability and exhibited preclinical activity in hematological malignancies and some solid tumors¹⁵⁶. Similarly, the next generation BET inhibitor PLX51107 was shown to overcome immunotherapy resistance in melanoma and displayed preclinical activity in AML^{157,158}. Most importantly, many of these BET inhibitors have shown preclinical efficacy in melanoma mainly when combined with other drugs^{153,157,159-163}. Consistently, the use of BET inhibitors alone has shown limited clinical efficacy¹⁶⁴.

While JQ1, OTX-015 and PLX51107 are pan-BET inhibitors targeting all BET-family proteins, recent advances in the design of selective BETi aimed to target either bromodomain (BD1 or BD2) which is believed to limit side-effects and toxicities¹⁵⁴. Such bromodomain-selective inhibitors include ABBV-744, GSK778 (iBET-BD1) and GSK046 (iBET-BD2)¹⁶⁵. Other efforts were geared towards designing BET protein degraders (PROTACs), which effectively cause E3-ubiquitin ligase mediated proteasomal degradation of BET-family proteins¹⁶⁶.

6.16. Crosstalk Between the MNK1/2-EIF4E Axis and BET-family Proteins

Various potential molecular interactions involving the BET-family proteins and the MNK1/2-eIF4E axis have been reported.

Gao et al. have shown suppression of NSCLC growth upon treatment with BET inhibitors JQ1 and I-BET151 or by BRD4 siRNA knockdown, which was also coupled with downregulation of eIF4E mRNA and protein levels¹⁶⁷. The mechanism by which JQ1 inhibited eIF4E promoter activity was through abrogation of BRD4 binding to the eIF4E promoter as assessed by chromatin immunoprecipitation (ChIP). Moreover, transcriptional regulation of eIF4E by JQ1 was also

recapitulated in xenograft nude mouse model. The authors suggested targeting eIF4E along with BET-family proteins as a novel therapeutic strategy.

Pham et al. aimed to investigate whether BET-inhibitor resistance can occur through activation of the translational machinery mediated by eIF4E¹⁶⁸. Initially, the authors showed that BET inhibition by JQ1 or the use of BET PROTACs increases MNK1-dependent phosphorylation of eIF4E in thyroid and pancreatic cancer grown in 3D collagen, a phenomenon that was dependent on p38 signaling and not MEK/ERK signaling. Most importantly, use of CGP57380 or siMNK1/2 potentiated the effect of JQ1 in decreasing tumor cell proliferation. Finally, CGP57380 and JQ1 co-treatment effectively decreased tumor size in syngeneic mice injected with thyroid cancer cells. The authors further suggested combining MNKi with BETi to treat solid tumors.

Bao et al. (2017) aimed to study the physiological function of BRD4 in inflammatory and immune responses. The authors initially generated a myeloid lineage-specific *BRD4* conditional-knockout mice and found that they were resistant to lipopolysaccharide (LPS)-induced septic shock and exhibited less lung inflammation and injury. BRD4-KO mice were more susceptible to bacterial infection which further supported the idea of BRD4 being important in the innate immune response. Furthermore, the authors showed that bone marrow-derived macrophages (BMDMs) from BRD4 KO mice display upregulated levels of *MKNK2*. Upon performing polysome profiling, levels of the *IκBα* gene (*Nfκbia*) were increased upon BRD4-KO and LPS stimulation. This increased IκBα synthesis was inversely correlated with the levels of nuclear RelA and increased IκBα levels reduced the ability of NFκB to bind to promoters of inflammatory genes as assessed by ChIP. The authors suggested that BRD4 may be regulating the expression of *MKNK2* either through posttranscriptional mechanisms (i.e. noncoding RNAs) or by recruiting a repressor of *MKNK2*.

Wan et al. also highlighted the ability of BRDT to regulate 4EBP1 levels in renal cell carcinoma (RCC)¹⁶⁹. Treatment with PLX51107 or BRDT knockdown compromised RCC proliferation while also decreasing 4EBP1 protein levels. While the authors showed direct interaction between BRDT and 4EBP1 by co-immunoprecipitation, whether acetylation of 4EBP1 is required for this interaction remains elusive.

Taken together, these studies suggest crosstalk between the MNK1/2-eIF4E axis and BET-family proteins. Such findings hint for a novel therapeutic strategy in cancer, whereby the MNK1/2-eIF4E axis and BET-family proteins are dually targeted.

7. METHODS

7.1. Cell lines and Reagents

A375, BLM, SK-MEL-28 and WM164 were cultured in Dulbecco's modified Eagle's medium (DMEM), while MM057 and MM164 were cultured in Ham's F10 medium. Both media were supplemented with 10% fetal bovine serum (FBS) and 1% penicillin/streptomycin antibiotics. Yummer 1.7 cells were cultured in DMEM/F12 supplemented with 10% FBS, 1% penicillin/streptomycin and 1X non-essential amino acids. MDMel WT and KI cell lines were cultured in advanced DMEM supplemented with 5% FBS, 1% penicillin/streptomycin and 1X glutamax. Cultured cell lines were kept in a 37°C humidified incubator maintained at 5% CO₂. SEL201, eFT508, OTX-015 and PLX51107 were dissolved in dimethyl sulfoxide (DMSO) to stock concentrations of 10mM and preserved in -80°C.

7.2. CRISPR-KO Screen

Methods of the CRISPR-KO screen were thoroughly described in¹⁷⁰. Briefly, an extended knockout library (EKO) of 278,754 sgRNA was used to transduce NALM-6 cells harboring a doxycycline-inducible Cas9. The EKO library targeted 19,084 RefSeq genes, 20,852 alternatively spliced exons and 3,872 hypothetical genes with 10 sgRNAs per gene. Transduced Cas9-NALM6 cells were selected with blasticidin for 6 days, followed by doxycycline induction for 7 days. Cells were then treated with 2.5uM of SEL201 or DMSO for 15 days after which sgRNAs were amplified and sequenced using Illumina HiSeq 2000.

7.3. Viral Transduction of A375

A375 cells were transduced using lentivirus with either a non-target shRNA (NT), shBRD2, shBRD3 or shBRD4. Two sequences were used for each shRNA except NT. Selection was performed using 2ug/mL of puromycin. Dose response curves and immunoblots experiments were only seeded after successful selection of transduced cells as determined by complete cell death of non-transduced cells.

7.4. Immunoblotting

Cells were seeded in 10cm dishes at appropriate sub-confluent densities (A375: 100,000; BLM: 150,000; SK-MEL-28: 200,000; WM164: 200,000) in 10mL of medium. For each time point, media

was aspirated, and cells were treated with 1X drug in 10mL of medium. At experimental endpoint, media was decanted, washed with 5mL of 1XPBS, and dishes were placed on ice. Cells were then lysed by adding 400uL of lysis buffer (supplemented with B-glycerophosphate, NaF, DTT and PMSF) per dish and sonicated at 20% amplitude for 3 seconds. Cells were then centrifuged at max speed at 4°C. Bradford assay was used to determine protein concentration and equalize concentrations across samples. Protein separation was performed by SDS-PAGE followed by transfer on PVDF or nitrocellulose membranes. Non-specific sites were blocked using 5% non-fat milk diluted in TBST for 1 hour. Following 16-hour primary antibody incubation (1:500-1:1000 or 1:5000 for loading controls), membranes were then washed 3X in TBST for 5 minutes each. Similar TBST washes were also performed after 1-hour secondary antibody incubation (1:3000 or 1:5000 for loading controls). Finally, proteins were revealed by enhanced chemiluminescence.

7.5. Dose Response Curves

Cells were seeded at appropriate densities depending on cell growth rate in 96-well plates, in triplicates, and in 100uL of medium/well. Specifically, we seeded 500 cells/well for each of A375, BLM, SK-MEL-28, WM164 and MM165 (fast growing), and 3000 cells/well for MM57 (slow growing). The next day, cells were treated by adding 100uL per well of 2X drug concentration (ranging from 0-100uM) diluted in medium. Three days later, media was decanted, and cells were washed with 1XPBS. Cells were then fixed with 4% paraformaldehyde (PFA) for 15 minutes and washed again with 1XPBS. Staining was then performed using 0.1% crystal violet diluted in 10% ethanol for 30 minutes. Following incubation, plates were washed in tap water and allowed to dry overnight. Finally, quantification was performed by reading the absorbance of crystal violet (590nm) after dilution in 10% acetic acid.

7.6. Cell Viability Assays

Performed similarly to dose response curve experiments, except DMSO concentration was maintained at 0.25% per well, and treatment duration was extended to four days. Concentrations used account for the IC50 of each drug for each cell line.

7.7. Colony Formation Assay

Similar cell densities were seeded as in dose response curve experiments (except 1000 cells/well for MM57) in 6-well plates, in triplicates, and in 1000uL of medium/well. The next day, cells were treated by adding 1000uL/well of 2X drug concentration diluted in medium. DMSO concentration

was maintained at 0.25% per well. Eleven days later, media was aspirated or decanted, and cells were stained with 0.5% crystal violet diluted in 70% ethanol for 30 minutes. Plates were then washed in tap water and allowed to dry overnight. Finally, plates were scanned, and quantification was performed by reading the absorbance of crystal violet (590nm) after dilution in 10% acetic acid.

7.8. Cell Cycle Analysis

A375 cells were seeded in 6-well plates at a density of 7500 cells/well in 1mL of medium. The following day, cells were treated with 1mL of 2X drug concentration or regular medium depending on treatment timepoint. DMSO concentration was maintained at 0.25% per well. At experimental endpoint, media was saved in 5mL round-bottom tubes and cells were trypsinized (1X Trypsin-EDTA). Cells were then washed with ice cold 1XPBS and fixed in ice cold 70% ethanol while vortexing and incubated for 30 minutes at 4°C. Following fixation, cells were washed twice with ice cold 1XPBS and stained with 50ug/1,000,000cells of propidium iodide (PI) and 100ug/mL RNase (diluted in 1XPBS) for 20 minutes in the dark. At least 20,000 events were acquired by flow cytometry (FACS CANTOII) at the lowest flow rate. Centrifugation was maintained at 300g for 5 minutes. Analysis was performed using ModFit software.

7.9. Annexin V-PI

Experiment was performed as described for cell cycle analysis. However, at experimental endpoint, A375 cells were stained using AP647-AnnexinV (1:1000) and PI (1uL/tube) diluted in 1X binding buffer. Cells were incubated for 15 minutes at room temperature in the dark. At least 50,000 events were recorded by flow cytometry (FACS CANTOII). Analysis was performed using FlowJo software.

7.10. CFSE Proliferation Assay

A375 cells were incubated in CFSE at a final concentration of 1nM diluted in PBS supplemented with 0.1% FBS for 10 minutes in a 37°C water bath. Thereafter, cells were washed 3 times with media and centrifuged at 290g. A375 cells were then seeded in 6-well plates at a density of 7500 cells/well in a total volume of 1mL of media. The following day, cells were treated with DMSO, SEL201 (2.5uM), OTX-015 (50nM) or the combination of both drugs for a final volume of 2mL. 96 hours post-treatment, cells were trypsinized and washed once with PBS after which FITC mean fluorescence intensity (MFI) was quantified by flow cytometry (FACS CANTOII – maximum events recorded).

7.11. Boyden Chamber Invasion Assay

Equal number of cells were seeded per condition in 10cm dishes. Prior to seeding the experiment, cells were serum-starved overnight. 12-well Boyden chamber inserts were coated with 300uL of 100uM/mL Matrigel diluted in coating buffer (0.01M Tris pH 8, 0.7% NaCl, ddH₂O as solvent) and allowed to incubate for 3 hours in a humidified incubator (37°C and 5% CO₂). Following matrigel polymerization, excess Matrigel solution was discarded. 30,000 serum-starved cells were seeded within inserts (upper chamber) in 1mL, and drugs diluted in serum-containing media were added in the well (lower chamber) in 1.5mL. The experiment was seeded in triplicate (i.e. 3 inserts per condition). Stock drug concentrations were adjusted to achieve a DMSO concentration of 0.25% per well. Cells were allowed to invade overnight, after which inserts were washed 3x in 1X PBS and cells were fixed in 5% glutaraldehyde for 30 minutes. Inserts were then washed again 3x in 1X PBS and stained with 0.5% crystal violet in 70% EtOH for 30 minutes. After a final 1X PBS wash, inserts were allowed to dry overnight. 3 random images were captured per insert using a brightfield microscope at 10X magnification. Analysis was performed by manual counting of cells per image using ImageJ software.

7.12. Senescence Assay

100 A375 cells were seeded per well in a 12-well plate in 500uL. The following day cells were treated with 2X drug concentration in 500uL while maintaining DMSO concentration at 0.25% per well. 7 days later, senescence staining was performed using the Senescence β -Galactosidase Staining Kit #9860 (Cell Signalling Technology). Briefly, media was aspirated, and cells were fixed using the provided fixative solution. Cells were then washed twice with 1X PBS and stained with 1mL of 1X β -Galactosidase Staining Solution (provided by manufacturer). Plates were then sealed in parafilm and incubated overnight in a 37°C dry incubator in the absence of CO₂. Following incubation period, 3 random images were captured per well using a brightfield microscope. Analysis was performed by manual counting of β -Gal(+) and (-) cells per image using ImageJ software. Staining solution was replaced by 70% glycerol and plates were kept at 4°C for long term storage.

7.13. *In Vivo* Mouse Study

500,000 Yumner 1.7 cells were subcutaneously injected in C57BL/6J mice. Once tumors were palpable, oral gavage treatment was initiated every weekday with 75mg/kg of SEL201 and/or 12.5-25mg/kg of OTX-015. SEL201 was diluted in DMSO, NMP and 40% captisol, while OTX-015 was

diluted in DMSO, vegetable oil and sterile water. Vehicle treatment included both SEL201 and OTX-015 drug solvents devoid of the drugs. Drug treatment conditions included the vehicle solution of its counterpart, that is mice treated with SEL201 also received the solvent of OTX-015 and vice-versa. Tumor sizes were measured using a caliper every 2 days and mice were weighed every day. Experimental endpoint was set at 2000mm³ tumor size, upon which tumor were harvested and formalin-fixed/paraffin embedded for immunohistochemistry.

7.14. Immunohistochemistry Staining MNK1

MNK1 IHC staining was performed on a breast cancer TMA of 150 cores (BR1505e – US Biomax Inc.). TMA slide was deparaffinized and hydrated by 3x 5-minute incubation in Xylene, 2x 5-minute incubation in 100% ethanol, 1x 5-minute incubation in 95% ethanol and 1x 5-minute incubation in 70% ethanol. The slide was then placed in running tap water for 5 minutes and rinsed twice with ddH₂O. Heat-induced epitope retrieval was performed using a pressure cooker in which slides were placed in a solution of 1X TRIS/EDTA buffer pH9. After 15 minutes at maximum pressure, the pressure cooker was allowed to depressurize, and slide was cooled down. TMA slide was rinsed twice in ddH₂O and PAP pen was used to delineate TMA cores. Slide was then rinsed 2x using wash buffer for 5 minutes each and endogenous peroxidase was quenched using 4.5% hydrogen peroxide and 24mM NaOH for 15 minutes. After 3x washes in wash buffer for 5 minutes each, non-specific sites were blocked using blocking buffer (1:10 donkey serum) for 1 hour. Slide was then rinsed 2x with wash buffer and incubated with 1:50 MNK1 (Cell Signalling Technology, C4C1) for 16 hours at 4°C. After 3x washes in wash buffer for 5 minutes each, 2 drops of HRP conjugate was applied and incubated for 1 hour. Slides were then rinsed again 4x in wash buffer after which the slide was incubated in magenta red solution for 10 minutes. Excess magenta red was removed using sulfuric acid for 45 seconds. Finally, TMA slide was rinsed in wash buffer and ddH₂O prior to counterstaining with hematoxylin. Slide was then dehydrated by 2-minute incubation in 95% ethanol, 2x 60s incubation in 100% ethanol and 3x 30s incubation in Xylene. Slide was mounted using permount and scanned at high resolution. Analysis was performed using QuPath software by single cells detection and by quantifying magenta red intensity by histoscore.

7.15. Immunohistochemistry Staining p-eIF4E

Yummer 1.7 tumor sections and BR1505e TMA were stained with p-eIF4E by IHC similar to MNK1 with a few differences. For p-eIF4E staining, blocking was performed in two steps. Blocking

buffer 1 (1:10 donkey serum) was incubated for 30 minutes followed by blocking buffer II (1:100 anti-mouse antibody diluted in Fc block) incubation for 30 minutes. Primary antibody (p-eIF4E, ab76256) was kept at 1:50 dilution and incubated for 30 minutes at 37°C in a humid chamber. Magenta red incubation only lasted for 2 minutes. Analysis was performed using QuPath software. For Yummer 1.7 tumor sections, mean magenta red intensity per tumor was determined. For p-eIF4E-stained BR1505e TMA, single cells were detected, and magenta red intensity was quantified by histoscore.

7.16. Immunohistochemistry Staining Ki67

Yummer 1.7 tumor sections were stained by Ki67 using a protocol similar to MNK1 staining, with a few differences. A 1X citrate buffer pH6 replaced the 1X TRIS/EDTA buffer pH9. Primary antibody was at 1:1000 dilution and incubated for 30 minutes at 37°C in a humid chamber. Chromogen incubation was achieved by 20-minute AEC incubation at room temperature. Slides were mounted using immumount. Analysis was performed using QuPath software by quantifying the proportion of Ki67+ cells.

7.17. Statistical Analyses

All statistical analyses were performed using GraphPad Prism 9 Software. Specific tests used are indicated in figure descriptions. Error bars represent standard deviations.

8. RESEARCH FINDINGS

8.1. A SEL201-CRISPR-KO Screen Suggests Synthetic Lethality Between BRD2 and MNK1/2 Kinases

With the aim of identifying targets that potentiate the cytostatic effect of MNK1/2 inhibition, we collaborated with the laboratory of Dr. Michael Tyers (IRIC) to perform a CRISPR-KO screen in a pre-B-cell lymphoma line – NALM6 – with the addition of a recently available MNK1/2 inhibitor termed SEL201. The laboratory of Dr. Tyers possesses significant expertise in the field of synthetic lethality and have efficiently optimized their CRISPR-KO screen method¹⁷⁰. Specifically, the NALM-6 cell line was chosen for exhibiting rapid doubling time (24 hours), for its growth in suspension (easily manageable in culture) and for exhibiting high transduction efficacy. Initially, NALM-6 cells engineered to express a doxycycline-inducible Cas9 were transduced with an extended-knockout (EKO) sgRNA library targeting a total of 19,084 RefSeq genes with 10 sgRNA per gene (details of the library described in ¹⁷⁰). The library transduction was performed while ensuring a low multiplicity of infection (MOI), with each cell containing at most 1 sgRNA per cell (figure 4A). Following selection for lentiviral integration with blasticidin and Cas9-expression using doxycycline, cells were treated with SEL201 or DMSO for 15 days, after which cells were subjected to next-generation sequencing. Ultimately, the frequency of sgRNA reads were assessed to determine whether knockout of a particular gene compromised cellular viability. A specific statistical tool, called robust analytics and normalization for knockout screens (RANKS), was used to assess the depletion of each sgRNA contained in the EKO library¹⁷⁰. In summary, genes exhibiting negative RANKS scores (i.e. synthetic lethal genes) suggest decreased cell viability when cells harboring the identified sgRNA are treated with SEL201 (figure 4B). In contrast, genes with positive RANKS scores (i.e. buffering genes) are genes whose knockout confers enhanced cell viability or resistance to SEL201 treatment. Through exploration of Gene Ontology (geneontology.org), negative RANKS score genes from the CRISPR-KO screen showed enrichment in several biological processes including DNA synthesis, regulation of S phase, infectious disease, regulation of M phase, HIV infection and were dominated by cell cycle-related processes (figure 4C). On the other hand, positive RANKS score genes showed enrichment in processes related to translation. Among the genes identified with a negative RANKS score, BRD2 caught our attention and enticed the investigation of synthetic lethal interactions between MNK1/2 and the BET-family of proteins (figure 1B). Therefore, we next sought to determine whether dual

inhibition of MNK1/2 kinases and BET-family of proteins decreased cellular viability of melanoma cells, compared to either monotherapy.

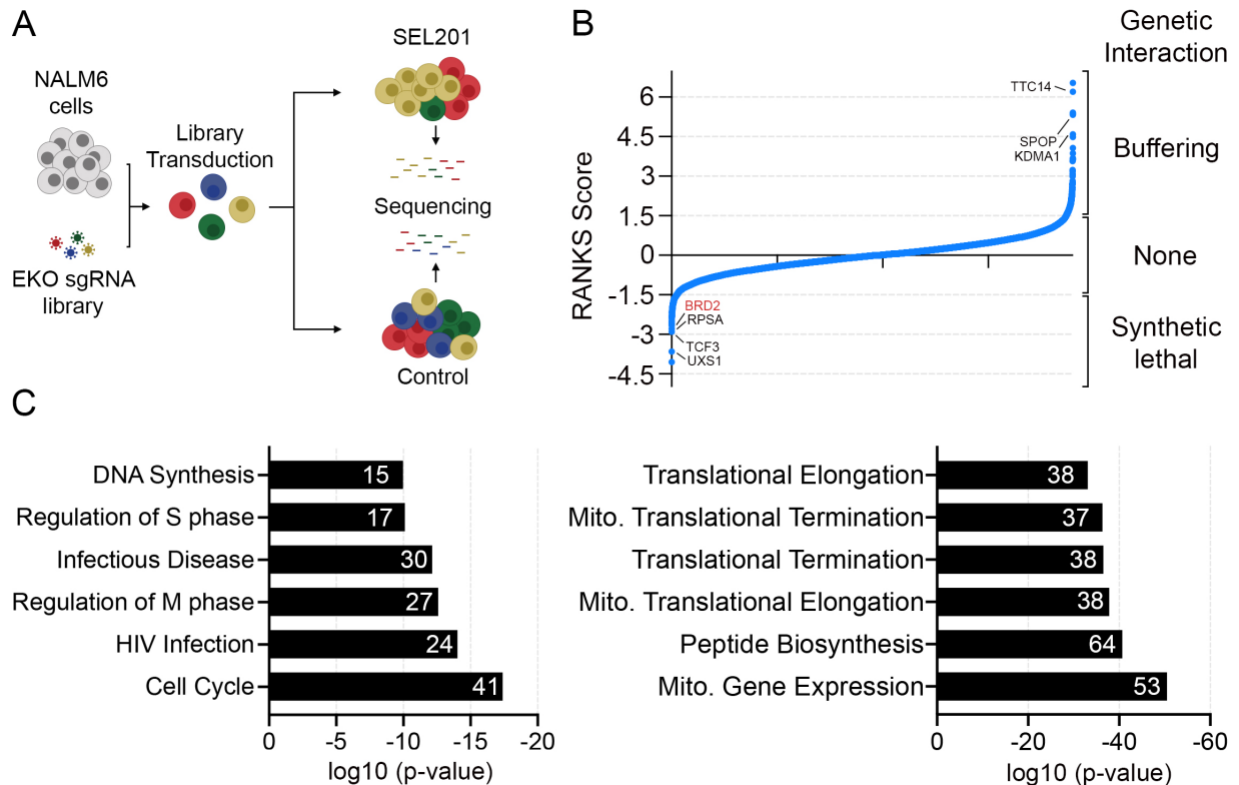


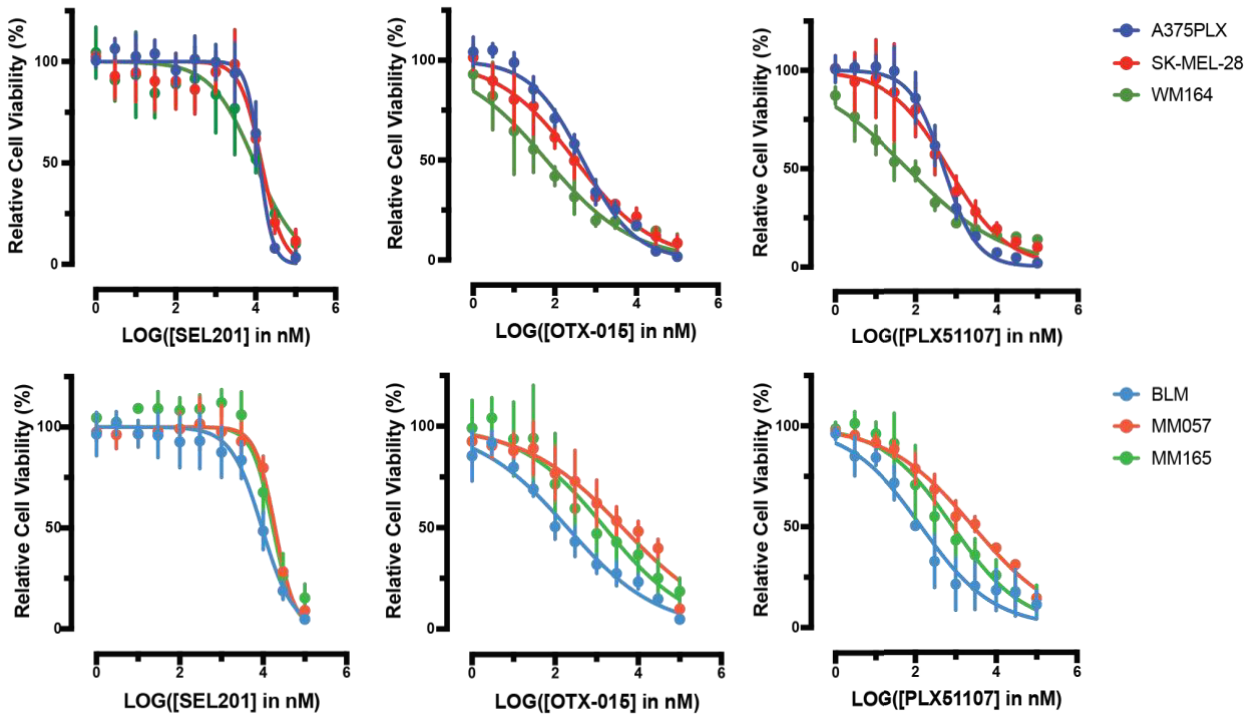
Figure 4. NALM-6 CRISPR-KO screen reveals synthetic lethality between MNK1/2 kinases and BRD2. A) Schematic depicting the main steps of the CRISPR-KO screen. Identically coloured cells signify transduction with the same gRNA. Cells harboring a non-synthetic lethal gRNA with SEL201 will exhibit enhanced viability. B) Top hit illustration of the CRISPR-KO screen based on gRNA sequence reads. Other BET proteins than BRD2 did not feature among the top hits. Data was analyzed using robust analytics and normalization for knockout screen (RANKS) statistical tool – see text. Cut-offs for top hits were arbitrarily set at +1.5 and -1.5 for positive and negative RANKS scores respectively. C) Gene Ontology analysis of major biological processes enriched for synthetic lethal genes (left panel) and buffering genes (right panel). Number of genes enriched for each biological process are indicated within bar charts.

8.2. Combining BET and MNK1/2 Inhibitors Compromises Melanoma Clonogenic Outgrowth Better Than Either Drug Alone

8.2.1. Establishing Drug Dose Response Curves to Determine Optimal Doses of MNK1/2 and BET Inhibitors

Prior to evaluating the effect of combining MNK and BET inhibitors, we analyzed the relative cellular viability at different drug concentrations to define a threshold beyond which cells experience excessive toxicity. Dose response curves were established for SEL201, OTX-015 and PLX51107 in six melanoma cell lines that express major genomic driver mutations, that is BRAF-mutant (A375, SK-MEL-28 and WM164 – figure 5a, upper panel) and NRAS-mutant (BLM, MM057 and MM165 – figure 2a, bottom panel). SEL201 exhibited relatively high IC₅₀ concentrations in all cell lines, ranging from 9-20 μ M (figure 5b). On the other hand, BET inhibitors OTX-015 and PLX51107 showed IC₅₀ concentrations in the nanomolar range for BLM, A375, SK-MEL-28 and WM164 (60-700nM), whereas MM057 and MM165 showed less sensitivity for BET inhibitors (IC₅₀: 0.8-4.5 μ M). Consequently, drug concentrations employed for subsequent experiments were maintained below the half maximal inhibitory concentration (IC₅₀) and were specific for each cell line.

A



B

DRUGS [nM]		CELL LINES		
		BLM	MM057	MM165
SEL201	IC5	755.3	3896.1	3115
	IC10	1431.3	5850.5	4800.1
	IC20	2864.2	9095	7674.7
	IC30	4542	12194.4	10484
	IC40	6628	15508.2	13538.6
	IC50	9376	19336	17119
OTX-015	IC5	0.1	1.4	1.6
	IC10	0.8	10.5	9.2
	IC20	6.1	95.4	61.5
	IC30	23.6	413.8	217.1
	IC40	71.6	1378	610.9
	IC50	198	4156	1578
PLX51107	IC5	0.3	1.8	2.2
	IC10	1.5	11.7	10
	IC20	7.8	86.7	51.2
	IC30	23.7	327.4	151.6
	IC40	59.3	973.5	369
	IC50	137.2	2646	834.9

DRUGS [nM]		CELL LINES		
		A375PLX	SK-MEL-28	WM164
SEL201	IC5	4008.5	2281.3	229
	IC10	5344.9	3617.3	589.4
	IC20	7303.9	5965.5	1644.4
	IC30	8988.5	8318.6	3252.1
	IC40	10655.5	10925.1	5687.7
	IC50	12456	14030	9500
OTX-015	IC5	6.3	0.5	0.05
	IC10	18.9	2.6	0.3
	IC20	62.3	15.1	2.1
	IC30	138	49.1	8
	IC40	264.6	129.2	23.2
	IC50	481.1	313.9	62.2
PLX51107	IC5	31.8	4.7	0.02
	IC10	64	16.4	0.1
	IC20	136.2	63.6	1.3
	IC30	225.2	156.3	5.8
	IC40	340.1	326.8	20.1
	IC50	496.5	643	62.3

Figure 5. Establishing toxicity thresholds for SEL201, OTX-015 and PLX51107 in *BRAF*- and *NRAS*-mutant melanoma cell lines. A) Dose response curves using MNK inhibitor SEL201 and BET inhibitors OTX-015 and PLX51107 in A375, SK-MEL-28, WM164 (*BRAF*-mutant) – upper

panel – and BLM, MM057 and MM165 (*NRAS*-mutant) – lower panel. B) IC5-IC50 drug concentrations are listed for all cell lines. All experiments were repeated at least three times.

8.2.2. Combining BET and MNK1/2 Inhibitors Further Decreases Cellular Proliferation in *BRAF*- and *NRAS*-Mutant Melanoma Cell Lines

Next, we sought to determine the effect of combining SEL201 and BET inhibitors OTX-015 and PLX51107 in *BRAF*- and *NRAS*-mutant melanoma cell lines. Cell viability assays were conducted by combining a range of non-toxic concentrations of SEL201 and OTX-015 (figure 6A) or SEL201 and PLX51107 (figure 6B) – as defined previously. Furthermore, by using the SynergyFinder software¹⁷¹, we established synergy distributions to determine whether combining specific drug doses exhibit potential synergistic effects as per the Bliss independence model¹⁷². Currently, the definition of synergy remains under debate between several competing models¹⁷³. Herein, we employ the Bliss model of independence which stipulates that if two drugs show no interaction (i.e., act independently), then their combined effect should be equal to the sum of their individual effects¹⁷⁴. This assumption is represented by the equation:

$$E(f_{ab}) = O(f_{ab}) \text{ or,}$$

$$f_a + f_b - f_a * f_b = O(f_{ab})$$

Where, $E(f_{ab})$ represents the expected fractional response when combining drugs a and b, whereas $O(f_{ab})$ defines the observed fractional response upon drug combination. f_a and f_b represent the individual fractional response of drugs a and b respectively. Specifically, the fractional response is the effect of the treatment relative to control, expressed as a proportion.

Departure from this assumption can be represented by the excess over bliss (EOB):

$$EOB = O(f_{ab}) - E(f_{ab})$$

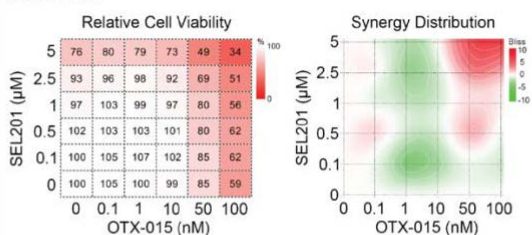
When the observed fractional response of the drug combination ($O(f_{ab})$) is greater than the expected fractional response ($E(f_{ab})$), we can infer potential synergistic interactions between both drugs. This is represented by a positive EOB score. In contrast, when the combination shows an observed fractional response that is less than the expected fractional response, this indicates potential antagonism, represented by a negative EOB score.

Overall, treatment of *BRAF*-mutant cell lines with combined SEL201 and OTX-015 (figure 6A – left panels) or SEL201 and PLX51107 (figure 6B – left panels) showed several potential

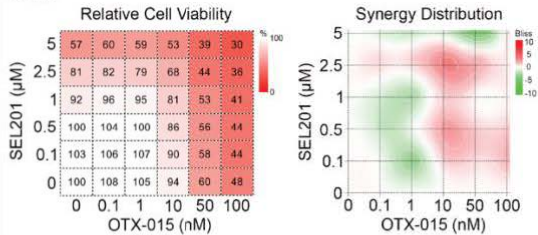
synergistic windows. Similarly, *NR4S*-mutant cell lines also showed potential synergy among specific drug concentrations, although to a lesser extent than *BR4F*-mutant cell lines (figure 6A-B – right panels). Whereas most cell lines showed several pairs of potentially synergistic concentrations, specific candidates were chosen for long-term colony formations assays. In particular, a 50nM concentration of OTX-015 and PLX51107 was used in A375, SK-MEL-28 and MM165, whereas a concentration of 10nM was employed for the more BETi-sensitive WM164 and BLM cell lines. MM057 showed different optimal concentrations for OTX-015 (50nM) and PLX51107 (10nM). SEL201 concentrations were maintained at 2.5uM for all cell lines, where we show robust repression of phospho-eIF4E, the best characterized substrate of MNK1/2 (figure 7)⁵⁷. Taken together, combining different concentrations of SEL201 and BET inhibitors in melanoma cells shows potential synergistic windows in assays done over the course of 96 hours. We next wanted to determine whether combined MNK1/2 and BET inhibition, at the selected concentrations, could be equally beneficial in long-term clonogenic outgrowth assays.

A

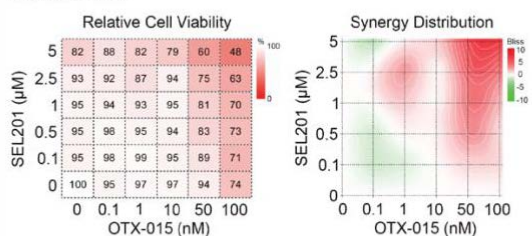
A375PLX



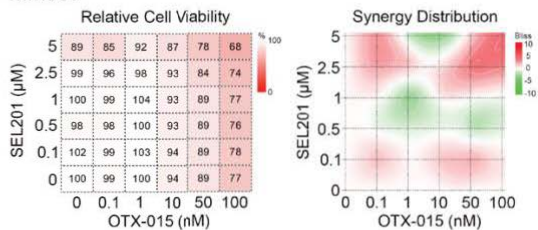
BLM



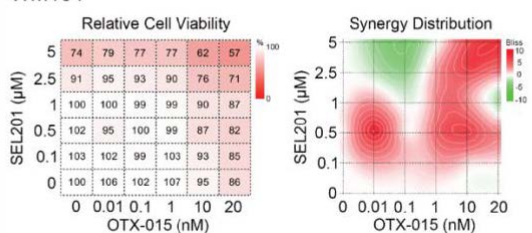
SK-MEL-28



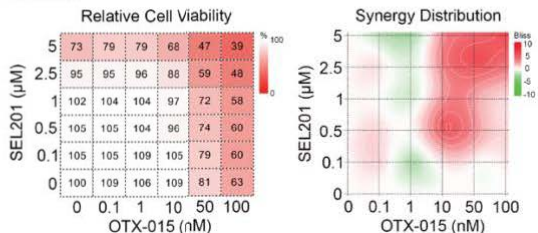
MM057



WM164

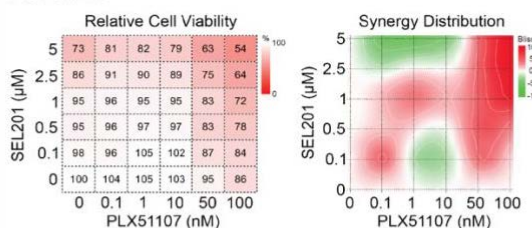


MM165

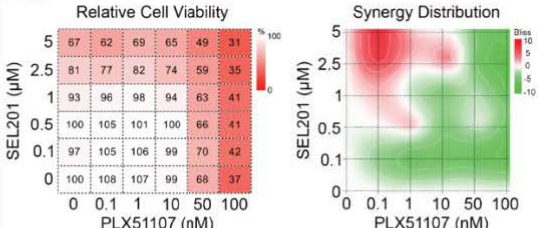


B

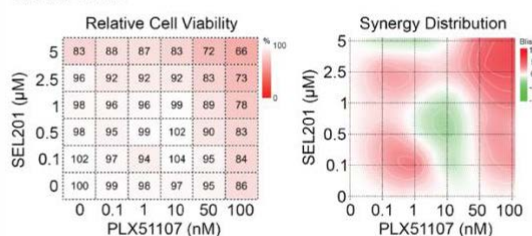
A375PLX



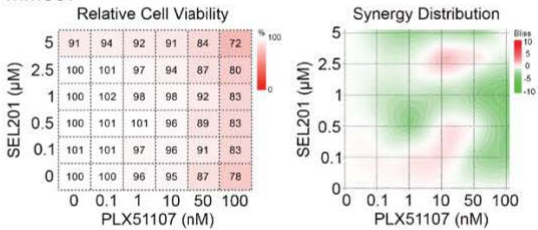
BLM



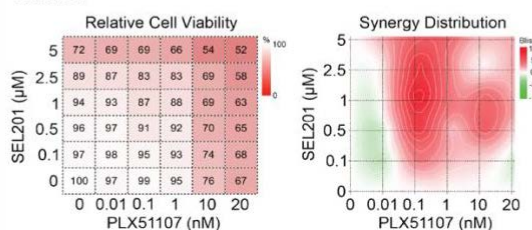
SK-MEL-28



MM057



WM164



MM165

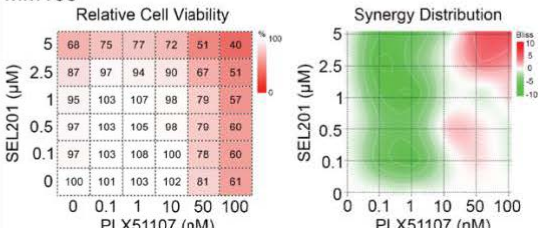


Figure 6. Identification of potential synergistic pairs of SEL201 and BET inhibitor concentrations. A) Cell viability of *BRAF*- (left panels) and *NRAS*- (right panels) mutant cell lines following combination of SEL201 and OTX-015 at non-toxic concentrations. For each cell line, the leftmost panel represents a table of viabilities (in % relative to DMSO control) for corresponding drug concentrations. The rightmost panel shows a heat map of the synergy distribution as calculated using SynergyFinder (synergyfinder.fimm.fi). Positive Bliss scores are represented in red whereas negative Bliss scores are shown in green. B) Similar to A), except PLX51107 was used instead of OTX-015.

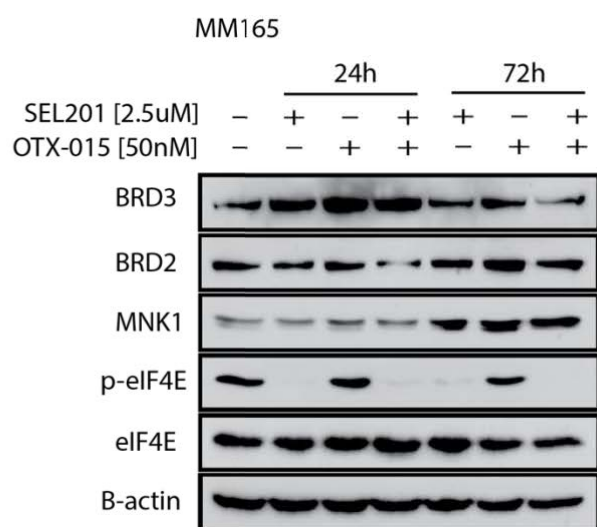
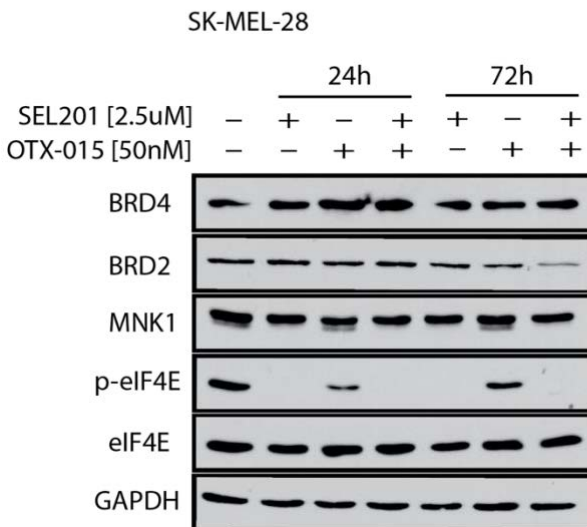
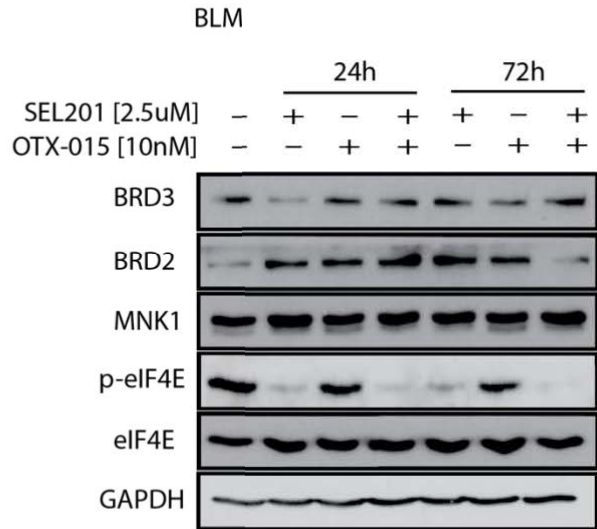
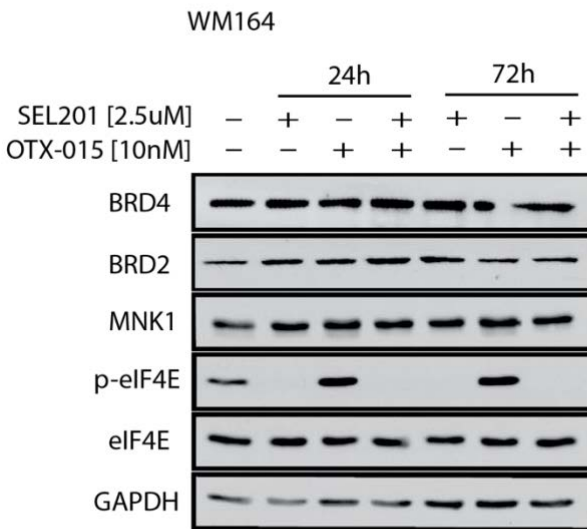
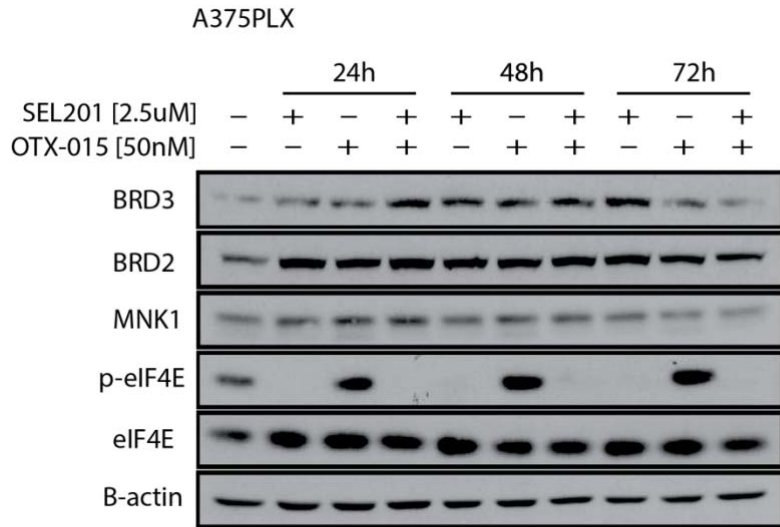
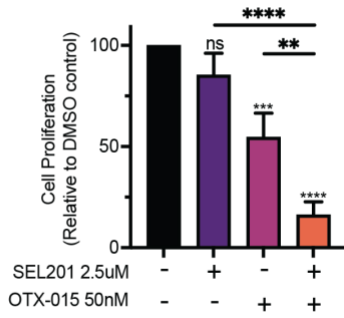


Figure 7. Treatment with 2.5uM SEL201 consistently suppressed p-eIF4E in melanoma cell lines. Western blots showing consistent decrease of p-eIF4E levels upon treatment with 2.5uM SEL201 at different timepoints in A375, WM164, SK-MEL28, BLM and MM165.

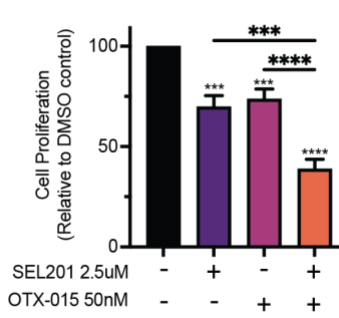
To this end, we performed colony formation assays in *BRAF*- and *NRAS*-mutant cell lines with dual treatment using either (a) SEL201 and OTX-015 or (b) SEL201 and PLX51107. Among the 6 cell lines tested, we observed a more robust decrease in clonogenic outgrowth when combining SEL201 and OTX-015 relative to either single agent (Figure 8A). Curiously, the combination of SEL201 and PLX51107 further suppressed clonogenic outgrowth exclusively in SK-MEL-28 and MM165 compared to monotherapy treatments (2 out of 6 cell lines tested – Figure 8B). Furthermore, among all cell lines with a significant drug combination effect, the computed excess over bliss showed positive values, which indicates a potential synergistic interaction between SEL201 and BET inhibitors in the long term. Specifically, upon combining SEL201 and OTX-015, EOB values were slightly increased in A375 (0.30), SK-MEL-28 (0.13) and MM165 (0.16) relative to WM164 (0.05), BLM (0.03) and MM057 (0.04). On the other hand, low EOB values are observed when combining SEL201 and PLX51107 in SK-MEL-28 (0.06) and MM165 (0.07). Taken together, these results highlight the efficacy of combining SEL201 with OTX-015 in *BRAF*- and *NRAS*-mutant melanoma cell lines, whereas similar efficacy is also partially shown when combining SEL201 and PLX51107.

A

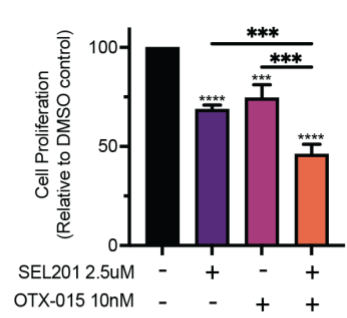
A375 PLX



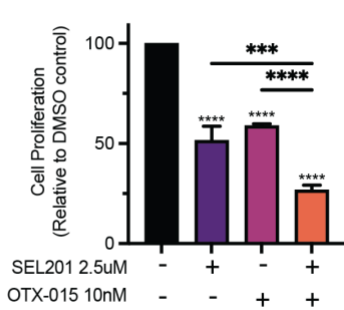
SK-MEL-28



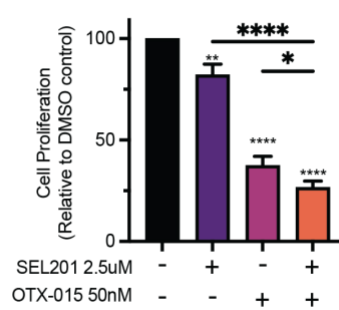
WM164



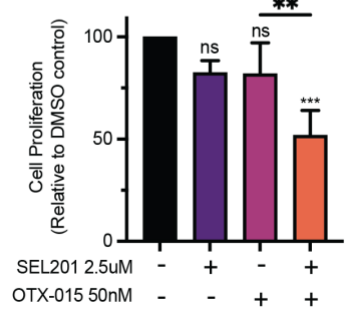
BLM



MM057

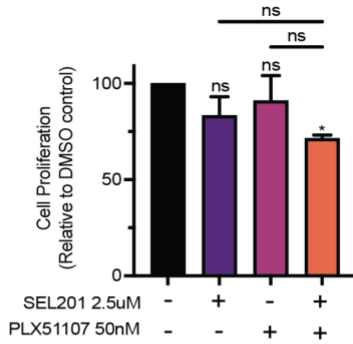


MM165

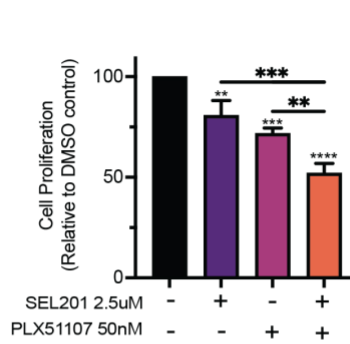


B

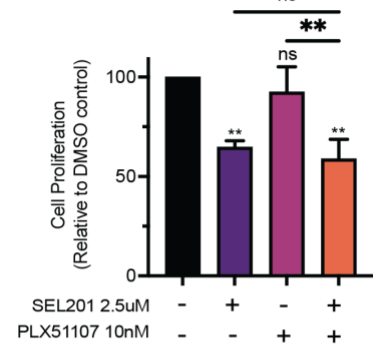
A375 PLX



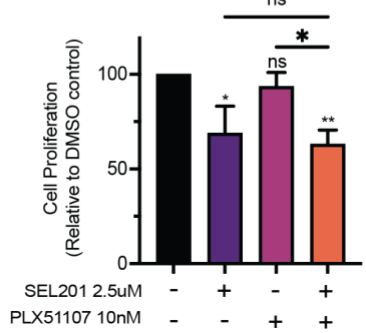
SK-MEL-28



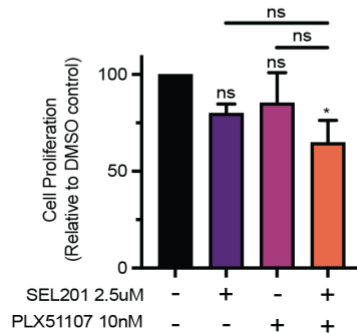
WM164



BLM



MM057



MM165

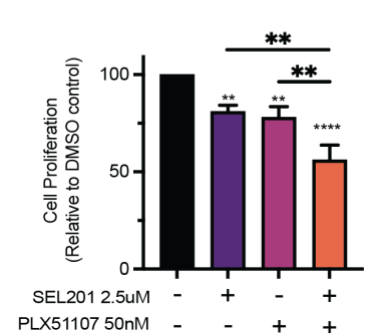


Figure 8. Combining SEL201 and OTX-015 further decreases *BRAF*- and *NRAS*-mutant melanoma cell proliferation in long term colony formation assays. A) Colony formation assays in *BRAF*- and *NRAS*-mutant cell lines treated with a combination of SEL201 and OTX-015. B) Similar to A) except OTX-015 is replaced by PLX51107. Quantification was performed by reading crystal violet absorbance (590 nm). At least three biological replicates were performed for each experiment. Statistical analyses were done by one-way ANOVA and Tuckey post-hoc test. ns: not significant (≥ 0.05); * $0.01 \leq p \leq 0.05$, ** $0.001 \leq p \leq 0.01$, *** $0.0001 \leq p \leq 0.001$, **** $p < 0.0001$.

8.3. BRD4 knockdown in A375 Recapitulates Pharmacological Effects of BETi in Combination Treatment

To determine which of the BET-family proteins effectively recapitulates pharmacological effects of BET inhibitors in melanoma when combined with MNK inhibitors, we performed shRNA knockdowns of BRD2, BRD3 and BRD4 in A375 and treated with different concentrations of SEL201 (figure 9). Surprisingly, unlike BRD2 or BRD3, knockdown of BRD4 sensitized A375 cells to SEL201 treatment. Thus, these results suggest that BRD4 is the main BET-family protein responsible for sensitivity to MNK inhibitors.

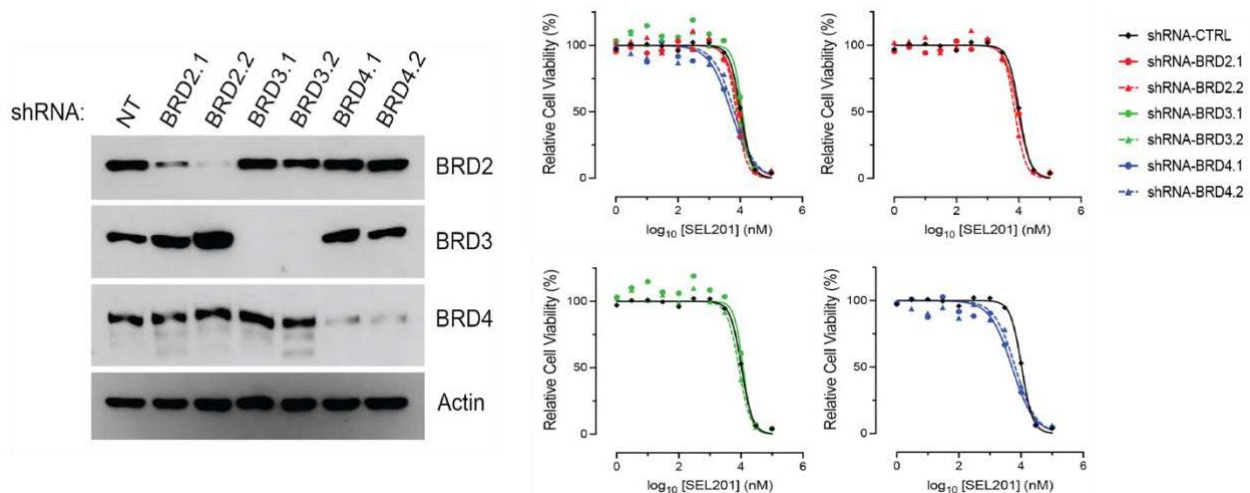


Figure 9. Knockdown of BRD4 in A375 exhibits sensitivity to SEL201. Left panel shows an immunoblot displaying knockdowns of BRD2, BRD3 and BRD4 proteins following transduction with respective shRNA in A375. Right panel shows SEL201 dose response curves of stable shBRD A375 cell lines.

8.4. EFT508 Recapitulates Pharmacological Effects of SEL201 in BLM but not in A375 when combined with OTX-015

We next aimed to test whether eFT508, a MNK1/2 inhibitor currently in clinical trials, produces similar effects to SEL201 when combined with OTX-015 in melanoma cells (figure 10). Thus, we performed colony formation assays by combining eFT508 and OTX-015 using A375 and BLM, two melanoma cell lines that showed decreased clonogenic outgrowth when treated with SEL201 and OTX-015. Unlike A375, BLM effectively showed an enhanced inhibition in colony formation relative to single agents when dually treated with eFT508 and OTX-015. Taken together, these results suggest that eFT508 only partially recapitulates the effect of SEL201 in melanoma when combined with OTX-015.

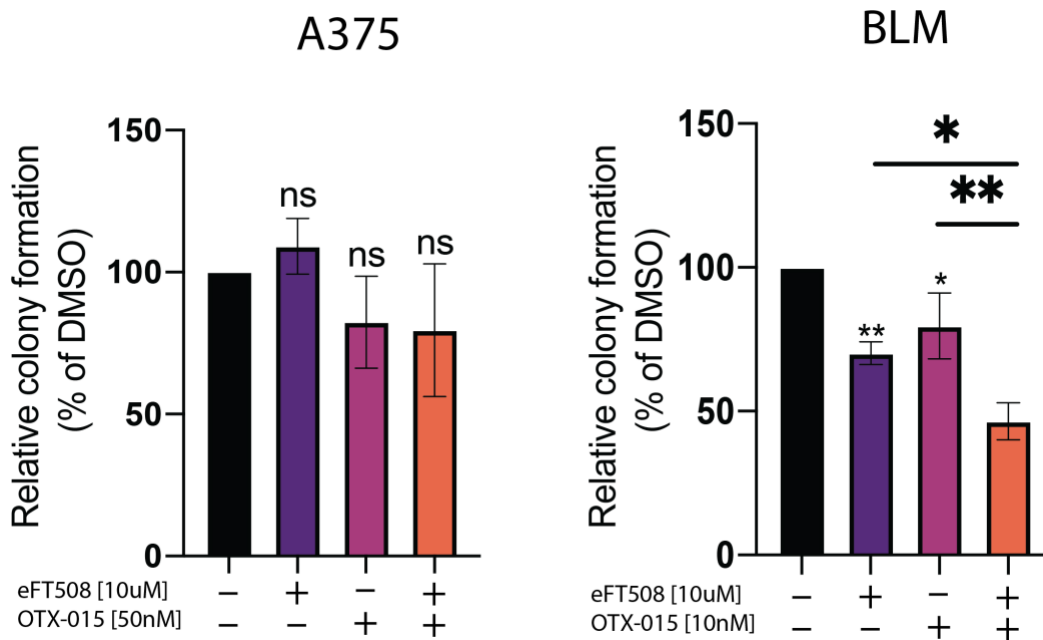


Figure 10. Combining eFT508 and OTX-015 suppresses clonogenic outgrowth in BLM but not in A375 relative to single agents. Quantification was performed by reading crystal violet absorbance (590 nm). At least three biological replicates were performed for each experiment. Statistical analyses were done by one-way ANOVA and Tuckey post-hoc test. ns: not significant (≥ 0.05); * $0.01 \leq p \leq 0.05$, ** $0.001 \leq p \leq 0.01$, *** $0.0001 \leq p \leq 0.001$, **** $p < 0.0001$.

8.5. Treatment of A375 Cells with OTX-015 and SEL201 Does not Induce Cell Cycle Arrest

To elucidate a mechanism through which the combined effect of SEL201 and OTX-015 inhibits melanoma cell viability and clonogenic outgrowth, we performed cell cycle analysis of A375 cells

treated with the combination (figure 11). Importantly, both MNK1/2 kinases and BET-family proteins have been shown to regulate the expression of cell cycle-related genes. On one hand, Zhan et al. showed that MNK1/2 mediate the translation but not the transcription of cyclin E1 (*CCNE1*)¹¹, while other studies highlighted the role of BRD2 in enhancing the promoter activity of cyclin D, cyclin E and cyclin A^{131,132}. Intriguingly, combining SEL201 and OTX-015 in A375 did not induce a cell cycle arrest at any phase across timepoints of 24, 48, and 72 hours. Taken together, these results suggest that the combination does not induce cell cycle arrest in A375 melanoma cells.

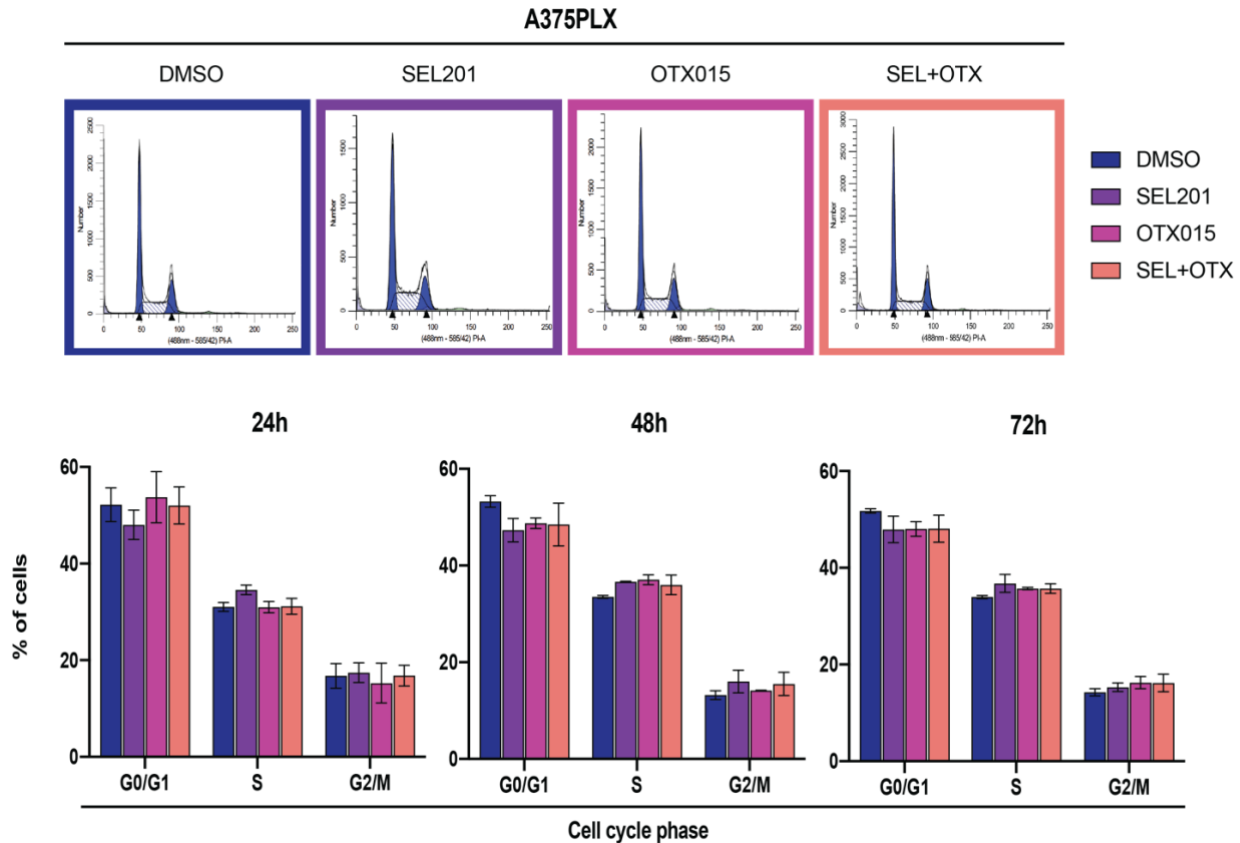


Figure 11. Combining SEL201 and OTX-015 in A375 does not induce cell cycle arrest. Upper panel shows representative cell cycle histograms at the 24h timepoint. Lower panel shows percentage of cells at different phases of the cell cycle. Experiment was repeated twice. Analysis done using ModFit software.

8.6. Combo-treated A375 Cells do not Exhibit Decreased Cellular Proliferation by CFSE Despite Showing Lower Cellular Abundance

Previous cell cycle analysis results indicated that the reduced cell viability and clonogenic outgrowth observed by combining SEL201 and OTX-015 is not attributable to an accumulation of

cells at a particular phase of the cell cycle. However, a possibility may be that the effect resides in inhibiting cellular proliferation without necessarily causing cell cycle arrest. To test this hypothesis, we performed Carboxyfluorescein succinimidyl ester (CFSE) staining of A375 cells and monitored their proliferation under dual treatment with SEL201 and OTX-015 (figure 12). Incorporation of CFSE into cells enables one to track proliferation over time, with rapidly proliferating cells typically displaying lower fluorescence intensity¹⁷⁵. While the combination treatment caused a decreased event count relative to single agents when samples were fully acquired by the cytometer, the mean fluorescence intensity of CFSE remained unchanged when compared to DMSO-treated cells. The measure of relative event count per condition was used as a control to verify that a similar trend to previous viability and clonogenic assays done in A375. Taken together, these results suggest that combo-treated A375 cells do not exhibit cell cycle arrest nor a decreased cellular proliferation, while still exhibiting lower event count than control or single agent-treated cells.

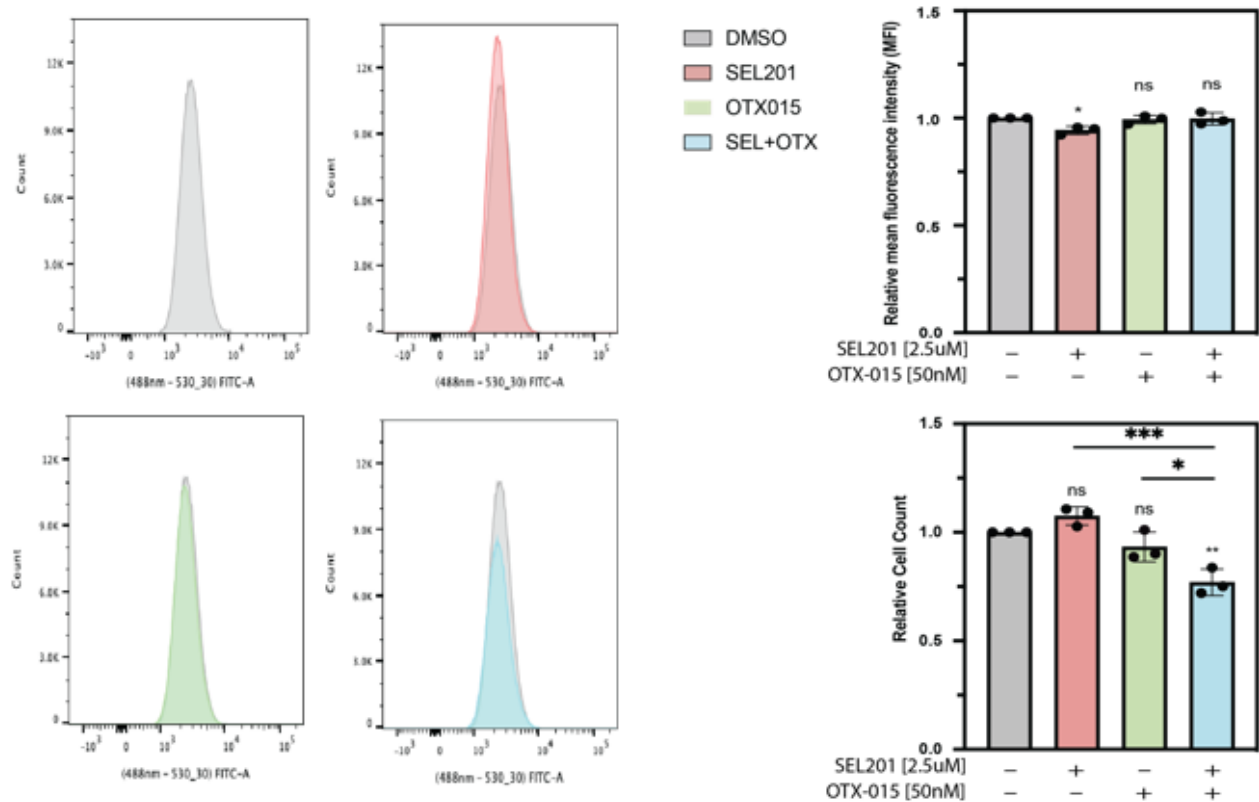


Figure 12. The combined effect of SEL201 and OTX-015 does not decrease cellular proliferation in A375. Leftmost panels show the distribution of FITC-fluorescent treated cells relative to DMSO-treated cells. Right upper panel shows the relative mean fluorescence intensity while the lower right panel represents the relative cell count (or events recorded when samples were fully

acquired) per condition. Samples were entirely recorded by the flow cytometer. Analysis done by FlowJo. At least three biological replicates were performed. Statistical analyses were done by one-way ANOVA and Tukey post-hoc test. ns: not significant (≥ 0.05); * $0.01 \leq p \leq 0.05$, ** $0.001 \leq p \leq 0.01$, *** $0.0001 \leq p \leq 0.001$, **** $p < 0.0001$.

8.7. The Combination of SEL201 and OTX-015 Does not Enhance Apoptosis in A375

Given that dual inhibition of A375 cells with SEL201 and OTX-015 does not induce cell cycle arrest or compromise cellular proliferation, we tested whether the combination exhibits cytotoxicity. To this end, we quantified the proportion of apoptotic A375 cells by annexin V-PI staining (figure 13). While the proportion of single-stain positive cells remained unchanged across timepoints (i.e. AnV-PI+ or AnV+PI-), we noted an increased proportion of late apoptotic or necrotic cells (An+PI+) in combo-treated A375 cells relative to single agents at 72h. However, no difference was noted relative to the DMSO-treated population. Taken together, these results indicate that combining SEL201 and OTX-015 results in decreased A375 clonogenic outgrowth and cell count through an unknown mechanism which excludes cell cycle arrest, reduced cellular proliferation or enhanced apoptosis.

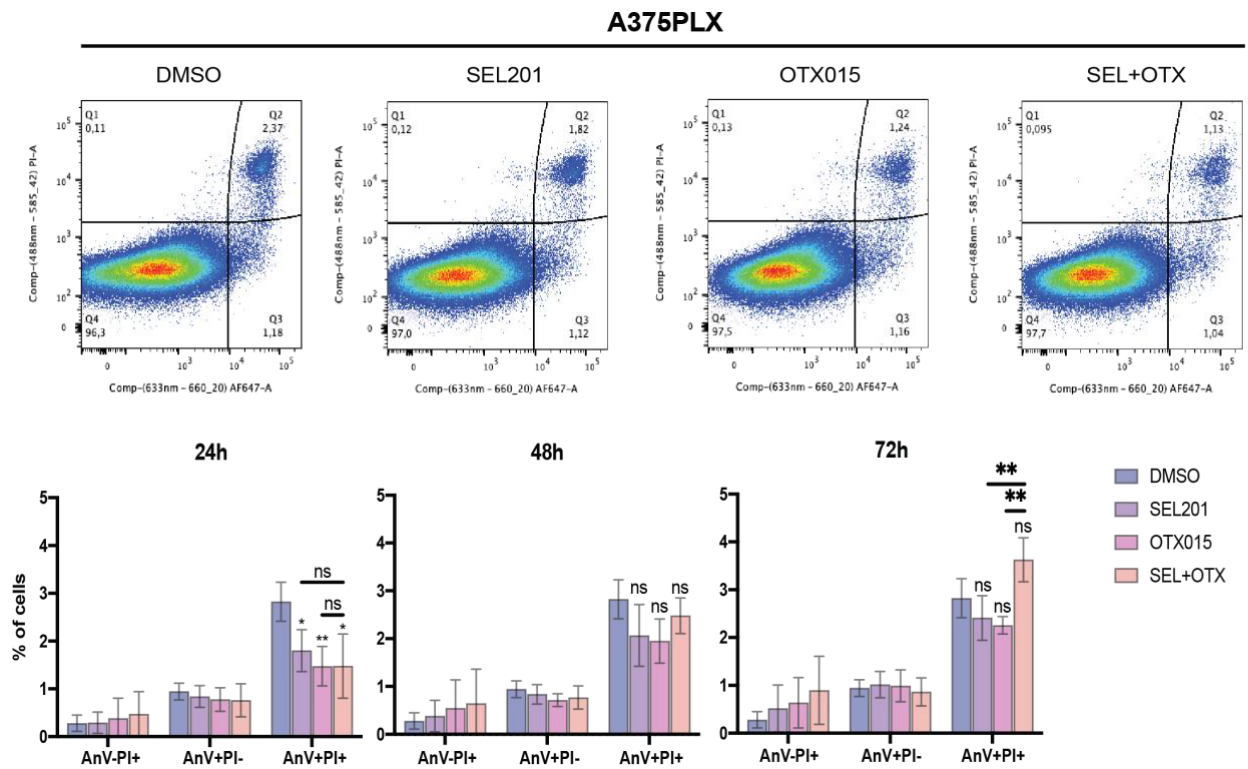


Figure 13. SEL201 and OTX-015 dual-treated A375 cells do not show enhanced cell death.

Upper panels show representative population distributions per treatment condition at the 24h timepoint. Gatings were maintained the same way across treatment conditions and timepoints. Lower panels display quantifications of the different populations undergoing early apoptosis (AnV+PI-), late apoptosis or necrosis (AnV+PI+) and non-viable cells (An-PI+) across timepoints. At least three biological replicates were performed for each experiment. Statistical analyses were done by two-way ANOVA and Tuckey post-hoc test. ns: not significant (≥ 0.05); * $0.01 \leq p \leq 0.05$, ** $0.001 \leq p \leq 0.01$, *** $0.0001 \leq p \leq 0.001$, **** $p < 0.0001$.

8.8. Dual Therapy Using SEL201 and OTX-015 Does not Induce Cellular Senescence in A375

Given that previous studies have highlighted the role of BRD4 in regulating cellular senescence¹⁷⁶, we next sought to determine whether enhanced cellular senescence could explain the mechanism through which SEL201 and OTX-015 inhibit A375 cell abundance and clonogenic outgrowth (figure 14). This was achieved by staining for senescence-associated β -galactosidase (SA- β -gal), a lysosomal protein that increases in senescent cells¹⁷⁷. β -galactosidase staining showed no further increase in the proportion of senescent cells in combo-treatment relative to single agents or DMSO-treated cells.

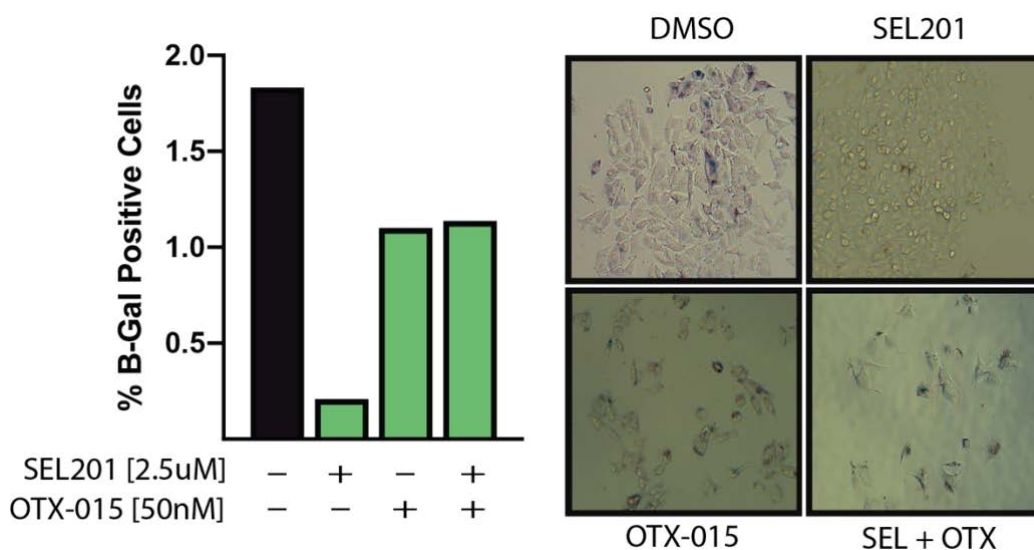


Figure 14. Preliminary β -galactosidase staining of A375 cells does not indicate senescence induction upon dual SEL201 and OTX-015 treatment. Representative images for each treatment condition are shown to the right (n=1).

8.9. Combining SEL201 and OTX-015 Does not Further Decrease the Invasive Potential *in vitro* of A375 and BLM Melanoma Cell Lines

Next, we aimed to determine whether combining SEL201 and OTX-015 decreases the invasive nature of melanoma cells. Specifically, we performed Boyden chamber invasion assays in A375 and BLM cell lines using Matrigel (figure 15). It is important to differentiate between Matrigel and collagen type I invasion assays, whereby each one of these assays recapitulates a different step of metastasis¹⁷⁸. On one hand, Matrigel is a mimic of the basement membrane, whereas collagen type I mimics the interstitial stroma. In practice, Boyden chamber inserts of 8 μm are coated with Matrigel, on top of which melanoma cells are seeded under treatment. 24 hours later, cells that have penetrated the Matrigel are quantified. In both A375 and BLM cell lines, we observed no significant decrease in invasion when combining SEL201 and OTX-015 relative to single agents alone. Despite A375 cells trending towards decreased invasiveness upon dual therapy, differences in invasiveness between the combination and OTX-015 were statistically non-significant. Taken together, these results suggest that the combination does not further decrease invasiveness across the basement membrane.

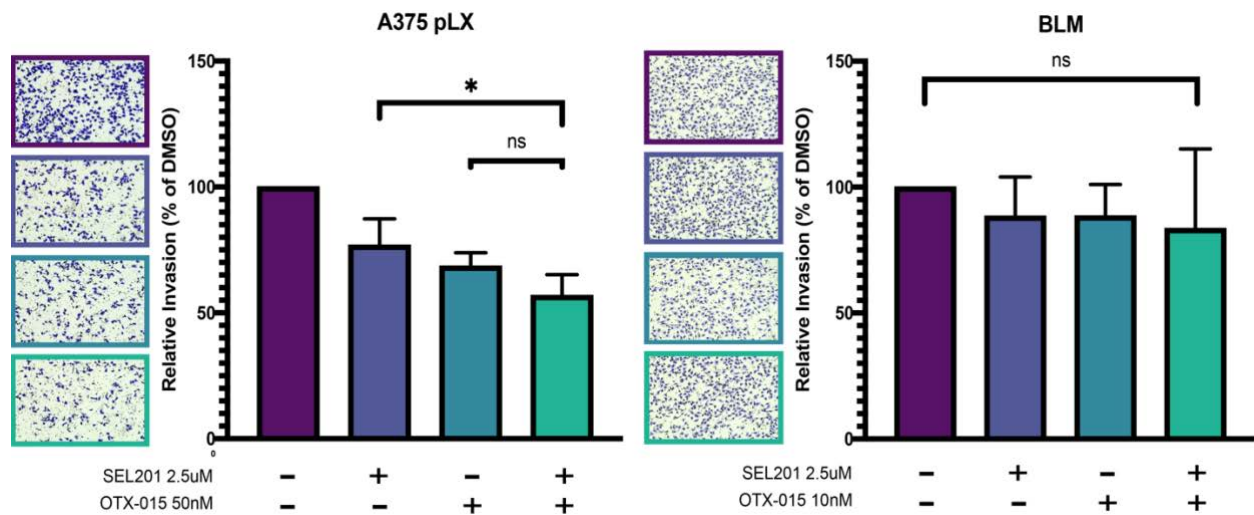


Figure 15. Combining SEL201 and OTX-015 does not exhibit efficacy in decreasing invasiveness in A375 and BLM. Representative images are shown for A375 (left panel) and BLM (right panel). At least three biological replicates were performed for each experiment. Statistical analysis by one-way ANOVA and Tuckey post-hoc test. ns: not significant (≥ 0.05); * $0.01 \leq p \leq 0.05$, ** $0.001 \leq p \leq 0.01$, *** $0.0001 \leq p \leq 0.001$, **** $p < 0.0001$.

8.10. Combining SEL201 and OTX-015 in a Syngeneic Mouse Model Shows Improved Survival Than Vehicle or Single Agent Treatments

Given that combining SEL201 and OTX-015 in melanoma showed efficacy *in vitro*, we next sought to determine whether the combination also recapitulates its effect in a syngeneic melanoma mouse model. Importantly, the choice of an immune-competent mouse model was justified given the mounting evidence on the role of BET-family proteins and the MNK1/2-eIF4E axis in modulating the immune system and the tumor microenvironment^{83,157}. To this end, we subcutaneously injected C57BL/6N mice with Yummer 1.7 melanoma cells, and upon palpable tumor size, mice underwent oral gavage with either vehicle, single-agent or dual treatment using SEL201 and OTX-015 until experimental endpoint (figure 16A). Of note, the Yummer 1.7 cell line was generated following UV-irradiation of the Yumm 1.7 cell line, which in turn enhances mutational burden and immunogenicity¹⁷⁹. Intriguingly, single-agent SEL201 or OTX-015 treatments showed poorer survival than vehicle-treated mice, with even poorer survival when OTX-015 concentration is lowered to 12.5mg/kg (figure 16B). Despite such results, combining SEL201 and OTX-015 at 75mg/kg and 25mg/kg respectively slightly improved survival relative to vehicle-treated mice. Unexpectedly, treatment with SEL201 did not inhibit p-eIF4E within the 4 tumors analyzed (i.e. 2 vehicle and 2 SEL201 tumors) (figure 16C). Similarly, combined SEL201 and OTX-015 treatment did not decrease cellular proliferation relative to vehicle- or single-agent-treated conditions, as assessed by Ki67 staining (figure 16D). These results are preliminary and the combination of SEL201 and OTX-015 requires further *in vivo* testing.

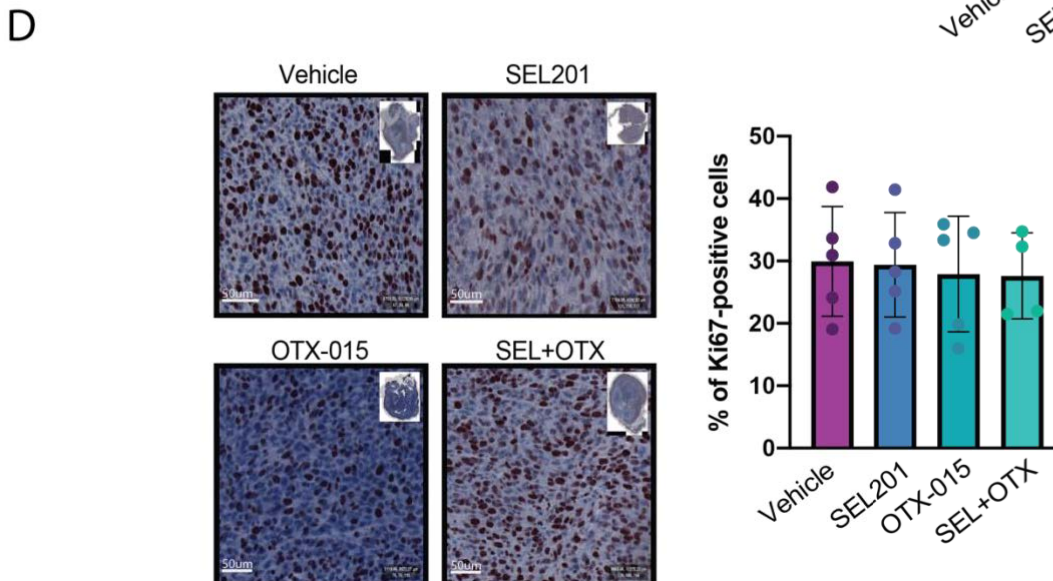
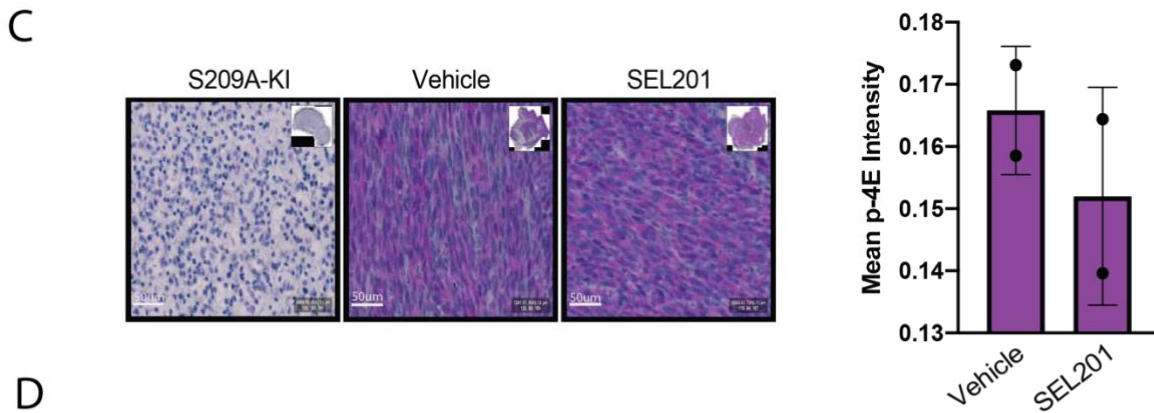
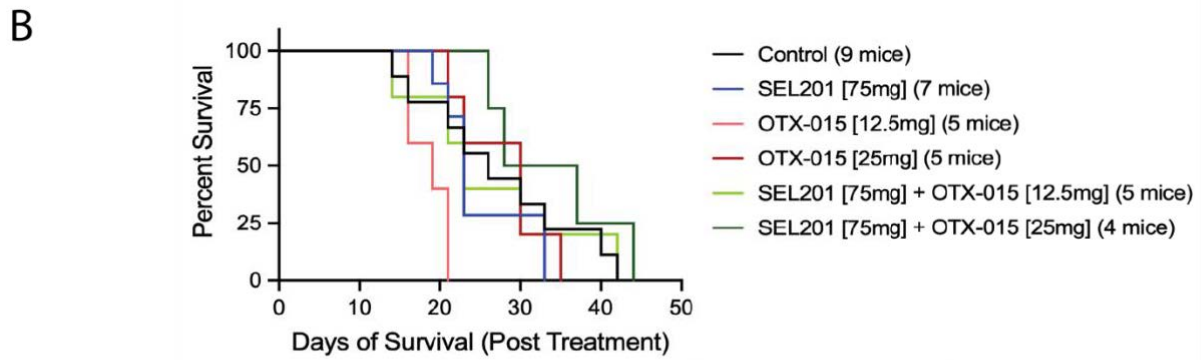
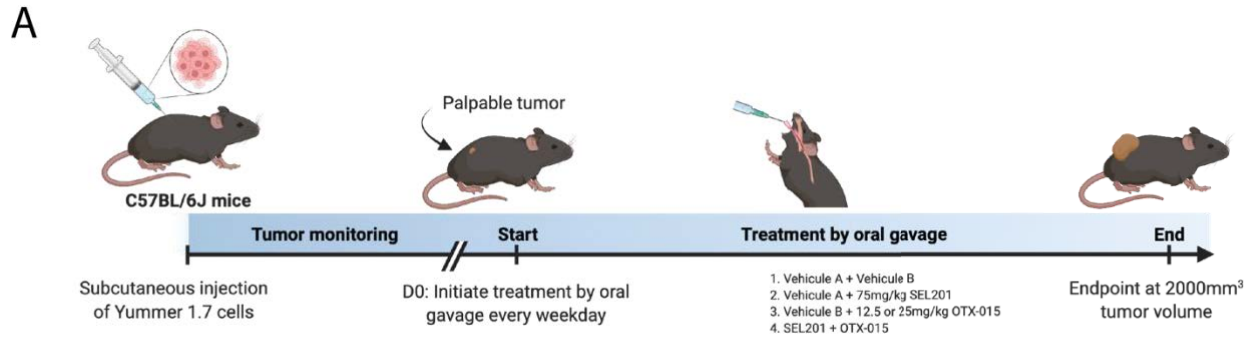
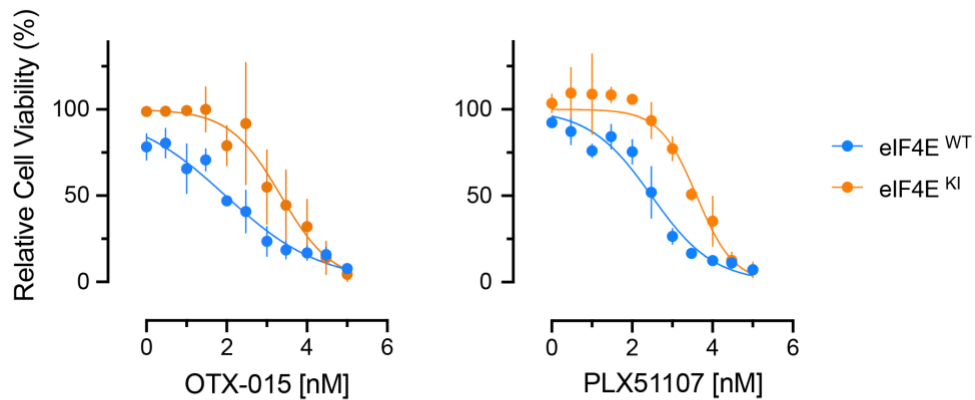


Figure 16. Combining SEL201 at 75mg/kg and OTX-015 at 25mg/kg slightly enhances survival of C57BL/6N mice subcutaneously injected with Yummer 1.7 melanoma cells. A) Schematic of the experimental method. See text for details. B) Kaplan-Meier plot displaying the survival of mice under different treatment arms. C) Overall tumor p-eIF4E expression in vehicle- and SEL201-treated mice as assessed by IHC. Only 2 tumors were stained per condition. S209A-KI: Tissue from a p-eIF4E serine to alanine (position 209) knock-in mice used as a negative control. D) Quantification of Ki67(+) cells within tumor tissues. OTX-015 and SEL+OTX conditions employ a concentration of 25mg/kg for OTX-015. Representative images are shown for each IHC staining. Each dot represents a mouse.

8.11. Pharmacological Effects of SEL201 in the Combination Treatment are Likely not Attributable to p-eIF4E Inhibition

Next, we aimed to determine whether the anti-tumorigenic effects of SEL201 and OTX-015 are dependent on p-eIF4E inhibition. While p-eIF4E is one of the best characterized substrates of MNK1/2, these kinases have been suggested to perform p-eIF4E-independent functions as well^{1,57}. Thus, we tested the sensitivity of two murine melanoma cell lines to BET inhibitors OTX-015 and PLX51107 (figure 17). Specifically, we compared murine MDMel melanoma cells harboring a non-phosphorylatable eIF4E (termed knock-in – eIF4E^{KI}) to their wild-type counterparts (eIF4E^{WT}). Both cell lines were derived by Huang et al.⁸³. Interestingly, eIF4E^{WT} MDMel cells showed enhanced sensitivity to BET inhibition than eIF4E^{KI}, as inferred by dose response curves. These results suggest that blocking the phosphorylation of eIF4E alone, is not sufficient to sensitize murine melanoma cells to BET inhibitors.



DRUGS [nM]		MDMel	
		eIF4E ^{WT}	eIF4E ^{KI}
OTX-015	IC50	93.45	2230
PLX51107	IC50	301.6	4006

Figure 17. MDMel melanoma cells harboring a non-phosphorylatable version of eIF4E do not exhibit enhanced sensitivity to BETi relative to its eIF4E wild-type counterpart. OTX-015 and PLX51107 dose response curves and associated IC50s are shown for both MDMel WT and MDMel KI cell lines. Experiments were repeated at least three times. Concentrations are in a logarithmic scale.

8.12. Treatment of Melanoma Cells With OTX-015 Does not Consistently Enhance p-eIF4E Expression

We tested whether BETi upregulate the phosphorylation of eIF4E in melanoma (figure 18), a phenotype previously shown in pancreatic and thyroid cancers¹⁶⁸. In only one of the four cell lines tested, that is BLM, did we observe a robust time- and OTX-015 concentration-dependent increase in p-eIF4E and total eIF4E. Of note, BRD4 has previously been shown to regulate the transcription of eIF4E in NSCLC¹⁶⁷. While still requiring further testing of MM165 and MM057 cell lines, these results nevertheless suggest an inconsistent enhancement of p-eIF4E expression in response to OTX-015 across melanoma cell lines.

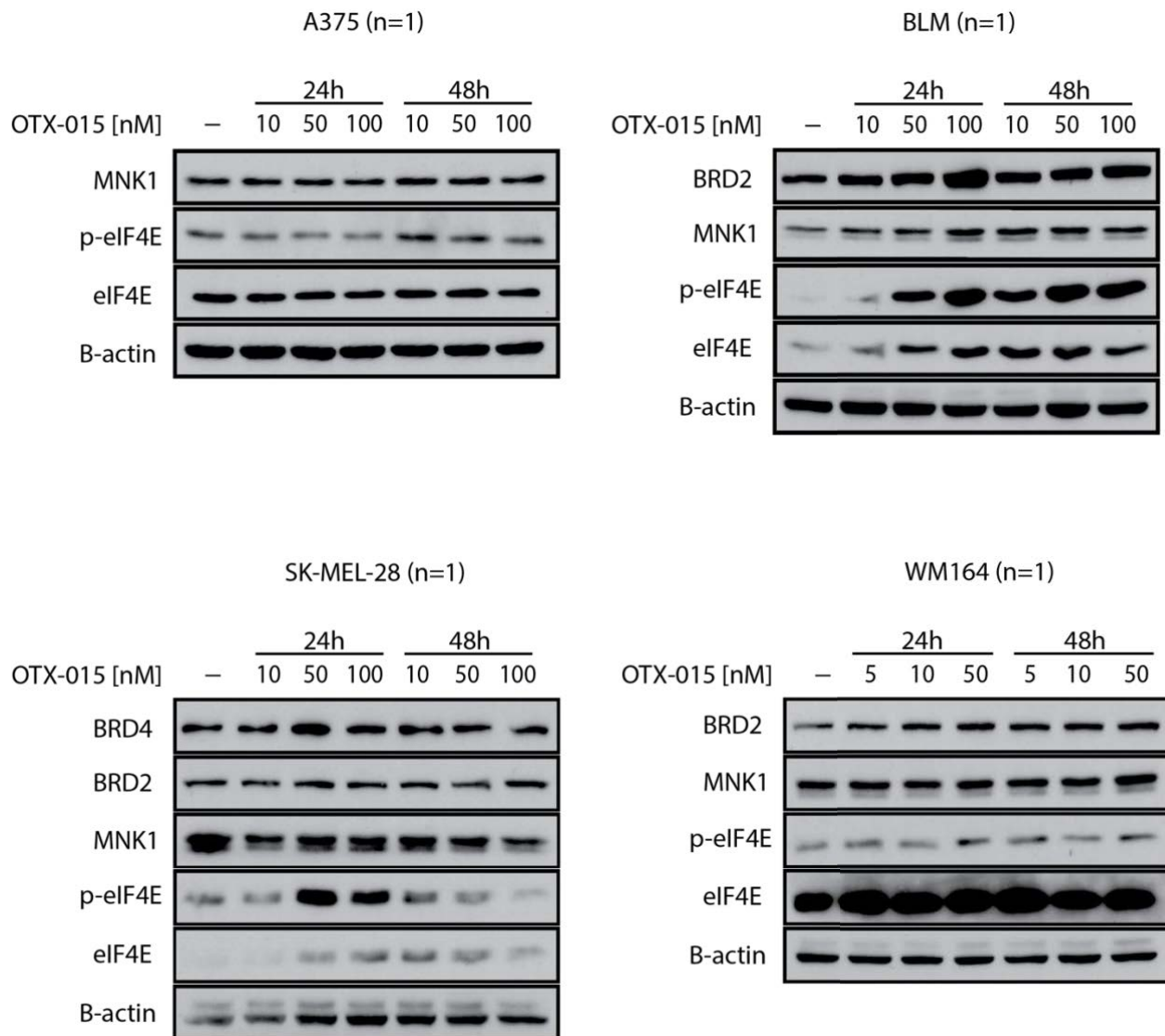


Figure 18. Treatment by OTX-015 does not consistently increase eIF4E phosphorylation in melanoma cells. Representative western blots shown for A375, BLM, SK-MEL-28 and WM164 under treatment with different concentrations of OTX-015 based on previously determined IC50s.

9. DISCUSSION

During the last decade, several targeted therapies have been approved for the treatment of malignant melanoma, which mainly target the BRAF and MEK oncogenes². Such therapies have successfully improved the progression free survival of patients despite almost always developing resistance. In addition, dual BRAF and MEK inhibition exhibit limited clinical efficacy in non-BRAF^{V600E}-mutant melanoma. Thus, novel targeted therapies are urgently needed to target the invasive nature of this disease. MNK1/2 kinases have been established as promising therapeutic targets in cancer and in melanoma⁵⁷. However, given the cytostatic nature of MNK inhibitors, these latter were suggested to be more efficient if used in combination therapy¹. To this end, we performed a CRISPR-KO screen in the NALM-6 pre-B cell lymphoma line in the presence of SEL201 to identify potential therapeutic partners with MNK1/2 inhibitors. Interestingly, BRD2 featured as a top hit among synthetic lethal genes, which enticed further investigations on dual MNK and BET-protein inhibition in melanoma.

Cell viability assays and colony formation assays highlighted the efficacy of combining SEL201 and OTX-015 in six melanoma cell lines. While the combination of SEL201 and OTX-015 exhibited efficacy in the predominant cutaneous melanoma subtype, that is *BRAF*-mutant, it is interesting to note that dual therapy using such drugs also showed considerable anti-tumorigenic activity in hard-to-treat *NRAS*-mutant melanomas. Further pre-clinical data are required to establish MNKi and BETi as a treatment option for non-BRAF^{V600E}-mutant melanoma. In contrast to OTX-015, the combination of PLX51107 with SEL201 showed efficacy in only 2 out of 6 cell lines tested. PLX51107 was suggested to cause fewer toxicities at pharmacologically effective doses than previous generation BETi JQ1 and OTX-015¹⁸⁰. Despite such advantages, the effect of PLX51107 in combination therapy with SEL201 showed reduced efficacy when compared to its BETi counterpart OTX-015, which may be due to different structural and functional properties of these drugs. While PLX51107 had shown efficacy when combined with immunotherapies in melanoma¹⁵⁷, OTX-015 decreased cell proliferation and induced cell cycle arrest in NSCLC and B-cell lymphoma^{181,182}. Thus, given our results, we employed OTX-015 for further experiments. Similarly, the use of eFT508 displayed lower efficacy than SEL201 when combined with OTX-015, despite inhibiting MNK1/2 kinases at lower doses⁹⁹. Taken together, these results established SEL201 and OTX-015 as an efficient dual therapy for *BRAF*- and *NRAS*-mutant melanoma cell lines.

While SEL201 treatment of five melanoma cell lines showed robust p-eIF4E suppression at a concentration of 2.5 μ M, a readout for BETi activity was not successfully shown. The use of OTX-015 at 10-50nM did not cause decreased BET protein levels nor a decrease in c-myc (data not shown), a known transcriptional target of BET-family proteins^{148,150}. Of note, the concentrations of BETi used throughout our *in vitro* experiments are significantly lower than in previous studies ranging between 300nM-1 μ M, which may account for the observed high c-myc expression across treatment conditions¹⁵⁴.

Through genetic knockdown experiments, BRD4 was defined as the main BET-family protein accounting for pharmacological effects of BETi when combined with SEL201. As opposed to BRD2 and BRD3, BRD4 knockdown sensitized A375 cells to SEL201 in short-term dose response assays. These results are in concordance with previous data by Segura et al. highlighting a pivotal role of BRD4 in melanoma¹⁵⁰. However, potential roles of BRD2 and BRD3 in the combination treatment cannot be fully eliminated. In other words, dose response experiments are performed under short treatment durations (3 days) which may have different dynamics than long-term colony formation assays (11 days). Moreover, we posit that dual and triple knockdown of BET proteins may enhance the sensitivity to SEL201 relative to BRD4 knockdown only. On the other hand, genetic abrogation of MNK1/2 is required to confirm the role of these kinases in the combination treatment.

The mechanism through which SEL201 and OTX-015 inhibit colony formation in A375 cells is currently under investigation by our team. While previous studies suggested the involvement of BET-family proteins and MNK1/2 kinases in the transcriptional and translational regulation of cell cycle genes respectively^{57,140}, our data suggested that A375 cells treated with the combination do not display cell cycle arrest. Moreover, CFSE experiments further showed no different proliferative capacity of combo-treated A375 cells relative to single agents alone or control. While such data encouraged investigations on the potential cytotoxic nature of combined SEL201 and OTX-015, we found no significant apoptosis in combo-treated A375 cells when compared to control- or single agent-treated cells across timepoints. While some differences in late apoptotic cells between treatment conditions are statistically significant (e.g. combo-treated cells displayed increased AnV+PI+ cells relative to single agents at 72h), such differences are very minimal – 1-2% – and are of little biological relevance. In other words, such slight increase in the percentage of late apoptotic cells, as observed by Annexin V-PI, are likely not to account for the considerable and potentially synergistic inhibitory effect of the combination as shown by viability assays and colony formation assays. In sum, our data

clearly showed that cell cycle arrest, inhibition of cellular proliferation and apoptosis do not individually explain the observed biological phenotype of the combination treatment in A375 cells. Furthermore, preliminary β -galactosidase staining of A375 cells did not show signs of a potentially senescent phenotype induced by combined SEL201 and OTX-015. We further attempted to characterize the invasive nature of A375 and BLM cells under SEL201 and OTX-015 dual treatment. Boyden chamber invasion assays using Matrigel showed no statistically significant cellular invasion between treatment conditions in A375 or BLM cells. Nevertheless, the use of other coating substrates (e.g. collagen I) may confer different invasive potential to melanoma cells.

RNA-seq and proteomics are required to elucidate a mechanism through which SEL201 and OTX-015 operate to inhibit melanoma cells. Several studies have highlighted the pivotal role of dysregulated epigenetics and mRNA translation in the process of melanoma phenotype switching^{103,107}. Thus, we expect dual BET and MNK inhibition to suppress the expression of genes with an invasive signature. Moreover, transcription factors with oncogenic properties (e.g. MYC) may further stimulate mRNA translation beyond its role in transcription, suggesting the dual targeting of transcription and translation to be a relevant therapeutic strategy in cancer¹⁸³. In the context of our data, pro-tumorigenic genes may be dually suppressed at the level of transcription – due to genetic silencing induced by BET inhibitors – and at the level of mRNA translation – due to the inhibition of MNK1/2 kinases.

Given the promising inhibitory effect of SEL201 and OTX-015 in melanoma cells, we further characterized the effects of the combination in a syngeneic melanoma mouse model with subcutaneously injected Yummer 1.7 cells. Interestingly, combination treated mice displayed a slight improvement in survival when compared to vehicle or single agent-treatment arms. However, single agent drugs did not show survival advantages over vehicle treatment. Such results are counter to previously published data, whereby SEL201 improved survival as monotherapy in the Yummer 1.7 subcutaneously injected mice⁸³. A potential reason for this observation may be the large variation in tumor growth of vehicle-treated mice which may be caused by technical problems in the experiment (supplemental figure 1). More replicates are required to further narrow the standard deviation and ultimately yield conclusive results. Preliminary p-eIF4E IHC staining of tumor tissues also showed no differences in staining intensity between vehicle- and SEL201-treated mice, thus pointing to a possibility of lack of effective dosing of the mice with the MNK1/2 inhibitor. Our group and others have shown effective on-target engagement and p-eIF4E repression by SEL201 in mouse models of melanoma, breast cancer and leukemia^{83,184,185}. Thus, the improved survival observed in combo-treated

mice may not be attributable to MNK1/2 kinase inhibition within the tumor tissue. Rather SEL201-treatment may operate pharmacologically on immune cells which in turn can cause tumor shrinkage. Such hypothetical mechanism of action needs further validation, namely through p-eIF4E staining of lymph nodes and assessment of T-cell activation. Furthermore, Ki67 IHC staining of tumor tissues showed no significant differences between treatment conditions. This can be explained as a result of the tumors manifesting logarithmic growth rates at endpoint (supplemental figure 1). In other words, despite delaying tumor growth, drug treatment is eventually rendered inefficient – potentially through acquired resistance – and drug-treated tumors resume exponential growth rates. As a result, Ki67 expression remains the same across conditions due to similar cellular proliferative activity. Future experiments aiming to assess Ki67 expression will require a predetermined endpoint based on time and not solely on tumor size. In other words, all tumors across conditions need to be harvested at a specific timepoint.

As the combination treatment enhanced survival in a syngeneic mouse model independently of p-eIF4E inhibition within tumors, we further questioned whether eIF4E phosphorylation recapitulates pharmacological effects of SEL201. Dose response curves using OTX-015 or PLX51107 showed an enhanced BETi sensitivity of eIF4E^{WT} cells relative to eIF4E^{KI} (devoid of p-eIF4E), thus excluding a role of p-eIF4E in the combination treatment. Pham et al. had shown upregulation of p-eIF4E in response to BETi treatment of thyroid and pancreatic cancer cells, which was determined to occur through p38 MAPK and Rac-signalling¹⁶⁸. In contrast to such results, we showed that OTX-015 treatment did not induce p-eIF4E consistently across melanoma cell lines. Taken together, this suggests that MNK1/2 kinases may perform pro-oncogenic functions independently of p-eIF4E.

While MNK1/2 kinases have been suggested to perform oncogenic functions through the canonical MNK-eIF4E axis, little is known about their roles beyond phosphorylating eIF4E. In fact, our data thus far may suggest that the combined anti-tumorigenic effect of SEL201 and OTX-015 is not dependent on p-eIF4E suppression (figure 17). One possibility is that MNK1/2 kinases target other proteins to induce tumor progression. Such assertion is supported by the subcellular localization of MNK1/2 kinases, which are expressed in the cytoplasm and in the nucleus⁵⁷. In other words, the expression of MNK1/2 kinases in the nucleus hint for unknown nuclear functions. Thus, to establish whether nuclear MNK kinase expression associates with oncogenicity, we performed MNK1 immunohistochemistry (IHC) staining in a breast cancer tumor microarray (TMA) composed of 150

cores, each representing individual patients (supplemental figure 2A). Histoscores were used to quantify the staining intensity of each core, denoted by the following equation:

$$\text{Histoscore} = (\% \text{ cells at intensity } 0) * 0 + (\% \text{ cells at intensity } 1) * 1 + (\% \text{ cells at intensity } 2) * 2 + (\% \text{ cells at intensity } 3) * 3,$$

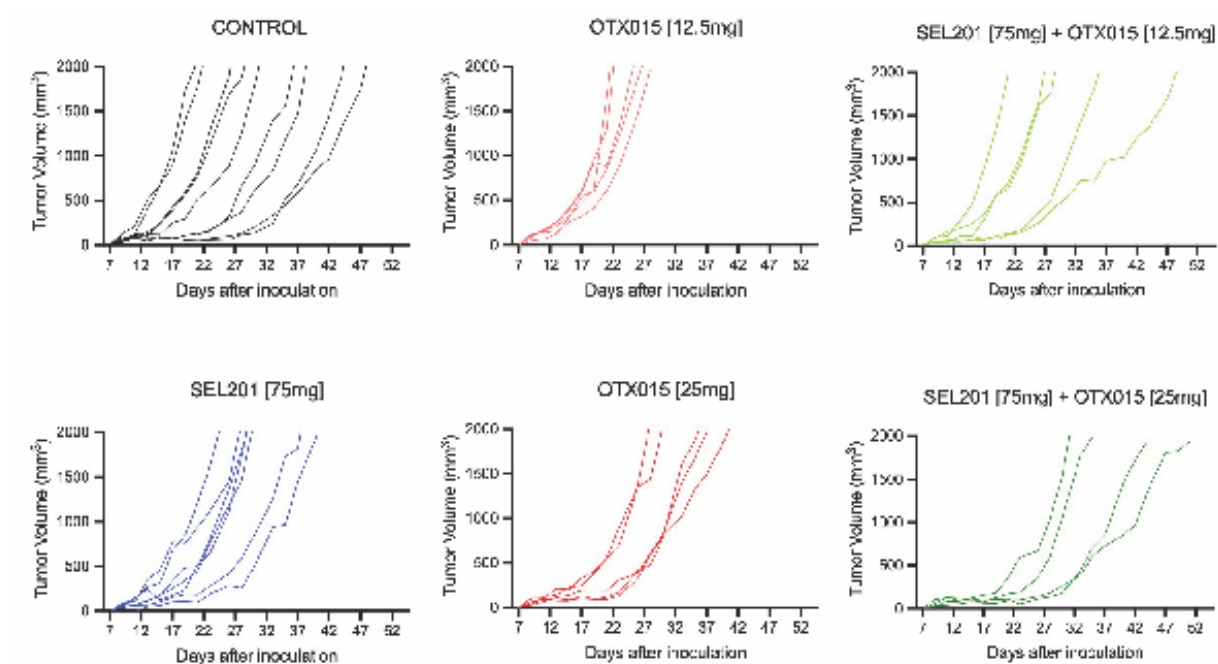
where 0, 1, 2, and 3 represent increasing staining intensities.

We found that MNK1 manifested higher nuclear than cytoplasmic expression. In 87 out of 150 cores, nuclear MNK1 expression exceeded a histoscore of 101, compared to 52 cores with such cytoplasmic MNK1 expression. In contrast, p-eIF4E expression did not show any differences in terms of nuclear and cytoplasmic staining intensity (supplemental figure 2B). These results hint for additional oncogenic functions of MNK1 that may be independent of eIF4E phosphorylation. Proteomic experiments are required to characterize targets and substrates of nuclear MNK1. Such nuclear MNK1 expression may be specifically attributable to the shorter isoform of MNK1 (MNK1b) which displays enhanced nuclear expression correlates with poor prognosis in breast cancer⁹². Thus, the mechanistic nature of dual MNK and BET inhibition may involve the cooperation between the shorter b isoforms of MNK kinases and BET proteins within the nucleus.

10. CONCLUSION

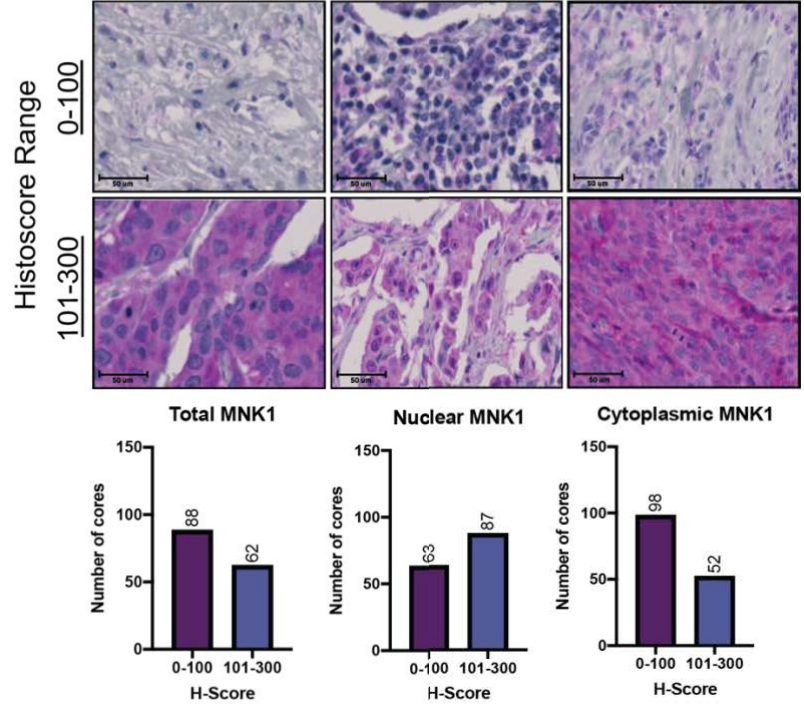
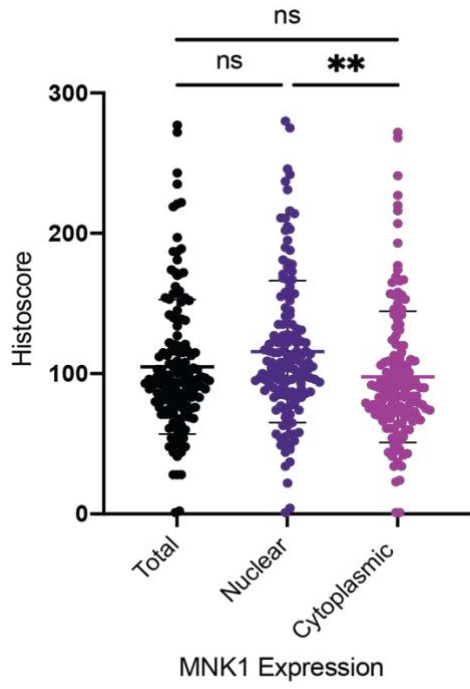
Melanoma, the deadliest form of skin cancer, rapidly develops resistance to currently available therapies. Furthermore, currently approved targeted therapies manifest limited efficacy in non- $BRAF^{V600E}$ molecular subtypes. Our research highlighted the promising activity of combined SEL201 and OTX-015 in the treatment of *BRAF*- and *NRAS*-mutant melanoma cells *in vitro* and *in vivo*. While additional experiments are required to fully validate the pre-clinical activity of this combination, our results provide a promising therapeutic alternative to currently available therapies in melanoma in resistant and hard-to-treat tumors.

11. SUPPLEMENTAL FIGURES

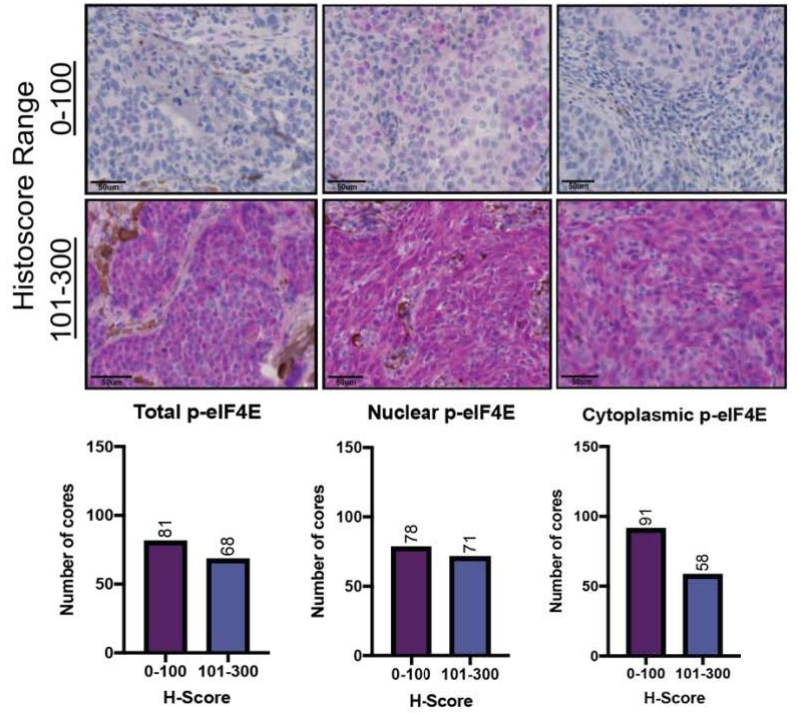
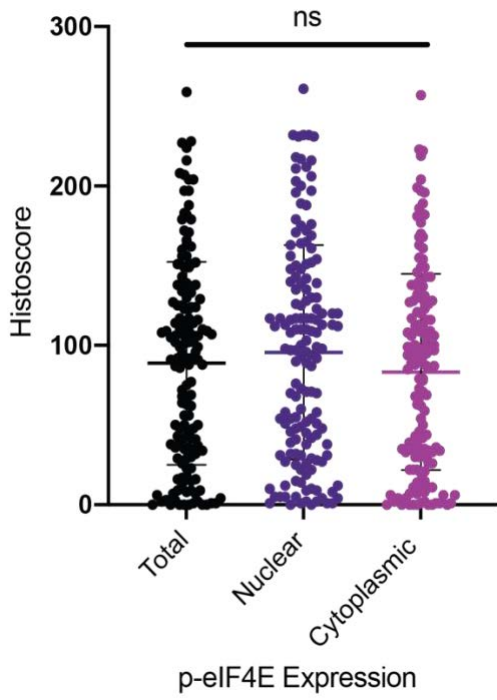


Supplemental figure 1. Tumor volume evolution in C57BL/6J mice subcutaneously injected with Yumrer 1.7 cells. Graphs showing the progressive tumor growth across treatment arms. See figure 16 for survival and IHC data. Each dotted line represents one mouse.

A



B



Supplemental figure 2. MNK1 displays higher nuclear than cytoplasmic expression in a breast cancer tissue microarray. A) Left panel shows histoscore distribution of total, nuclear and cytoplasmic expression of MNK1. Each dot represents a single core within the TMA (total of 150 cores). Count of cores falling within specific histoscore ranges and associated representative images are shown to the right. B) Similar to A) except p-eIF4E replaces MNK1. Statistical analysis by one-way ANOVA and Tuckey post-hoc test. ns: not significant (≥ 0.05); * $0.01 \leq p \leq 0.05$, ** $0.001 \leq p \leq 0.01$, *** $0.0001 \leq p \leq 0.001$, **** $p < 0.0001$

12. REFERENCES

- 1 Xie, J., Merrett, J. E., Jensen, K. B. & Proud, C. G. The MAP kinase-interacting kinases (MNKs) as targets in oncology. *Expert Opin Ther Targets* **23**, 187-199, doi:10.1080/14728222.2019.1571043 (2019).
- 2 Curti, B. D. & Faries, M. B. Recent Advances in the Treatment of Melanoma. *N Engl J Med* **384**, 2229-2240, doi:10.1056/NEJMra2034861 (2021).
- 3 Davis, L. E., Shalin, S. C. & Tackett, A. J. Current state of melanoma diagnosis and treatment. *Cancer Biol Ther* **20**, 1366-1379, doi:10.1080/15384047.2019.1640032 (2019).
- 4 Siegel, R. L., Miller, K. D., Fuchs, H. E. & Jemal, A. Cancer Statistics, 2021. *CA Cancer J Clin* **71**, 7-33, doi:10.3322/caac.21654 (2021).
- 5 Rabbie, R., Ferguson, P., Molina-Aguilar, C., Adams, D. J. & Robles-Espinoza, C. D. Melanoma subtypes: genomic profiles, prognostic molecular markers and therapeutic possibilities. *J Pathol* **247**, 539-551, doi:10.1002/path.5213 (2019).
- 6 Pfeifer, G. P. Environmental exposures and mutational patterns of cancer genomes. *Genome Med* **2**, 54, doi:10.1186/gm175 (2010).
- 7 Patrawala, S. *et al.* Discordance of histopathologic parameters in cutaneous melanoma: Clinical implications. *J Am Acad Dermatol* **74**, 75-80, doi:10.1016/j.jaad.2015.09.008 (2016).
- 8 Cancer Genome Atlas, N. Genomic Classification of Cutaneous Melanoma. *Cell* **161**, 1681-1696, doi:10.1016/j.cell.2015.05.044 (2015).
- 9 Leonardi, G. C. *et al.* Cutaneous melanoma: From pathogenesis to therapy (Review). *Int J Oncol* **52**, 1071-1080, doi:10.3892/ijo.2018.4287 (2018).
- 10 Sun, J., Carr, M. J. & Khushalani, N. I. Principles of Targeted Therapy for Melanoma. *Surg Clin North Am* **100**, 175-188, doi:10.1016/j.suc.2019.09.013 (2020).
- 11 Boespflug, A., Caramel, J., Dalle, S. & Thomas, L. Treatment of NRAS-mutated advanced or metastatic melanoma: rationale, current trials and evidence to date. *Ther Adv Med Oncol* **9**, 481-492, doi:10.1177/1758834017708160 (2017).
- 12 Nassar, K. W. & Tan, A. C. The mutational landscape of mucosal melanoma. *Semin Cancer Biol* **61**, 139-148, doi:10.1016/j.semcancer.2019.09.013 (2020).
- 13 Zhan, Y. *et al.* MNK1/2 inhibition limits oncogenicity and metastasis of KIT-mutant melanoma. *J Clin Invest* **127**, 4179-4192, doi:10.1172/JCI91258 (2017).

- 14 Abbaspour Babaei, M., Kamalidehghan, B., Saleem, M., Huri, H. Z. & Ahmadipour, F. Receptor tyrosine kinase (c-Kit) inhibitors: a potential therapeutic target in cancer cells. *Drug Des Devel Ther* **10**, 2443-2459, doi:10.2147/DDDT.S89114 (2016).
- 15 Shain, A. H. & Bastian, B. C. From melanocytes to melanomas. *Nat Rev Cancer* **16**, 345-358, doi:10.1038/nrc.2016.37 (2016).
- 16 Shain, A. H. *et al.* The Genetic Evolution of Melanoma from Precursor Lesions. *N Engl J Med* **373**, 1926-1936, doi:10.1056/NEJMoa1502583 (2015).
- 17 Heidenreich, B. & Kumar, R. TERT promoter mutations in telomere biology. *Mutat Res Rev Mutat Res* **771**, 15-31, doi:10.1016/j.mrrev.2016.11.002 (2017).
- 18 Serrano, M., Hannon, G. J. & Beach, D. A new regulatory motif in cell-cycle control causing specific inhibition of cyclin D/CDK4. *Nature* **366**, 704-707, doi:10.1038/366704a0 (1993).
- 19 Ozenne, P., Eymin, B., Brambilla, E. & Gazzeri, S. The ARF tumor suppressor: structure, functions and status in cancer. *Int J Cancer* **127**, 2239-2247, doi:10.1002/ijc.25511 (2010).
- 20 Kadoch, C. *et al.* Proteomic and bioinformatic analysis of mammalian SWI/SNF complexes identifies extensive roles in human malignancy. *Nat Genet* **45**, 592-601, doi:10.1038/ng.2628 (2013).
- 21 Chen, C. Y., Chen, J., He, L. & Stiles, B. L. PTEN: Tumor Suppressor and Metabolic Regulator. *Front Endocrinol (Lausanne)* **9**, 338, doi:10.3389/fendo.2018.00338 (2018).
- 22 Hafner, A., Bulyk, M. L., Jambhekar, A. & Lahav, G. The multiple mechanisms that regulate p53 activity and cell fate. *Nat Rev Mol Cell Biol* **20**, 199-210, doi:10.1038/s41580-019-0110-x (2019).
- 23 Dankort, D. *et al.* Braf(V600E) cooperates with Pten loss to induce metastatic melanoma. *Nat Genet* **41**, 544-552, doi:10.1038/ng.356 (2009).
- 24 Naffa, R. *et al.* P38 MAPK Promotes Migration and Metastatic Activity of BRAF Mutant Melanoma Cells by Inducing Degradation of PMCA4b. *Cells* **9**, doi:10.3390/cells9051209 (2020).
- 25 Wen, S. Y. *et al.* Roles of p38alpha and p38beta mitogenactivated protein kinase isoforms in human malignant melanoma A375 cells. *Int J Mol Med* **44**, 2123-2132, doi:10.3892/ijmm.2019.4383 (2019).
- 26 Ivanov, V. N. & Ronai, Z. p38 protects human melanoma cells from UV-induced apoptosis through down-regulation of NF-kappaB activity and Fas expression. *Oncogene* **19**, 3003-3012, doi:10.1038/sj.onc.1203602 (2000).

- 27 Cuenda, A. & Rousseau, S. p38 MAP-kinases pathway regulation, function and role in human diseases. *Biochim Biophys Acta* **1773**, 1358-1375, doi:10.1016/j.bbamcr.2007.03.010 (2007).
- 28 Loesch, M. & Chen, G. The p38 MAPK stress pathway as a tumor suppressor or more? *Front Biosci* **13**, 3581-3593, doi:10.2741/2951 (2008).
- 29 Chiacchiera, F. *et al.* p38alpha blockade inhibits colorectal cancer growth in vivo by inducing a switch from HIF1alpha- to FoxO-dependent transcription. *Cell Death Differ* **16**, 1203-1214, doi:10.1038/cdd.2009.36 (2009).
- 30 Chapman, P. B. *et al.* Improved survival with vemurafenib in melanoma with BRAF V600E mutation. *N Engl J Med* **364**, 2507-2516, doi:10.1056/NEJMoa1103782 (2011).
- 31 Ballantyne, A. D. & Garnock-Jones, K. P. Dabrafenib: first global approval. *Drugs* **73**, 1367-1376, doi:10.1007/s40265-013-0095-2 (2013).
- 32 Shi, H. *et al.* Acquired resistance and clonal evolution in melanoma during BRAF inhibitor therapy. *Cancer Discov* **4**, 80-93, doi:10.1158/2159-8290.CD-13-0642 (2014).
- 33 Das Thakur, M. *et al.* Modelling vemurafenib resistance in melanoma reveals a strategy to forestall drug resistance. *Nature* **494**, 251-255, doi:10.1038/nature11814 (2013).
- 34 Paraiso, K. H. *et al.* Recovery of phospho-ERK activity allows melanoma cells to escape from BRAF inhibitor therapy. *Br J Cancer* **102**, 1724-1730, doi:10.1038/sj.bjc.6605714 (2010).
- 35 Johannessen, C. M. *et al.* COT drives resistance to RAF inhibition through MAP kinase pathway reactivation. *Nature* **468**, 968-972, doi:10.1038/nature09627 (2010).
- 36 Greger, J. G. *et al.* Combinations of BRAF, MEK, and PI3K/mTOR inhibitors overcome acquired resistance to the BRAF inhibitor GSK2118436 dabrafenib, mediated by NRAS or MEK mutations. *Mol Cancer Ther* **11**, 909-920, doi:10.1158/1535-7163.MCT-11-0989 (2012).
- 37 Long, G. V. *et al.* Long-Term Outcomes in Patients With BRAF V600-Mutant Metastatic Melanoma Who Received Dabrafenib Combined With Trametinib. *J Clin Oncol* **36**, 667-673, doi:10.1200/JCO.2017.74.1025 (2018).
- 38 Larkin, J. *et al.* Combined vemurafenib and cobimetinib in BRAF-mutated melanoma. *N Engl J Med* **371**, 1867-1876, doi:10.1056/NEJMoa1408868 (2014).
- 39 Dummer, R. *et al.* Encorafenib plus binimetinib versus vemurafenib or encorafenib in patients with BRAF-mutant melanoma (COLUMBUS): a multicentre, open-label, randomised phase 3 trial. *Lancet Oncol* **19**, 603-615, doi:10.1016/S1470-2045(18)30142-6 (2018).

- 40 Welsh, S. J., Rizos, H., Scolyer, R. A. & Long, G. V. Resistance to combination BRAF and MEK inhibition in metastatic melanoma: Where to next? *Eur J Cancer* **62**, 76-85, doi:10.1016/j.ejca.2016.04.005 (2016).
- 41 Long, G. V. *et al.* Increased MAPK reactivation in early resistance to dabrafenib/trametinib combination therapy of BRAF-mutant metastatic melanoma. *Nat Commun* **5**, 5694, doi:10.1038/ncomms6694 (2014).
- 42 Heinzerling, L. *et al.* Tolerability of BRAF/MEK inhibitor combinations: adverse event evaluation and management. *ESMO Open* **4**, e000491, doi:10.1136/esmoopen-2019-000491 (2019).
- 43 Alexandrov, L. B. *et al.* Signatures of mutational processes in human cancer. *Nature* **500**, 415-421, doi:10.1038/nature12477 (2013).
- 44 Topalian, S. L., Drake, C. G. & Pardoll, D. M. Immune checkpoint blockade: a common denominator approach to cancer therapy. *Cancer Cell* **27**, 450-461, doi:10.1016/j.ccell.2015.03.001 (2015).
- 45 Patel, S. P. & Kurzrock, R. PD-L1 Expression as a Predictive Biomarker in Cancer Immunotherapy. *Mol Cancer Ther* **14**, 847-856, doi:10.1158/1535-7163.MCT-14-0983 (2015).
- 46 Larkin, J. *et al.* Five-Year Survival with Combined Nivolumab and Ipilimumab in Advanced Melanoma. *N Engl J Med* **381**, 1535-1546, doi:10.1056/NEJMoa1910836 (2019).
- 47 Simeone, E. *et al.* Immunotherapy in metastatic melanoma: a novel scenario of new toxicities and their management. *Melanoma Manag* **6**, MMT30, doi:10.2217/mmt-2019-0005 (2019).
- 48 Baxi, S. *et al.* Immune-related adverse events for anti-PD-1 and anti-PD-L1 drugs: systematic review and meta-analysis. *BMJ* **360**, k793, doi:10.1136/bmj.k793 (2018).
- 49 Gutzmer, R. *et al.* Atezolizumab, vemurafenib, and cobimetinib as first-line treatment for unresectable advanced BRAF(V600) mutation-positive melanoma (IMspire150): primary analysis of the randomised, double-blind, placebo-controlled, phase 3 trial. *Lancet* **395**, 1835-1844, doi:10.1016/S0140-6736(20)30934-X (2020).
- 50 Tangella, L. P., Clark, M. E. & Gray, E. S. Resistance mechanisms to targeted therapy in BRAF-mutant melanoma - A mini review. *Biochim Biophys Acta Gen Subj* **1865**, 129736, doi:10.1016/j.bbagen.2020.129736 (2021).
- 51 Paraiso, K. H. *et al.* PTEN loss confers BRAF inhibitor resistance to melanoma cells through the suppression of BIM expression. *Cancer Res* **71**, 2750-2760, doi:10.1158/0008-5472.CAN-10-2954 (2011).

- 52 Jiang, C. C. *et al.* MEK-independent survival of B-RAFV600E melanoma cells selected for resistance to apoptosis induced by the RAF inhibitor PLX4720. *Clin Cancer Res* **17**, 721-730, doi:10.1158/1078-0432.CCR-10-2225 (2011).
- 53 Bedard, P. L. *et al.* First-in-human trial of the PI3Kbeta-selective inhibitor SAR260301 in patients with advanced solid tumors. *Cancer* **124**, 315-324, doi:10.1002/cncr.31044 (2018).
- 54 Lassen, A. *et al.* Effects of AKT inhibitor therapy in response and resistance to BRAF inhibition in melanoma. *Mol Cancer* **13**, 83, doi:10.1186/1476-4598-13-83 (2014).
- 55 Wang, B. *et al.* Targeting mTOR signaling overcomes acquired resistance to combined BRAF and MEK inhibition in BRAF-mutant melanoma. *Oncogene* **40**, 5590-5599, doi:10.1038/s41388-021-01911-5 (2021).
- 56 Subbiah, V. *et al.* Phase I Study of the BRAF Inhibitor Vemurafenib in Combination With the Mammalian Target of Rapamycin Inhibitor Everolimus in Patients With BRAF-Mutated Malignancies. *JCO Precis Oncol* **2**, doi:10.1200/PO.18.00189 (2018).
- 57 Prabhu, S. A., Moussa, O., Miller, W. H., Jr. & Del Rincon, S. V. The MNK1/2-eIF4E Axis as a Potential Therapeutic Target in Melanoma. *Int J Mol Sci* **21**, doi:10.3390/ijms21114055 (2020).
- 58 Ueda, T., Watanabe-Fukunaga, R., Fukuyama, H., Nagata, S. & Fukunaga, R. Mnk2 and Mnk1 are essential for constitutive and inducible phosphorylation of eukaryotic initiation factor 4E but not for cell growth or development. *Mol Cell Biol* **24**, 6539-6549, doi:10.1128/MCB.24.15.6539-6549.2004 (2004).
- 59 Sonenberg, N. eIF4E, the mRNA cap-binding protein: from basic discovery to translational research. *Biochem Cell Biol* **86**, 178-183, doi:10.1139/O08-034 (2008).
- 60 Merrick, W. C. eIF4F: a retrospective. *J Biol Chem* **290**, 24091-24099, doi:10.1074/jbc.R115.675280 (2015).
- 61 Marcotrigiano, J., Gingras, A. C., Sonenberg, N. & Burley, S. K. Cap-dependent translation initiation in eukaryotes is regulated by a molecular mimic of eIF4G. *Mol Cell* **3**, 707-716, doi:10.1016/s1097-2765(01)80003-4 (1999).
- 62 Pinto-Diez, C., Ferreras-Martin, R., Carrion-Marchante, R., Gonzalez, V. M. & Martin, M. E. Deeping in the Role of the MAP-Kinases Interacting Kinases (MNKs) in Cancer. *Int J Mol Sci* **21**, doi:10.3390/ijms21082967 (2020).

- 63 Lazaris-Karatzas, A., Montine, K. S. & Sonenberg, N. Malignant transformation by a eukaryotic initiation factor subunit that binds to mRNA 5' cap. *Nature* **345**, 544-547, doi:10.1038/345544a0 (1990).
- 64 Graff, J. R. *et al.* eIF4E activation is commonly elevated in advanced human prostate cancers and significantly related to reduced patient survival. *Cancer Res* **69**, 3866-3873, doi:10.1158/0008-5472.CAN-08-3472 (2009).
- 65 Coleman, L. J. *et al.* Combined analysis of eIF4E and 4E-binding protein expression predicts breast cancer survival and estimates eIF4E activity. *Br J Cancer* **100**, 1393-1399, doi:10.1038/sj.bjc.6605044 (2009).
- 66 Holm, N. *et al.* A prospective trial on initiation factor 4E (eIF4E) overexpression and cancer recurrence in node-negative breast cancer. *Ann Surg Oncol* **15**, 3207-3215, doi:10.1245/s10434-008-0086-9 (2008).
- 67 Zhou, S., Wang, G. P., Liu, C. & Zhou, M. Eukaryotic initiation factor 4E (eIF4E) and angiogenesis: prognostic markers for breast cancer. *BMC Cancer* **6**, 231, doi:10.1186/1471-2407-6-231 (2006).
- 68 Wang, R. *et al.* Overexpression of eukaryotic initiation factor 4E (eIF4E) and its clinical significance in lung adenocarcinoma. *Lung Cancer* **66**, 237-244, doi:10.1016/j.lungcan.2009.02.001 (2009).
- 69 Fang, D., Peng, J., Wang, G., Zhou, D. & Geng, X. Upregulation of eukaryotic translation initiation factor 4E associates with a poor prognosis in gallbladder cancer and promotes cell proliferation in vitro and in vivo. *Int J Mol Med* **44**, 1325-1332, doi:10.3892/ijmm.2019.4317 (2019).
- 70 Niu, Z. *et al.* Protein expression of eIF4E and integrin alphavbeta6 in colon cancer can predict clinical significance, reveal their correlation and imply possible mechanism of interaction. *Cell Biosci* **4**, 23, doi:10.1186/2045-3701-4-23 (2014).
- 71 Chen, Y. T., Tsai, H. P., Wu, C. C., Wang, J. Y. & Chai, C. Y. Eukaryotic translation initiation factor 4E (eIF-4E) expressions are associated with poor prognosis in colorectal adenocarcinoma. *Pathol Res Pract* **213**, 490-495, doi:10.1016/j.prp.2017.02.004 (2017).
- 72 Jiang, X. M. *et al.* Prognostic significance of eukaryotic initiation factor 4E in hepatocellular carcinoma. *J Cancer Res Clin Oncol* **142**, 2309-2317, doi:10.1007/s00432-016-2232-2 (2016).

- 73 Salehi, Z. & Mashayekhi, F. Expression of the eukaryotic translation initiation factor 4E (eIF4E) and 4E-BP1 in esophageal cancer. *Clin Biochem* **39**, 404-409, doi:10.1016/j.clinbiochem.2005.11.007 (2006).
- 74 Salehi, Z., Mashayekhi, F. & Shahosseini, F. Significance of eIF4E expression in skin squamous cell carcinoma. *Cell Biol Int* **31**, 1400-1404, doi:10.1016/j.cellbi.2007.06.006 (2007).
- 75 Topisirovic, I., Ruiz-Gutierrez, M. & Borden, K. L. Phosphorylation of the eukaryotic translation initiation factor eIF4E contributes to its transformation and mRNA transport activities. *Cancer Res* **64**, 8639-8642, doi:10.1158/0008-5472.CAN-04-2677 (2004).
- 76 Martinez-Saez, E. *et al.* pEIF4E as an independent prognostic factor and a potential therapeutic target in diffuse infiltrating astrocytomas. *Cancer Med* **5**, 2501-2512, doi:10.1002/cam4.817 (2016).
- 77 Yoshizawa, A. *et al.* Overexpression of phospho-eIF4E is associated with survival through AKT pathway in non-small cell lung cancer. *Clin Cancer Res* **16**, 240-248, doi:10.1158/1078-0432.CCR-09-0986 (2010).
- 78 Zheng, J. *et al.* Phosphorylated Mnk1 and eIF4E are associated with lymph node metastasis and poor prognosis of nasopharyngeal carcinoma. *PLoS One* **9**, e89220, doi:10.1371/journal.pone.0089220 (2014).
- 79 Hou, S. *et al.* Significance of MNK1 in prognostic prediction and chemotherapy development of epithelial ovarian cancer. *Clin Transl Oncol* **19**, 1107-1116, doi:10.1007/s12094-017-1646-x (2017).
- 80 Wang, X., Wang, Y., Zhang, Q., Zhuang, H. & Chen, B. MAP Kinase-Interacting Kinase 1 Promotes Proliferation and Invasion of Hepatocellular Carcinoma and Is an Unfavorable Prognostic Biomarker. *Med Sci Monit* **24**, 1759-1767, doi:10.12659/msm.909012 (2018).
- 81 Guo, Z. *et al.* MAP kinase-interacting serine/threonine kinase 2 promotes proliferation, metastasis, and predicts poor prognosis in non-small cell lung cancer. *Sci Rep* **7**, 10612, doi:10.1038/s41598-017-10397-9 (2017).
- 82 Carter, J. H. *et al.* Phosphorylation of eIF4E serine 209 is associated with tumour progression and reduced survival in malignant melanoma. *Br J Cancer* **114**, 444-453, doi:10.1038/bjc.2015.450 (2016).
- 83 Huang, F. *et al.* Inhibiting the MNK1/2-eIF4E axis impairs melanoma phenotype switching and potentiates antitumor immune responses. *J Clin Invest* **131**, doi:10.1172/JCI140752 (2021).

- 84 Furic, L. *et al.* eIF4E phosphorylation promotes tumorigenesis and is associated with prostate cancer progression. *Proc Natl Acad Sci U S A* **107**, 14134-14139, doi:10.1073/pnas.1005320107 (2010).
- 85 Truitt, M. L. *et al.* Differential Requirements for eIF4E Dose in Normal Development and Cancer. *Cell* **162**, 59-71, doi:10.1016/j.cell.2015.05.049 (2015).
- 86 Slentz-Kesler, K. *et al.* Identification of the human Mnk2 gene (MKNK2) through protein interaction with estrogen receptor beta. *Genomics* **69**, 63-71, doi:10.1006/geno.2000.6299 (2000).
- 87 Fukunaga, R. & Hunter, T. MNK1, a new MAP kinase-activated protein kinase, isolated by a novel expression screening method for identifying protein kinase substrates. *EMBO J* **16**, 1921-1933, doi:10.1093/emboj/16.8.1921 (1997).
- 88 Waskiewicz, A. J., Flynn, A., Proud, C. G. & Cooper, J. A. Mitogen-activated protein kinases activate the serine/threonine kinases Mnk1 and Mnk2. *EMBO J* **16**, 1909-1920, doi:10.1093/emboj/16.8.1909 (1997).
- 89 O'Loghlen, A. *et al.* Identification and molecular characterization of Mnk1b, a splice variant of human MAP kinase-interacting kinase Mnk1. *Exp Cell Res* **299**, 343-355, doi:10.1016/j.yexcr.2004.06.006 (2004).
- 90 Parra, J. L., Buxade, M. & Proud, C. G. Features of the catalytic domains and C termini of the MAPK signal-integrating kinases Mnk1 and Mnk2 determine their differing activities and regulatory properties. *J Biol Chem* **280**, 37623-37633, doi:10.1074/jbc.M508356200 (2005).
- 91 Scheper, G. C. *et al.* The N and C termini of the splice variants of the human mitogen-activated protein kinase-interacting kinase Mnk2 determine activity and localization. *Mol Cell Biol* **23**, 5692-5705, doi:10.1128/MCB.23.16.5692-5705.2003 (2003).
- 92 Pinto-Diez, C. *et al.* Increased expression of MNK1b, the spliced isoform of MNK1, predicts poor prognosis and is associated with triple-negative breast cancer. *Oncotarget* **9**, 13501-13516, doi:10.18632/oncotarget.24417 (2018).
- 93 Goto, S., Yao, Z. & Proud, C. G. The C-terminal domain of Mnk1a plays a dual role in tightly regulating its activity. *Biochem J* **423**, 279-290, doi:10.1042/BJ20090228 (2009).
- 94 Karni, R. *et al.* The gene encoding the splicing factor SF2/ASF is a proto-oncogene. *Nat Struct Mol Biol* **14**, 185-193, doi:10.1038/nsmb1209 (2007).

- 95 Adesso, L. *et al.* Gemcitabine triggers a pro-survival response in pancreatic cancer cells through activation of the MNK2/eIF4E pathway. *Oncogene* **32**, 2848-2857, doi:10.1038/onc.2012.306 (2013).
- 96 Maimon, A. *et al.* Mnk2 alternative splicing modulates the p38-MAPK pathway and impacts Ras-induced transformation. *Cell Rep* **7**, 501-513, doi:10.1016/j.celrep.2014.03.041 (2014).
- 97 Jin, X., Yu, R., Wang, X., Proud, C. G. & Jiang, T. Progress in developing MNK inhibitors. *Eur J Med Chem* **219**, 113420, doi:10.1016/j.ejmech.2021.113420 (2021).
- 98 Beggs, J. E. *et al.* The MAP kinase-interacting kinases regulate cell migration, vimentin expression and eIF4E/CYFIP1 binding. *Biochem J* **467**, 63-76, doi:10.1042/BJ20141066 (2015).
- 99 Reich, S. H. *et al.* Structure-based Design of Pyridone-Aminal eFT508 Targeting Dysregulated Translation by Selective Mitogen-activated Protein Kinase Interacting Kinases 1 and 2 (MNK1/2) Inhibition. *J Med Chem* **61**, 3516-3540, doi:10.1021/acs.jmedchem.7b01795 (2018).
- 100 Jauch, R. *et al.* Mitogen-activated protein kinases interacting kinases are autoinhibited by a reprogrammed activation segment. *EMBO J* **25**, 4020-4032, doi:10.1038/sj.emboj.7601285 (2006).
- 101 Hou, J., Lam, F., Proud, C. & Wang, S. Targeting Mnks for cancer therapy. *Oncotarget* **3**, 118-131, doi:10.18632/oncotarget.453 (2012).
- 102 Neagu, M. Metabolic Traits in Cutaneous Melanoma. *Front Oncol* **10**, 851, doi:10.3389/fonc.2020.00851 (2020).
- 103 Huang, F., Santinon, F., Flores Gonzalez, R. E. & Del Rincon, S. V. Melanoma Plasticity: Promoter of Metastasis and Resistance to Therapy. *Front Oncol* **11**, 756001, doi:10.3389/fonc.2021.756001 (2021).
- 104 Strub, T., Ballotti, R. & Bertolotto, C. The "ART" of Epigenetics in Melanoma: From histone "Alterations, to Resistance and Therapies". *Theranostics* **10**, 1777-1797, doi:10.7150/thno.36218 (2020).
- 105 Hoek, K. S. *et al.* In vivo switching of human melanoma cells between proliferative and invasive states. *Cancer Res* **68**, 650-656, doi:10.1158/0008-5472.CAN-07-2491 (2008).
- 106 Sensi, M. *et al.* Human cutaneous melanomas lacking MITF and melanocyte differentiation antigens express a functional Axl receptor kinase. *J Invest Dermatol* **131**, 2448-2457, doi:10.1038/jid.2011.218 (2011).

- 107 Suva, M. L., Riggi, N. & Bernstein, B. E. Epigenetic reprogramming in cancer. *Science* **339**, 1567-1570, doi:10.1126/science.1230184 (2013).
- 108 Manning, C. S., Hooper, S. & Sahai, E. A. Intravital imaging of SRF and Notch signalling identifies a key role for EZH2 in invasive melanoma cells. *Oncogene* **34**, 4320-4332, doi:10.1038/onc.2014.362 (2015).
- 109 Ferretti, R., Bhutkar, A., McNamara, M. C. & Lees, J. A. BMI1 induces an invasive signature in melanoma that promotes metastasis and chemoresistance. *Genes Dev* **30**, 18-33, doi:10.1101/gad.267757.115 (2016).
- 110 Lee, L. J. *et al.* Cancer Plasticity: The Role of mRNA Translation. *Trends Cancer* **7**, 134-145, doi:10.1016/j.trecan.2020.09.005 (2021).
- 111 Falletta, P. *et al.* Translation reprogramming is an evolutionarily conserved driver of phenotypic plasticity and therapeutic resistance in melanoma. *Genes Dev* **31**, 18-33, doi:10.1101/gad.290940.116 (2017).
- 112 Wek, R. C. Role of eIF2alpha Kinases in Translational Control and Adaptation to Cellular Stress. *Cold Spring Harb Perspect Biol* **10**, doi:10.1101/cshperspect.a032870 (2018).
- 113 Robichaud, N. *et al.* Phosphorylation of eIF4E promotes EMT and metastasis via translational control of SNAIL and MMP-3. *Oncogene* **34**, 2032-2042, doi:10.1038/onc.2014.146 (2015).
- 114 Gkogkas, C. G. *et al.* Pharmacogenetic inhibition of eIF4E-dependent Mmp9 mRNA translation reverses fragile X syndrome-like phenotypes. *Cell Rep* **9**, 1742-1755, doi:10.1016/j.celrep.2014.10.064 (2014).
- 115 Baylin, S. B. & Jones, P. A. Epigenetic Determinants of Cancer. *Cold Spring Harb Perspect Biol* **8**, doi:10.1101/cshperspect.a019505 (2016).
- 116 Audia, J. E. & Campbell, R. M. Histone Modifications and Cancer. *Cold Spring Harb Perspect Biol* **8**, a019521, doi:10.1101/cshperspect.a019521 (2016).
- 117 Venza, M. *et al.* Epigenetic regulation of p14ARF and p16INK4A expression in cutaneous and uveal melanoma. *Biochim Biophys Acta* **1849**, 247-256, doi:10.1016/j.bbagr.2014.12.004 (2015).
- 118 Di Martile, M., Del Bufalo, D. & Trisciuglio, D. The multifaceted role of lysine acetylation in cancer: prognostic biomarker and therapeutic target. *Oncotarget* **7**, 55789-55810, doi:10.18632/oncotarget.10048 (2016).

- 119 Bechter, O. & Schoffski, P. Make your best BET: The emerging role of BET inhibitor treatment in malignant tumors. *Pharmacol Ther* **208**, 107479, doi:10.1016/j.pharmthera.2020.107479 (2020).
- 120 Allfrey, V. G., Faulkner, R. & Mirsky, A. E. Acetylation and Methylation of Histones and Their Possible Role in the Regulation of Rna Synthesis. *Proc Natl Acad Sci U S A* **51**, 786-794, doi:10.1073/pnas.51.5.786 (1964).
- 121 Filippakopoulos, P. & Knapp, S. The bromodomain interaction module. *FEBS Lett* **586**, 2692-2704, doi:10.1016/j.febslet.2012.04.045 (2012).
- 122 Fujisawa, T. & Filippakopoulos, P. Functions of bromodomain-containing proteins and their roles in homeostasis and cancer. *Nat Rev Mol Cell Biol* **18**, 246-262, doi:10.1038/nrm.2016.143 (2017).
- 123 Spriano, F., Stathis, A. & Bertoni, F. Targeting BET bromodomain proteins in cancer: The example of lymphomas. *Pharmacol Ther*, 107631, doi:10.1016/j.pharmthera.2020.107631 (2020).
- 124 Bourova-Flin, E., Chuffart, F., Rousseaux, S. & Khochbin, S. The Role of Bromodomain Testis-Specific Factor, BRDT, in Cancer: A Biomarker and A Possible Therapeutic Target. *Cell J* **19**, 1-8, doi:10.22074/cellj.2017.5060 (2017).
- 125 Scanlan, M. J. *et al.* Expression of cancer-testis antigens in lung cancer: definition of bromodomain testis-specific gene (BRDT) as a new CT gene, CT9. *Cancer Lett* **150**, 155-164, doi:10.1016/s0304-3835(99)00385-7 (2000).
- 126 Wu, S. Y., Lee, A. Y., Lai, H. T., Zhang, H. & Chiang, C. M. Phospho switch triggers Brd4 chromatin binding and activator recruitment for gene-specific targeting. *Mol Cell* **49**, 843-857, doi:10.1016/j.molcel.2012.12.006 (2013).
- 127 Hsu, S. C. & Blobel, G. A. The Role of Bromodomain and Extraterminal Motif (BET) Proteins in Chromatin Structure. *Cold Spring Harb Symp Quant Biol* **82**, 37-43, doi:10.1101/sqb.2017.82.033829 (2017).
- 128 Cheung, K. L., Kim, C. & Zhou, M. M. The Functions of BET Proteins in Gene Transcription of Biology and Diseases. *Front Mol Biosci* **8**, 728777, doi:10.3389/fmolb.2021.728777 (2021).
- 129 Donati, B., Lorenzini, E. & Ciarrocchi, A. BRD4 and Cancer: going beyond transcriptional regulation. *Mol Cancer* **17**, 164, doi:10.1186/s12943-018-0915-9 (2018).
- 130 Wu, T. & Donohoe, M. E. The converging roles of BRD4 and gene transcription in pluripotency and oncogenesis. *RNA Dis* **2** (2015).

- 131 Allen, B. L. & Taatjes, D. J. The Mediator complex: a central integrator of transcription. *Nat Rev Mol Cell Biol* **16**, 155-166, doi:10.1038/nrm3951 (2015).
- 132 Hargreaves, D. C., Horng, T. & Medzhitov, R. Control of inducible gene expression by signal-dependent transcriptional elongation. *Cell* **138**, 129-145, doi:10.1016/j.cell.2009.05.047 (2009).
- 133 Li, Y., Liu, M., Chen, L. F. & Chen, R. P-TEFb: Finding its ways to release promoter-proximally paused RNA polymerase II. *Transcription* **9**, 88-94, doi:10.1080/21541264.2017.1281864 (2018).
- 134 Falchook, G. *et al.* Development of 2 Bromodomain and Extraterminal Inhibitors With Distinct Pharmacokinetic and Pharmacodynamic Profiles for the Treatment of Advanced Malignancies. *Clin Cancer Res* **26**, 1247-1257, doi:10.1158/1078-0432.CCR-18-4071 (2020).
- 135 Wu, S. Y. *et al.* Opposing Functions of BRD4 Isoforms in Breast Cancer. *Mol Cell* **78**, 1114-1132 e1110, doi:10.1016/j.molcel.2020.04.034 (2020).
- 136 Crowley, T., Brunori, M., Rhee, K., Wang, X. & Wolgemuth, D. J. Change in nuclear-cytoplasmic localization of a double-bromodomain protein during proliferation and differentiation of mouse spinal cord and dorsal root ganglia. *Brain Res Dev Brain Res* **149**, 93-101, doi:10.1016/j.devbrainres.2003.12.011 (2004).
- 137 Peng, J. *et al.* Brd2 is a TBP-associated protein and recruits TBP into E2F-1 transcriptional complex in response to serum stimulation. *Mol Cell Biochem* **294**, 45-54, doi:10.1007/s11010-006-9223-6 (2007).
- 138 Denis, G. V., Vaziri, C., Guo, N. & Faller, D. V. RING3 kinase transactivates promoters of cell cycle regulatory genes through E2F. *Cell Growth Differ* **11**, 417-424 (2000).
- 139 Kanno, T. *et al.* Selective recognition of acetylated histones by bromodomain proteins visualized in living cells. *Mol Cell* **13**, 33-43, doi:10.1016/s1097-2765(03)00482-9 (2004).
- 140 Sinha, A., Faller, D. V. & Denis, G. V. Bromodomain analysis of Brd2-dependent transcriptional activation of cyclin A. *Biochem J* **387**, 257-269, doi:10.1042/BJ20041793 (2005).
- 141 Hsu, S. C. *et al.* The BET Protein BRD2 Cooperates with CTCF to Enforce Transcriptional and Architectural Boundaries. *Mol Cell* **66**, 102-116 e107, doi:10.1016/j.molcel.2017.02.027 (2017).
- 142 Cheung, K. L. *et al.* Distinct Roles of Brd2 and Brd4 in Potentiating the Transcriptional Program for Th17 Cell Differentiation. *Mol Cell* **65**, 1068-1080 e1065, doi:10.1016/j.molcel.2016.12.022 (2017).

- 143 Lamonica, J. M. *et al.* Bromodomain protein Brd3 associates with acetylated GATA1 to promote its chromatin occupancy at erythroid target genes. *Proc Natl Acad Sci U S A* **108**, E159-168, doi:10.1073/pnas.1102140108 (2011).
- 144 Sarnik, J., Poplawski, T. & Tokarz, P. BET Proteins as Attractive Targets for Cancer Therapeutics. *Int J Mol Sci* **22**, doi:10.3390/ijms222011102 (2021).
- 145 Xie, X. H. *et al.* Clinical features, treatment, and survival outcome of primary pulmonary NUT midline carcinoma. *Orphanet J Rare Dis* **15**, 183, doi:10.1186/s13023-020-01449-x (2020).
- 146 French, C. A. *et al.* BRD4-NUT fusion oncogene: a novel mechanism in aggressive carcinoma. *Cancer Res* **63**, 304-307 (2003).
- 147 Eagen, K. P. & French, C. A. Supercharging BRD4 with NUT in carcinoma. *Oncogene* **40**, 1396-1408, doi:10.1038/s41388-020-01625-0 (2021).
- 148 Delmore, J. E. *et al.* BET bromodomain inhibition as a therapeutic strategy to target c-Myc. *Cell* **146**, 904-917, doi:10.1016/j.cell.2011.08.017 (2011).
- 149 Marcotte, R. *et al.* Functional Genomic Landscape of Human Breast Cancer Drivers, Vulnerabilities, and Resistance. *Cell* **164**, 293-309, doi:10.1016/j.cell.2015.11.062 (2016).
- 150 Segura, M. F. *et al.* BRD4 sustains melanoma proliferation and represents a new target for epigenetic therapy. *Cancer Res* **73**, 6264-6276, doi:10.1158/0008-5472.CAN-13-0122-T (2013).
- 151 Gallagher, S. J. *et al.* Control of NF- κ B activity in human melanoma by bromodomain and extra-terminal protein inhibitor I-BET151. *Pigment Cell Melanoma Res* **27**, 1126-1137, doi:10.1111/pcmr.12282 (2014).
- 152 Konieczkowski, D. J. *et al.* A melanoma cell state distinction influences sensitivity to MAPK pathway inhibitors. *Cancer Discov* **4**, 816-827, doi:10.1158/2159-8290.CD-13-0424 (2014).
- 153 Tiago, M. *et al.* Targeting BRD/BET proteins inhibits adaptive kinome upregulation and enhances the effects of BRAF/MEK inhibitors in melanoma. *Br J Cancer* **122**, 789-800, doi:10.1038/s41416-019-0724-y (2020).
- 154 Shorstova, T., Foulkes, W. D. & Witcher, M. Achieving clinical success with BET inhibitors as anti-cancer agents. *Br J Cancer* **124**, 1478-1490, doi:10.1038/s41416-021-01321-0 (2021).
- 155 Filippakopoulos, P. *et al.* Selective inhibition of BET bromodomains. *Nature* **468**, 1067-1073, doi:10.1038/nature09504 (2010).
- 156 Odore, E. *et al.* Phase I Population Pharmacokinetic Assessment of the Oral Bromodomain Inhibitor OTX015 in Patients with Haematologic Malignancies. *Clin Pharmacokinet* **55**, 397-405, doi:10.1007/s40262-015-0327-6 (2016).

- 157 Erkes, D. A. *et al.* The next-generation BET inhibitor, PLX51107, delays melanoma growth in a CD8-mediated manner. *Pigment Cell Melanoma Res* **32**, 687-696, doi:10.1111/pcmr.12788 (2019).
- 158 Grieselhuber, N. R. *et al.* The Novel BET Inhibitor PLX51107 Has In Vitro and In Vivo Activity Against Acute Myeloid Leukemia. *Blood* **128**, doi:DOI 10.1182/blood.V128.22.3941.3941 (2016).
- 159 Deng, G. *et al.* BET inhibitor suppresses melanoma progression via the noncanonical NF-kappaB/SPP1 pathway. *Theranostics* **10**, 11428-11443, doi:10.7150/thno.47432 (2020).
- 160 Nikbakht, N., Tiago, M., Erkes, D. A., Chervoneva, I. & Aplin, A. E. BET Inhibition Modifies Melanoma Infiltrating T Cells and Enhances Response to PD-L1 Blockade. *J Invest Dermatol* **139**, 1612-1615, doi:10.1016/j.jid.2018.12.024 (2019).
- 161 Emran, A. A. *et al.* A Combination of Epigenetic BET and CDK9 Inhibitors for Treatment of Human Melanoma. *J Invest Dermatol* **141**, 2238-2249 e2212, doi:10.1016/j.jid.2020.12.038 (2021).
- 162 Badamchi-Zadeh, A. *et al.* Combined HDAC and BET Inhibition Enhances Melanoma Vaccine Immunogenicity and Efficacy. *J Immunol* **201**, 2744-2752, doi:10.4049/jimmunol.1800885 (2018).
- 163 Echevarria-Vargas, I. M. *et al.* Co-targeting BET and MEK as salvage therapy for MAPK and checkpoint inhibitor-resistant melanoma. *EMBO Mol Med* **10**, doi:10.15252/emmm.201708446 (2018).
- 164 Stathis, A. & Bertoni, F. BET Proteins as Targets for Anticancer Treatment. *Cancer Discov* **8**, 24-36, doi:10.1158/2159-8290.CD-17-0605 (2018).
- 165 Gilan, O. *et al.* Selective targeting of BD1 and BD2 of the BET proteins in cancer and immunoinflammation. *Science* **368**, 387-394, doi:10.1126/science.aaz8455 (2020).
- 166 Zhou, B. *et al.* Discovery of a Small-Molecule Degradator of Bromodomain and Extra-Terminal (BET) Proteins with Picomolar Cellular Potencies and Capable of Achieving Tumor Regression. *J Med Chem* **61**, 462-481, doi:10.1021/acs.jmedchem.6b01816 (2018).
- 167 Gao, Z. *et al.* Targeting BRD4 proteins suppresses the growth of NSCLC through downregulation of eIF4E expression. *Cancer Biol Ther* **19**, 407-415, doi:10.1080/15384047.2018.1423923 (2018).

- 168 Pham, T. N. D. *et al.* Induction of MNK Kinase-dependent eIF4E Phosphorylation by Inhibitors Targeting BET Proteins Limits Efficacy of BET Inhibitors. *Mol Cancer Ther* **18**, 235-244, doi:10.1158/1535-7163.MCT-18-0768 (2019).
- 169 Wan, P. *et al.* BRDT is a novel regulator of eIF4EBP1 in renal cell carcinoma. *Oncol Rep* **44**, 2475-2486, doi:10.3892/or.2020.7796 (2020).
- 170 Bertomeu, T. *et al.* A High-Resolution Genome-Wide CRISPR/Cas9 Viability Screen Reveals Structural Features and Contextual Diversity of the Human Cell-Essential Proteome. *Mol Cell Biol* **38**, doi:10.1128/MCB.00302-17 (2018).
- 171 Ianevski, A., Giri, A. K. & Aittokallio, T. SynergyFinder 2.0: visual analytics of multi-drug combination synergies. *Nucleic Acids Res* **48**, W488-W493, doi:10.1093/nar/gkaa216 (2020).
- 172 BLISS, C. I. THE TOXICITY OF POISONS APPLIED JOINTLY1. *Annals of Applied Biology* **26**, 585-615, doi:<https://doi.org/10.1111/j.1744-7348.1939.tb06990.x> (1939).
- 173 Tang, J., Wennerberg, K. & Aittokallio, T. What is synergy? The Saariselka agreement revisited. *Front Pharmacol* **6**, 181, doi:10.3389/fphar.2015.00181 (2015).
- 174 Amzallag, A., Ramaswamy, S. & Benes, C. H. Statistical assessment and visualization of synergies for large-scale sparse drug combination datasets. *BMC Bioinformatics* **20**, 83, doi:10.1186/s12859-019-2642-7 (2019).
- 175 Quah, B. J. & Parish, C. R. The use of carboxyfluorescein diacetate succinimidyl ester (CFSE) to monitor lymphocyte proliferation. *J Vis Exp*, doi:10.3791/2259 (2010).
- 176 Dong, X., Hu, X., Chen, J., Hu, D. & Chen, L. F. BRD4 regulates cellular senescence in gastric cancer cells via E2F/miR-106b/p21 axis. *Cell Death Dis* **9**, 203, doi:10.1038/s41419-017-0181-6 (2018).
- 177 Lee, B. Y. *et al.* Senescence-associated beta-galactosidase is lysosomal beta-galactosidase. *Aging Cell* **5**, 187-195, doi:10.1111/j.1474-9726.2006.00199.x (2006).
- 178 Van Hoorde, L., Van Aken, E. & Mareel, M. Collagen type I: a substrate and a signal for invasion. *Prog Mol Subcell Biol* **25**, 105-134, doi:10.1007/978-3-642-59766-4_7 (2000).
- 179 Wang, J. *et al.* UV-induced somatic mutations elicit a functional T cell response in the YUMMER1.7 mouse melanoma model. *Pigment Cell Melanoma Res* **30**, 428-435, doi:10.1111/pcmr.12591 (2017).
- 180 Ozer, H. G. *et al.* BRD4 Profiling Identifies Critical Chronic Lymphocytic Leukemia Oncogenic Circuits and Reveals Sensitivity to PLX51107, a Novel Structurally Distinct BET Inhibitor. *Cancer Discov* **8**, 458-477, doi:10.1158/2159-8290.CD-17-0902 (2018).

- 181 Boi, M. *et al.* The BET Bromodomain Inhibitor OTX015 Affects Pathogenetic Pathways in Preclinical B-cell Tumor Models and Synergizes with Targeted Drugs. *Clin Cancer Res* **21**, 1628-1638, doi:10.1158/1078-0432.CCR-14-1561 (2015).
- 182 Riveiro, M. E. *et al.* OTX015 (MK-8628), a novel BET inhibitor, exhibits antitumor activity in non-small cell and small cell lung cancer models harboring different oncogenic mutations. *Oncotarget* **7**, 84675-84687, doi:10.18632/oncotarget.13181 (2016).
- 183 Rebello, R. J. *et al.* The Dual Inhibition of RNA Pol I Transcription and PIM Kinase as a New Therapeutic Approach to Treat Advanced Prostate Cancer. *Clin Cancer Res* **22**, 5539-5552, doi:10.1158/1078-0432.CCR-16-0124 (2016).
- 184 Guo, Q. *et al.* The MNK1/2-eIF4E Axis Supports Immune Suppression and Metastasis in Postpartum Breast Cancer. *Cancer Res* **81**, 3876-3889, doi:10.1158/0008-5472.CAN-20-3143 (2021).
- 185 Altman, J. K. *et al.* Inhibition of Mnk kinase activity by cercosporamide and suppressive effects on acute myeloid leukemia precursors. *Blood* **121**, 3675-3681, doi:10.1182/blood-2013-01-477216 (2013).